LLDPE/SEBS/SILANE MODIFIED ZEOLITE ZSM-5 BLEND FILM WITH HIGH PERMSELECTIVITY FOR ETHYLENE PERMEATION

KRITSANA MAKPHON

A THESIS SUBMITTED IN PARTIAL FULFILLMENT OF THE REQUIREMENT FOR THE DEGREE OF MASTER OF SCIENCE IN POLYMER TECHNOLOGY

DEPARTMENT OF CHEMISTRY
FACULTY OF SCIENCE
KING MONGKUT'S INSTITUTE OF TECHNOLOGY LADKRABANG

2017

KMITL-2017-SC-M-014-028

Faculty of Science
King Mongkut's Institute of Technology Ladkrabang
Thesis Certification

Thesis Title	"LLDPE/SEBS/SILANE MODIFIED ZEOLITE ZSM-5 BLEND FILM WITH HIGH PERMSELECTIVITY FOR ETHYLENE PERMEATION"
Student Name	Miss Kritsana Makphon
Student ID	57605051
Degree	Master of Science (Polymer Technology)
Department	Chemistry
Thesis Advisor	Asst.Prof.Dr. Chonlada Ritvirulh
Thesis Co-advisor	Asst.Prof.Dr. Suparat Rukchonlatee
Thesis Co-advisor	Assoc.Prof.Dr. Tawan Sooknoi

Thesis Committee	Signatures
Assoc.Prof.Dr. Ittipol Jangchud Chairperson	
Assoc.Prof.Dr. Jutarat Prachayawarakorn Examiner	
Assoc.Prof.Dr. Kalyanee Sirisinha External Examiner	
Asst.Prof.Dr. Suparat Rukchonlatee Thesis Co-Advisor	
Assoc.Prof.Dr. Tawan Sooknoi Thesis Co-Advisor	
Asst.Prof.Dr. Chonlada Ritvirulh Thesis Advisor	

Examination Date 4th July 2017 **Time** 09.00-12.00 a.m.
Place Faculty of Science room 304

Approved by Faculty of Science

(Assoc.Prof.Dr. Dusanee Thanaboripat)
Dean
Date 19 Jul 2017

หัวข้อวิทยานิพนธ์	ฟิล์มพอลิเมอร์ผสมแอลแอลดีพีอี/เอสอีบีเอส/ซีโอไลต์ ZSM-5 ดัดแปรด้วยไซเลนที่มีความจำเพาะเจาะจงสูงสำหรับการซึมผ่านก๊าซเอทิลีน
ชื่อนักศึกษา	นางสาวกฤษณา มรรคผล
รหัสประจำตัว	57605051
ปริญญา	วิทยาศาสตรมหาบัณฑิต (เทคโนโลยีพอลิเมอร์)
ภาควิชา	เคมี
พ.ศ.	2560
อาจารย์ที่ปรึกษาวิทยานิพนธ์	ผศ.ดร.ชลลดา ฤตวิรุฬห์
อาจารย์ที่ปรึกษาวิทยานิพนธ์ร่วม	รศ.ดร.ตะวัน สุขน้อย ผศ.ดร.สุภารัตน์ รักชลธี

บทคัดย่อ

งานวิจัยนี้ทำการพัฒนาฟิล์มพอลิเมอร์ผสมของพอลิเอทิลีนชนิดความหนาแน่นต่ำเชิงเส้น (LLDPE)/พอลิสไตรีน เอทิลีน-บิวทิลีน สไตรีน (SEBS) และซีโอไลต์ HZSM-5 ที่ดัดแปรเพื่อเพิ่มความสามารถในการซึมผ่านก๊าซเอทิลีนของฟิล์มบรรจุภัณฑ์ โดยมีปัจจัยศึกษาที่มีผลต่อการซึมผ่านก๊าซเอทิลีนของฟิล์มพอลิเมอร์ผสม คือการดัดแปรพื้นผิวของซีโอไลต์และปริมาณของซีโอไลต์ (5-15%wt) การดัดแปรพื้นผิวด้วยออกตะเดกซิลไตรคลอโรไซเลน (OTS) และ 3-อะมิโนโพรพิลไตรเอทอกซีไซเลน (APS)/พอลิเอทิลีนต่อกิ่งด้วยมาเลอิกแอนไฮดรายด์ (PE-g-MA) เพื่อเพิ่มความสามารถในการเข้ากันได้ระหว่างซีโอไลต์กับพอลิเมอร์ โดยศึกษาสมบัติเชิงกล สมบัติทางความร้อน สัณฐานวิทยา และอัตราการซึมผ่านก๊าซเอทิลีนของฟิล์ม จากการศึกษาพบว่าฟิล์มที่ใช้ซีโอไลต์ชนิดปรับปรุงด้วย OTS มีอัตราการซึมผ่านก๊าซเอทิลีนและสมบัติในการรับแรงดึงดีกว่าฟิล์มที่ใช้ซีโอไลต์ชนิดปรับปรุงด้วย APS/PE-g-MA และจากผลของสัณฐานวิทยาพบว่าฟิล์มที่ใช้ซีโอไลต์ชนิดปรับปรุงด้วย APS/PE-g-MA มีวัฏภาคกระจายขนาดใหญ่กว่าฟิล์มที่ใช้ซีโอไลต์ชนิดปรับปรุงด้วย OTS ซึ่งเกิดจากวัฏภาคกระจาย SEBS รวมตัวกัน แสดงว่า PE-g-MA ในฟิล์มที่ใช้ซีโอไลต์ชนิดปรับปรุงด้วย APS/PE-g-MA ลดความเข้ากันได้ระหว่าง LLDPE และ SEBS โดยการเพิ่มความเร็วรอบในการผสมทำให้ความสามารถในการเข้ากันได้และอัตราการซึมผ่านก๊าซเอทิลีนของฟิล์มที่ใช้ซีโอไลต์ชนิดปรับปรุงด้วย APS/PE-g-MA มีค่าเพิ่มขึ้น และจากผลของปริมาณของซีโอไลต์พบว่าฟิล์มที่ใช้ซีโอไลต์ชนิดไม่ปรับปรุงและปรับปรุงพื้นผิวด้วย OTS มีสมบัติในการรับแรงดึงและอัตราการซึมผ่านก๊าซเอทิลีนเพิ่มขึ้นเมื่อปริมาณซีโอไลต์มากขึ้น เนื่องจากซีโอไลต์ทำให้ระยะแพร่ผ่านของก๊าซเอทิลีนในฟิล์มสั้นลงและมีความแตกต่างของความเข้มข้นของก๊าซเอทิลีนสูง เป็นผลให้การซึมผ่านก๊าซเอทิลีนง่ายขึ้น

ฟิล์มที่ใช้ซีโอไลต์ชนิดไม่ปรับปรุงพื้นผิวมีอัตราการซึมผ่านก๊าซเอทิลีนและคาร์บอนไดออกไซด์เพิ่มขึ้นอย่างมากเมื่อมีซีโอไลต์ปริมาณสูง (10-15%wt) ค่าอัตราการซึมผ่านที่ไม่เฉพาะเจาะจงชนิดของก๊าซเป็นผลจากการมีช่องว่างที่เกิดจากรอยต่อระหว่างวัฏภาคในเนื้อฟิล์ม

คำสำคัญ : การซึมผ่านของก๊าซเอทิลีน ซีโอไลต์แซดเอสเอ็ม-5 พอลิเมอร์ผสม พอลิสไตรีน-เอทิลีน/บิวทิลีน-สไตรีน พอลิเอทิลีนชนิดความหนาแน่นต่ำเชิงเส้น

Thesis Title	LLDPE/SEBS/silane modified zeolite ZSM-5 blend film with high permselectivity for ethylene permeation
Student Name	Miss Kritsana Makphon
Student ID	57605051
Degree	Master of Science (Polymer Technology)
Department	Chemistry
Year	2017
Thesis Advisor	Asst.Prof.Dr. Chonlada Ritvirulh
Thesis Co-advisors	Assoc.Prof.Dr. Tawan Sooknoi
	Asst.Prof.Dr. Suparat Rukchonlatee

Abstract

In this research, polymer blend film of linear low density polyethylene (LLDPE)/polystyrene ethylene-butylene styrene copolymer (SEBS) with modified zeolite HZSM-5 were developed to improve ethylene gas permeation for packaging applications. The factors affecting ethylene gas permeation of the polymer blend film were studied, including zeolite surface modification and zeolite loading (5-15%wt). Octadecyltrichlorosilane (OTS) and 3-aminopropyltri-ethoxysilane (APS)/maleic anhydride grafted polyethylene (PE-g-MA) were used to modify zeolite surface, in order to improve compatibility between zeolite and polymers. Mechanical and thermal properties, morphology, ethylene transmission rates (ETR) of the films were investigated. It was found that OTS-modified zeolite-filled film possessed ETR and tensile properties greater than those of APS/PE-g-MA-modified one. The dispersed phase size of APS-modified zeolite-filled film was larger than that of OTS-modified sample because the dispersed SEBS phase was coalescence. This was suggested that PE-g-MA in APS/PE-g-MA-modified zeolite-filled film reduced compatibility between LLDPE and SEBS. An improved compatibility and ETR of the APS/PE-g-MA-modified zeolite-filled film can be obtained by increasing the mixing speed. It was also found that the tensile strength and ETR of both unmodified and OTS-modified zeolite-filled films were

increased with the zeolite loading. This is because the zeolite had shortens diffusion pathway in the film for ethylene gas and high virtual ethylene concentration gradient, resulting in facilitated ethylene permeation. Although the ETR and CO_2 transmission rate (CO_2TR) of unmodified zeolite-filled film was largely increased at high zeolite loading (10-15%wt), this non-selective transmission rate was due to interfacial void of this film.

Keywords : Ethylene permeation, Zeolite ZSM-5, Polymer blends, SEBS, LLDPE

Acknowledgements

The author would like to express my profound gratitude to my advisors, Asst.Prof.Dr. Chonlada Ritvirulh, Assoc.Prof.Dr. Tawan Sooknoi and Asst.Prof.Dr. Suparat Rukchonlatee for their supervisions, helpful suggestion and encouragement throughout this thesis.

The author is also grateful to Assoc.Prof.Dr. Ittipol Jangchud, Assoc.Prof.Dr. Jutarat Prachayawarakorn and Assoc.Prof.Dr. Kalyanee Sirisinha for serving as the chairperson and the committees.

The author would like to extend this sincere appreciation to Prof.Dr. Masayuki Yamaguchi for guidance advice and support during my visit at Japan Advanced Institute of Science and Technology.

The author would like to thanks to all my teacher, friends and research team for their constant guidance advice, support and encouragement.

Sincere thanks to the Department of Chemistry, Faculty of Science, King Mongkut's Institute of Technology Ladkrabang for equipment, chemicals and facilities.

Finally, the author thanks and give to parents and family for the constant love and encouragement.

Miss Kritsana Makphon

Table of Contents

Table of Contents (Continued)

Table of Contents (Continued)

Table of Contents (Continued)

List of Tables

List of Figures

List of Figures (Continued)

List of Figures (Continued)

List of Figures (Continued)

List of Figures (Continued)

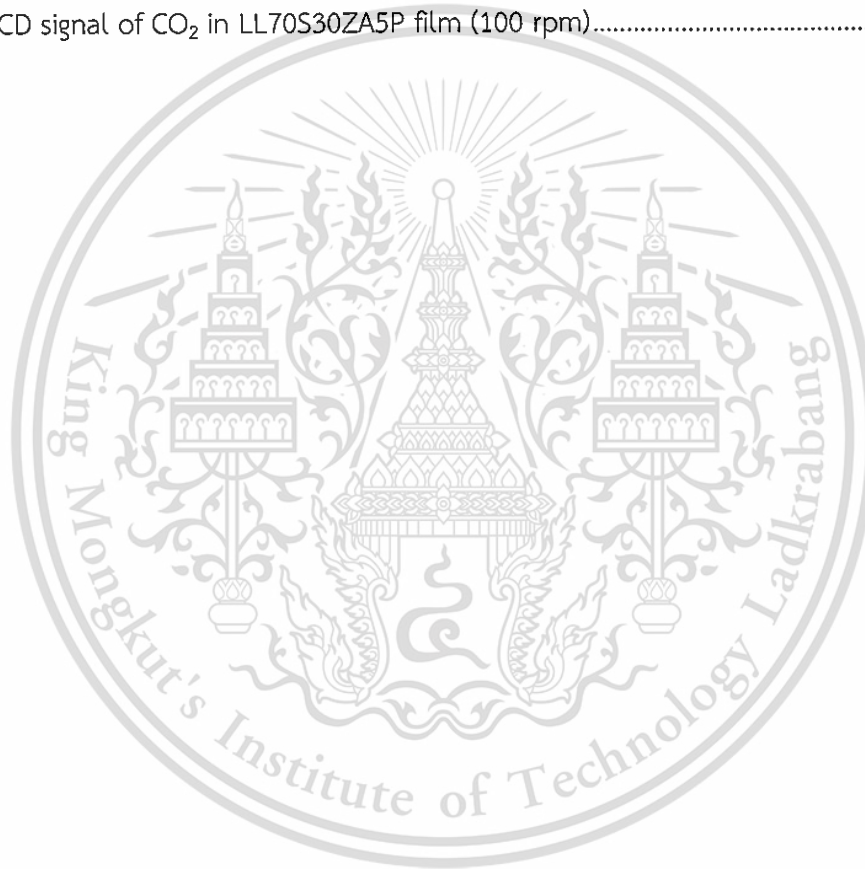

Abbreviations

APS	3-aminopropyltriethoxysilane
Å	Angstrom
$CaCO_3$	Calcium carbonate
°C	Degree Celsius
C_2H_4	Ethylene
DMA	Dynamic mechanical properties
CO_2	Carbon dioxide
CO_2P	Carbon dioxide permeation
CO_2TR	Carbon dioxide transmission rate
DSC	Differential scanning calorimetry
E′	Storage modulus of tension mode
E″	Loss modulus of tension mode
EN	Electronegativity
EP	Ethylene permeation
ETS	Ethyltrichlorosilane
ETR	Ethylene transmission rate
FE-SEM	Field emission scanning electron microscopy
G′	Storage modulus of shear mode
G″	Loss modulus of shear mode
He	Helium
$KMnO_4$	Potassium permanganate
LLDPE	Linear low density polyethylene
MAP	Modified atmosphere packaging
MPa	Megapascal
N_2	Nitrogen
O_2	Oxygen
OTS	Octadecyltrichlorosilane
PE	Polyethylene
PE-g-MA	Maleic anhydride grafted polyethylene
PP	Polypropylene

Abbreviations (Continued)

ppb	Part per billion
ppm	Part per million
rpm	Revolutions per minute
SEBS	Polystyrene ethylene-butylene styrene
SEM	Scanning electron microscopy
T	Temperature
tan δ	Ratio of loss modulus to the storage modulus
T_c	Crystallization temperature
TCD	Thermal conductivity detector
T_g	Glass transition temperature
TGA	Thermogravimetric analyzer
THF	Tetrahydrofuran
T_m	Melting temperature
TPEs	Thermoplastic elastomers
μm	Micrometer
ω	Angular frequency
X_c	Crystallinity
XPS	X-ray photoelectron spectrophotometer

Chapter 1
Introduction

1.1 Research Motivation

Thailand is one of the most world-leading manufacturers and exporters of agricultural products. However, freshness of agricultural products have to be preserved before reaching the consumer [1]. The plant respiration process is the major cause for loss of vegetables and fruits freshness. Some vegetables and fruits in climacteric group such as banana, mango and tomato, can generate ethylene gas after harvesting. Ethylene gas is a plant hormone that can accelerate the ripening process of vegetables and fruits in this climacteric group. In addition, ethylene gas causes discoloration, odor and a decrease in nutritional value of vegetables and fruits [2]. In order to delay the ripening process during storage and transportation, the packaging of those vegetables and fruits should be able to reduce accumulation of the ethylene gas produced.

Most packaging films are produced from polyethylene (PE) because of its low cost, high flexibility, long shelf life [3]. However, PE is low gas permeability. Therefore, packaging films with polymer blends of polyethylene and thermoplastic elastomers (TPEs) should be developed to enhance gas permeability. In previous work [4], the blend film of linear low density polyethylene (LLDPE) and poly(styrene-ethylene/butylene-styrene) (SEBS) exhibited high ethylene permeability. The SEBS contains ethylene-butylene segment that causes high elasticity and low polarity. High ethylene-butylene content in LLDPE/SEBS film led to an increase in ethylene gas permeability. However, tensile stress at yield of LLDPE/SEBS films were decreased with SEBS loading. It was found that the LLDPE/SEBS film with a 70/30 ratio gave an acceptable tensile strength and the highest ethylene transmission rate (ETR). This agreed with another work [5] that carried out the research on the LLDPE/SEBS films. In addition, the high ETR was caused by large size of the SEBS dispersed phase. Moreover, ethylene gas permeability of polymer blend film was successfully improved when zeolite ZSM-5 having porous structure and continuous channel was added [5]. This composite film showed a high selectivity to ethylene gas adsorption.

This is because the porous material possesses selectivity with ethylene, leading to an increase in adsorption of the ethylene. Consequently, the adsorption ability of porous material causes an increase in ethylene concentration gradient in the film. Hence, ethylene gas permeability of such film would be higher. However, porous material is relatively high polar, as compared to the polymers. This results in low compatibility of porous material with LLDPE/SEBS. Hence, surface modification of porous material should be applied to reduce its polarity and also increase its compatibility with the polymer matrix. It was found that ethylene gas permeation of LLDPE/SEBS/zeolite Y composite film was successfully improved when zeolite Y was modified with octadecyltrichlorosilane (OTS) that increases surface hydrophobicity of the zeolite [6]. However, zeolite Y with high polarity is not selective for adsorption of hydrocarbon, such as ethylene.

Hence, in this study, the LLDPE/SEBS blend film at 70/30 weight ratio with zeolite ZSM-5 (Si/Al = 15-infinity) because it has low polarity than zeolite Y (Si/Al = 1.5-3) that zeolite ZSM-5 is more selective for ethylene adsorption. Nevertheless, zeolite ZSM-5 surface is relatively polar, as compared to the polymers. Therefore surface modification of zeolite ZSM-5 was functionalized with OTS. The OTS could successfully reduce surface polarity of the polar materials such as zeolite Y [6-7]. In addition, to study effect of surface modifier type, 3-aminopropyltriethoxysilane (APS) was employed in this research. The use of APS as surface modifier for solid filler was previously reported [8]. After zeolite ZSM-5 was surface treated with APS, the amine group in APS could react with maleic anhydride of the maleic anhydride grafted polyethylene (PE-g-MA). This may result in better compatibility between modified zeolite ZSM-5 and polymers. In addition, the effects of zeolite content (5-15%wt) in the LLDPE/SEBS films were investigated.

1.2 Objectives of the study

1) To develop the films with high permselectivity for ETR.

2) To understand the effect of OTS and APS with PE-g-MA for zeolite ZSM-5 on mechanical properties and gas permeation of LLDPE/SEBS films.

3) To understand the effect of zeolite ZSM-5 loading in the LLDPE/SEBS films.

1.3 Scopes of the study

1) Surface modification of zeolite ZSM-5 with OTS and APS/PE-g-MA.

2) Characterization of modified zeolite using X-ray photoelectron spectrophotometer (XPS).

3) Mixing of LLDPE/SEBS/zeolite ZSM-5 and LLDPE/SEBS/modified zeolite ZSM-5 (OTS and APS/PE-g-MA) with various zeolite contents at 5, 10, and 15%wt using an internal mixer.

4) Preparation of LLDPE/SEBS/zeolite ZSM-5 composite films using a compression molding technique.

5) Characterization of thermal properties and morphology of LLDPE/SEBS/zeolite ZSM-5 composite films using differential scanning calorimetry (DSC) and field emission scanning electron microscopy (FE-SEM), respectively.

6) Study on mechanical properties of LLDPE/SEBS/zeolite ZSM-5 composite films.

7) Study on permeation of ethylene gas and carbon dioxide gas of LLDPE/SEBS/zeolite ZSM-5 composite films.

1.4 Benefits of the study

LLDPE/SEBS/modified zeolite ZSM-5 packaging films with enhanced ethylene gas permeation and acceptable tensile properties can be obtained. The films can be applied for long shelf-life of fresh vegetables and fruits.

Chapter 2

Theory and Literature Reviews

2.1 Respiration in fresh produces [9-12]

Process of respiration involves combining O_2 in the air with organic molecules in the tissue i.e. sugar to form various intermediate compounds and eventually CO_2 and water. The energy and organic molecules produced during respiration are used by other metabolic processes to maintain the health of the commodity. The overall equation for respiration can be written in the following equation (2.1).

$$C_6H_{12}O_6 + 6O_2 \longrightarrow 6CO_2 + 6H_2O + \text{energy and/or heat} \quad (2.1)$$

This respiration activity contributes to aging or senescence of the fresh produces. If this activity is decreased or slow down, the postharvest storage life can be prolonged. Practically, the decreased respiration is obtained from either decreasing oxygen or increasing carbon dioxide. This is a main concept of the modified atmosphere packaging (MAP). In MAP, the oxygen content is decreased to approximately 1-5% (down from 20.99% in the ambient air). On the other hand, the carbon dioxide content is approximately 5-10% (typically 0.03% in the ambient air).

In addition, fresh produces can also generate the ethylene gas (C_2H_4) that is a natural growth hormone. According to their ethylene productions, classification of fresh produces is shown in Table 2.1. The ethylene can affect on the fresh produces in many difference ways due to its biologically active at very low concentration (ppb-ppm range). Although some effects of ethylene are viewed as beneficial, the most of them are detrimental effect that is senescence. In particular, for a climacteric fruit, the ethylene can accelerate unusual fast respiration.

Table 2.1 Classification of the fresh produces that is classified by ethylene production rate [13]

Class	Range at 20°C (68°F) (μl C_2H_4/kg-h)	Commodities
Very low	<0.1	Asparagus, cauliflower, cherry, orange, grape, pomegranate, vegetables, root vegetables, potato, most cut flower.
Low	0.1–1.0	Blueberry, cranberry, cucumber, eggplant, okra, olive, pepper, persimmon, pineapple, pumpkin, raspberry, watermelon.
Moderate	1.0-10.0	Banana, fig, guava, melon, mango, tomato
High	10.0-100.0	Apple, apricot, avocado, cantaloupe, kiwifruit (Ripe), nectarine, papaya, peach, pear, plum
Very high	>100.0	Passion fruit

2.2 Ripening of fruits [14-15]

Fresh fruits undergo a natural stage of development known as ripening. This occurs when the fruits have ceased growing and are counted to be mature. Ripeness is followed by aging (often called senescence) and breakdown of the fruits. Typically, there are two characteristic types of fruit ripening due to different patterns of respiration:

1. Climacteric fruit

Climacteric fruits refer to fruits that can be harvested when mature. These fruits may be ripened naturally or artificially. The start of ripening is accompanied by a rapid rise in respiration rate, called the respiratory climacteric. After the climacteric, the respiration can be slow down as the fruit ripens and develops tasted quality. Examples of climacteric fruits are apple, avocado, banana, kiwifruit, mango, papaya, passion fruit, peach, pear, tomato and watermelon etc. Pattern of climacteric fruit is illustrated in Figure 2.1.

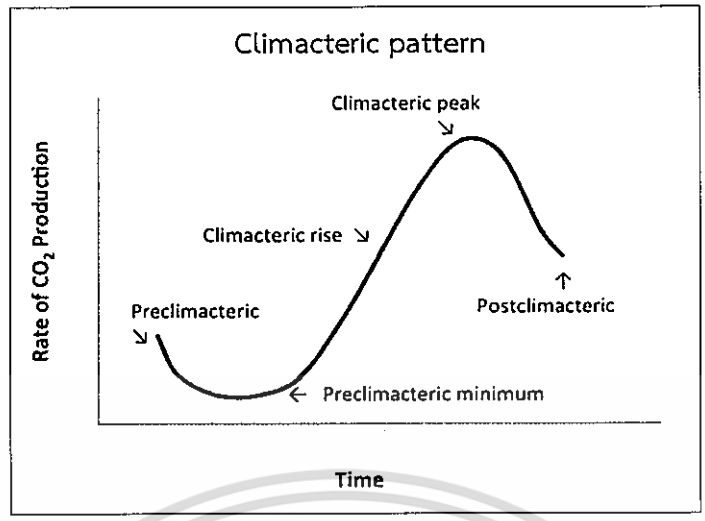

Figure 2.1 The climacteric pattern of respiration in ripening fruit [16]

2. Non-climacteric fruit

Non-climacteric fruits refer to those fruits, which ripen only while still attached to the parent plant. Their eating qualities suffer if they are harvested before fully ripe. This is because their sugar and acid content do not increase further. Respiration rate is gradually slow during growth and after harvest. Maturation and ripening are a gradual process. Examples of non-climacteric fruits are blueberry, cherry, cucumber, grape, lemon, lime, olive, orange, pepper, pineapple, strawberry etc. Pattern of non-climacteric fruit is illustrated in Figure 2.2.

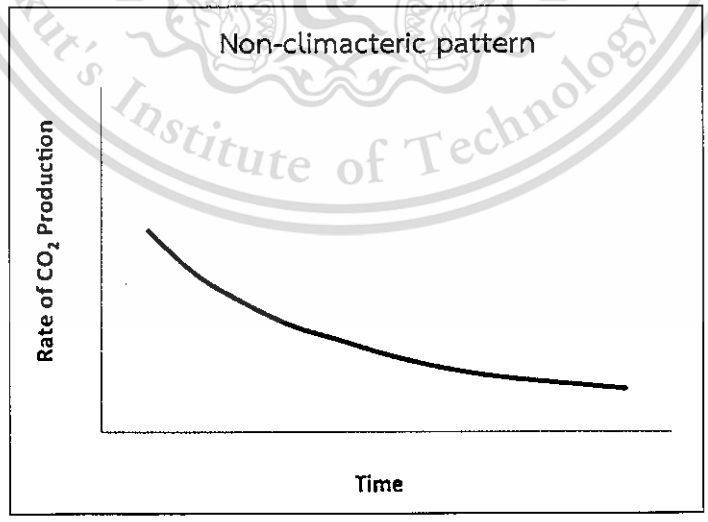

Figure 2.2 The non-climacteric pattern of respiration in ripening fruit [16]

2.3 Modified atmosphere packaging [17-21]

Modified atmosphere packaging (MAP) concept for packaged goods can be achieved by modifying the atmosphere surrounding a food product by vacuum, gas flushing or controlled permeability of the pack. Thus controlling the biochemical, enzymatic and microbial actions lead to a decrease in main degradations that might occur. These allow the preservation of the fresh state of the produces without the temperature or chemical treatments used by competitive preservation techniques such as canning, freezing, dehydration and other processes.

2.3.1 Methods of MAP conditions

MAP can be categorized into passive MAP and active MAP:

1. Passive MAP

MAP can passively evolve within a hermetically sealed package as a consequence of a commodity's respiration, i.e. O_2 consumption and CO_2 evolution. If a commodity's respiration characteristics are properly matched to film permeability values, then a beneficial modified atmosphere can be passively created within a package. If a film of correct selectivity permeability is chosen, then a desirable equilibrium modified atmosphere is established when the rate of O_2 transmission through the package equals a respiration rate of the product.

2. Active MAP

Active MAP can be defined as the incorporation of an active system into a packaging film or container to modify the packaging atmosphere and maintain the quality or extend the shelf-life of the product. The active system can be either a solid material or gas. Typical systems used include O_2, CO_2, ethylene scavengers/ emitters, moisture absorbers and gas flushing such as O_2, CO_2, CO, N_2, argon and the combination of two or more of these gases.

2.3.2 Advantages and disadvantages of MAP

The normal composition of air is 20.99% O_2, 78.03% N_2, 0.03% CO_2 and 0.95% other gases. Modification of the atmosphere within the package by reducing the O_2 content while increasing the levels of CO_2 and/or N_2 has been shown to significantly extend the shelf-life of perishable foods at chill temperatures.

Advantages of MAP

1) Increased shelf-life allowing less frequent loading of retail display shelves

2) Reduction in retail waste

3) Improved presentation-clear view of product and all round visibility

4) Hygienic stackable pack, sealed and free from product drip and odor

5) Easy separation of sliced products

6) Little or no need for chemical preservation

7) Increased distribution area and reduced transport costs due to less frequent deliveries

8) Centralized packaging and portion control

9) Reduction in production and storage costs due to better utilization of labor, space and equipment

Disadvantages of MAP

1) Capital cost of gas packaging machinery

2) Cost of gases and packaging materials

3) Cost of analytical equipment to ensure that correct gas mixtures are being used

4) Cost of quality assurance systems to prevent the distribution of leakers, etc

5) Increased pack volume which will adversely affect transport costs and retail display space

6) Potential growth of food-borne pathogens due to temperature abuse by retailers and consumers

7) Benefits of MAP are lost once the pack is opened or leaked

2.4 Membrane technology

2.4.1 Membrane description [22-23]

Membrane is a thin layer of materials that are capable for separation substance as a function of their chemical or physical properties when a suitable driving force is applied. Membranes are available in different configurations: plate and frame, tubular, hollow fiber and spiral wound. They are made of various materials such as polymer, metal and ceramic.

The basic concept of membrane separation is shown in Figure 2.3. A feed stream enters the system of membrane and a suitable driving force (such as differential concentration or pressure) is applied across the membrane. This leads to preferential transport of one or more components. Certain components (solutes, solvents or gases) pass through the membrane. Other components do not pass through the membrane or pass through very slowly. The selective transport (called permeation) forms the basis of membrane separations, which generally involve the separation of solutes or fluids. The stream containing the components that permeate through membrane is called the permeate or filtrate and the stream containing retained components is called the retentate or concentrate.

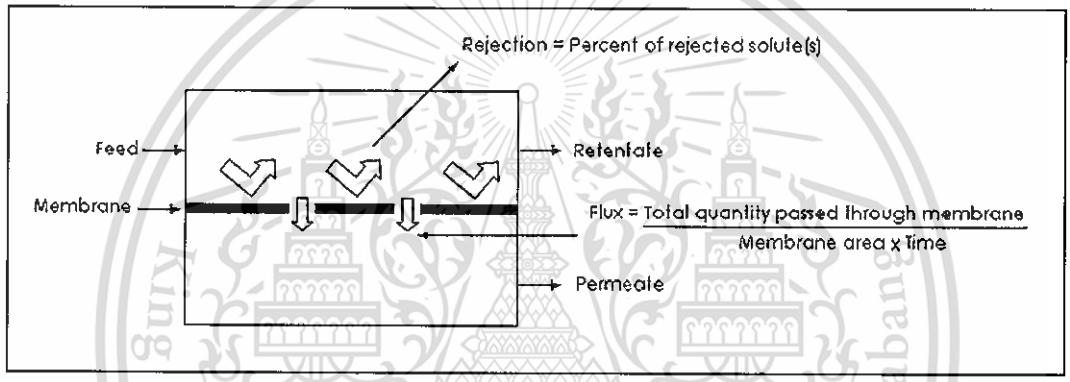

Figure 2.3 Transport of membrane [24]

2.4.2 Applications of membrane [25]

Membrane technology has become a dignified separation technology over the past decennia and is being used increasingly in a broad range of applications. The main force of membrane technology is the fact that it works without an addition of chemicals, with a relatively low energy use, easily and well-arranged process conductions. The important property of membrane, which is exploited in every application, is the ability of a membrane to control the permeation of chemical species in contact with it. Applications of membrane are shown in Table 2.2

Table 2.2 Industrial applications of membrane separation processes [25]

Industrial applications	Membrane separation processes
Reverse osmosis	- Desalinization of brackish water - Treatment of wastewater to remove a wide variety of impurity - Treatment of surface and ground water - Concentration of foodstuffs - Removal of alcohol from beer and wine
Dialysis	- Separation of nickel sulfate from sulfuric acid - Hemodialysis (Removal of waste metalbolites, excess body water and restoration of electrolyte balance in blood)
Electrodialysis	- Production table salt from seawater - Treatment of wastewater from electroplating - Demineralization of cheese whey - Production of ultra pure water for the semiconductor
Microfiltration	- Sterilization of drug - Purification of antibiotic - Separation of mammalian cell from liquid
Ultrafiltration	- Preconcentration of milk before making cheese - Recovery of vaccine and antibiotic from fermentation broth - Color removal from Kraft black in paper making
Pervaporation	- Dehydration of ethanol-water azeotrope - Removal of water from organic solvent - Removal of organic from water
Gas permeation	- Separation of CO_2 and H_2 from methane and other hydrocarbons - Adjustment of the H_2/CO ratio in synthesis gas - Recovery of helium - Recovery methane from biogas
Liquid membrane	Recovery of zinc from wastewater in the viscous fiber industry

2.4.3 Gas permeation of polymer membrane [24, 26-27]

Gas permeation is a technique for fractionating gas mixtures using nonporous polymer membranes having a selective permeability to gas according to a dissolution-diffusion mechanism. In this membrane process, membrane devices for gas or vapor separation usually operate under continuous steady-state conditions with three streams (feed, permeate and retentate). Gas is made to pass through the membrane by applying a pressure difference on either side of the membrane. This differential pressure causes a difference in dissolved gas concentration between the two faces of the membrane and hence a diffusional gas flows through the membrane. Membrane selectivity is based on the relative permeation rates of the components through the membrane. Each gaseous component transporting through the membrane has a characteristic permeation rate that is a function of the ability to dissolve and diffuse through the membrane material.

Membranes utilized in separation process are required to possess both high selectivity and high permeation (high permselectivity). The selectivity of the membrane to specific gas molecules is the ability of the molecules to diffuse through the membrane. Diffusion of molecules through the polymer is dependent upon various properties of polymer; for example, crosslinking density, chain stiffness, glass transition temperature (T_g), crystallinity, crystallite size and distribution, and solubility of the molecules in the polymer membrane.

Chain stiffness and crystallinity affect the free volume of the polymer. Crystallites restrict the free volume, making diffusion more difficult. Increasing the chain stiffness in the amorphous regions essentially restricts the free volume. Having small, uniformly distributed crystallites in the polymer creates more tortuous pathways for the diffusing molecules. Polarity due to functional groups inside the membrane and Van Der Waals forces due to hydrocarbon fragments can also have a significant influence on separation processes, depending on the nature of the gas molecules.

Permselective polymeric membranes can be divided into two basic categories: glassy and rubbery. Glassy polymers have low chain intrasegmental mobility and long relaxation times, while rubbery polymers exhibit the opposite characteristics, namely high intrasegmental mobility and short relaxation times. Permeation behavior in each type of polymer is shown in Table 2.3.

Table 2.3 Permeation behavior of polymeric materials [27]

Glassy polymer	Rubbery polymer
Diffusion controlled permeation	Solubility controlled permeation
Little movement of polymer segments	Continuous movement of holes
Permeation dependent upon size of permeating molecules	Permeation dependent upon ability to dissolve intermolecular interaction and increase moving polymer segment

Membrane separation processes offer numerous industrial advantages over distillation or disposal. Energy requirements are lower, providing for lower overhead costs. The equipment necessary for liquid and gas separations is significantly more compact, simple to build and reasonably easy to operate. Handling various volumes of separated product is accomplished without having to utilize different equipments because the equipments can be scaled up or operated at partial capacity without problems. Furthermore, permselective membranes have utility not only in industrial processes involving basic chemicals but also in commercial products. Polymer films, such as polyethylene, used in packaging of meats, fruits and vegetables are essential to have a certain amount of oxygen permeability and diffusion through the packaging while holding back water. This minimum diffusion, especially in meat packaging, allows the meat to retain a more desirable coloring for the consumer.

2.5 Polymer blend [28-30]

A polymer blend is a mixture of two or more polymers that have been blended together to create a new material with different physical, chemical and mechanical properties. Generally, there are five main types of polymer blend; thermoplastic–thermoplastic blends, thermoplastic-rubber blends, thermoplastic-thermosetting blends, rubber–thermosetting blends and polymer-filler blends, all of which have been extensively studied. Polymer blending has attracted much attention as an easy and cost-effective method of developing polymeric materials that have versatility for commercial applications. In other words, the properties of the blends can be manipulated according to their end uses by correct selection of the component polymers.

Nowadays, the market competition is so high. Therefore, producers of plastics are required to provide better and more economic materials with superior combinations of properties as a replacement for the traditional metals and polymers.

Extent of mixing is related to time as mixing requires sufficient time to allow the polymer chains to mix. Thus, for miscible blends particular structures can be "frozen in" by rapid cooling when the desired mixing is achieved. Miscibility or immiscibility can be described in simple thermodynamic terms in the following equation (2.2).

$$\Delta G_m = \Delta H_m - T\Delta S \quad (2.2)$$

When, ΔG_m = Gibbs free energy of mixing (J/mol)

ΔH = Enthalpy of mixing (J)

ΔS_m = Entropy of mixing (J)

T = Temperature (K)

Mixing is exactly analogous with polymer solubility. The driving force for mixing and solubility is the entropy or random-related term. The entropy-related term must overcome the opposing enthalpy energy term. In a more complete treatment, temperature and volume fraction must be considered. Generally, polymer blend can be divided into two categories.

1. Miscible blend

Polymer blend is homogeneous down to the molecular level associated with the negative value of the free energy of mixing; $\Delta G_m \sim \Delta H_m < 0$. Normally, amorphous polymers can be mixed to be miscible blend easier than semi-crystalline polymers. This is because amorphous polymer has higher disorder chains, resulting in high entropy (ΔS_m) and hence miscible mixing can occur. In some cases, special attractions allow polymers to be miscible.

Generally, miscible blends will have properties somewhere between those of the unblended polymers. These properties will be dependent on the ratio of the two polymers and this ratio is often used to obtain a particular property. These properties include mechanical, chemical, thermal, weathering, etc. However, most of polymer blends prefer to be immiscible blend because of the positive free energy of mixing; $\Delta G_m \sim \Delta H_m > 0$.

2. Immiscible blends

The polymers cannot be truly mixed together. They exhibit phase separation. In general, the morphology on a molecular level varies with the fraction of each component in the blends. In general term, there are a continuous phase (matrix) and a discontinuous phase (dispersed phase). For a combination of polymer A and B, at low amount of A, polymer A typically acts as a discontinuous phase with spherical form surrounded by B. As the fraction of polymer A increases, the spheres eventually become so large and coalesce together forming cylinder, lamellae, and hence two continuous phases are present. As the fraction of A continues to increase, polymer B becomes the discontinuous phase surrounded by the continuous phase of polymer A. Morphologies of proportions of polymers as shown in Figure 2.4.

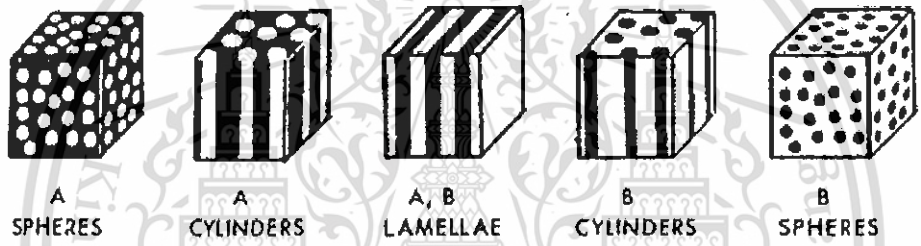

Figure 2.4 Morphologies of polymer blends by increasing ratio of polymer A/B [31]

The discontinuous phase generally reveals the rough shape of the sphere to minimize the exposure of surface area to another phase. The size of the spheres influences the overall properties and varies with concentration. Larger sphere sizes are promoted because they give less relative contact area with another phase. The small dispersed phase size indicates that compatibility of polymer blend is increased.

Generally, miscible (single phase) blends are usually optically transparent and are homogeneous to the polymer segmental level. For example, polystyrene (PS)/ poly(phenylene oxide) (PPO) and poly(styrene-acrylonitrile) (SAN)/polymethyl methacrylate (PMMA) are miscible blends, while polypropylene (PP)/PS and PP/polyethylene (PE) are immiscible blends.

2.6 Polymer

2.6.1 Linear low density polyethylene [32-34]

Linear low density polyethylene (LLDPE) is a thermoplastic polymer. It can be produced under pressure less than 300 psi at 100°C. The production of LLDPE is initiated by transition metal catalysts, particularly Ziegler-Natta (Figure 2.5) or Philips catalyst. The actual polymerization process can be done either in solution phase or in gas phase reactors. Usually, octene is the comonomer in solution phase while butene and hexene are copolymerized with ethylene in a gas phase reactor. LLDPEs do not contain the long branches in comparison with LDPEs. The structure of LLDPE is shown in Figure 2.6.

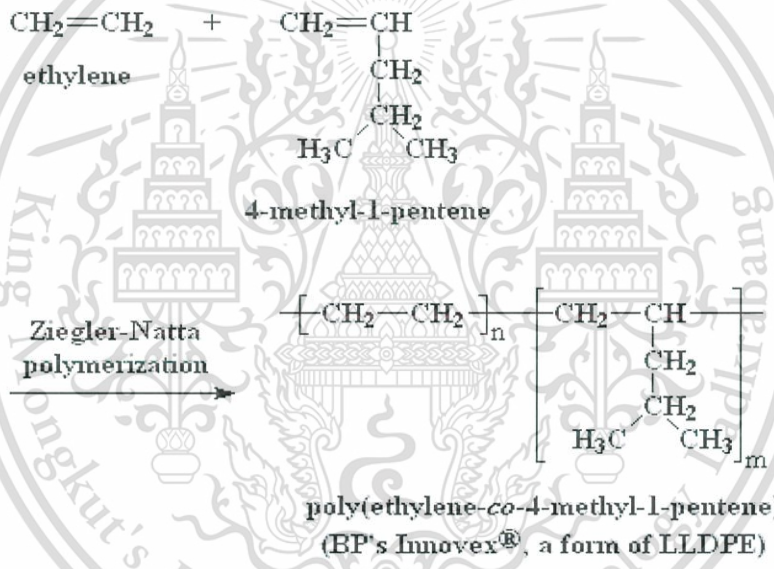

Figure 2.5 Polymerization of LLDPE using Ziegler-Natta [33]

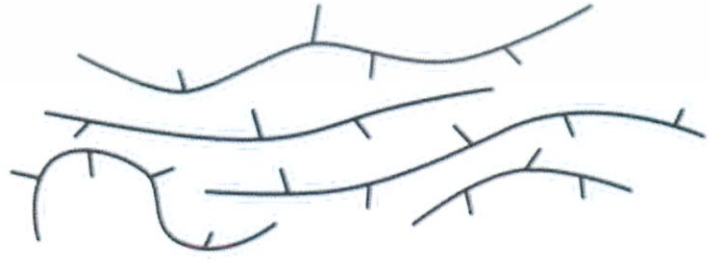

Figure 2.6 Structure of LLDPE [35]

2.6.1.1 Properties of LLDPE

LLDPE has tensile strength, impact and puncture resistance higher than LDPE. It is very flexible and elongates under stress. It can be used to make thinner films, with better environmental stress cracking resistance. It has good resistance to chemicals and good electrical properties. Example of LLDPE properties are listed in Table 2.4.

Table 2.4 Example of LLDPE properties [32]

Property	Value
Density	0.915 g/cm^3
Surface hardness	SD48
Tensile strength	30 MPa
Flexural modulus	0.35 GPa
Notched izod	1.06 kJ/m
Linear expansion	20×10^{-5}/°C
Elongation at break	500%
Strain at yield	20%
Water absorption	0.01%
Oxygen index	17%
Flammability UL94	HB
Volume resistivity	10^{16} Ω·cm
Dielectric strength	25 MV/m
Dielectric constant 1 kHz	2.3
HDT @ 0.45 MPa	45°C
HDT @ 1.80 MPa	37°C
Material drying	NA
Melting temperature Range	120 to 160°C
Mould Shrinkage	3%
Mould temperature range	22 to 60°C

LDPE and LLDPE have unique rheological or melt flow properties. LLDPE is less shear sensitive because of its narrower molecular weight distribution and shorter chain branching. During a shearing process, such as extrusion, LLDPE remains more

viscous and, therefore, its fabrication is more difficult than LDPE of equivalent melt index. The lower shear sensitivity of LLDPE allows for a faster stress relaxation of the polymer chains during extrusion. Thus, the physical properties are susceptible to changes in blow-up ratios. In melt extension, LLDPE has lower viscosity at all strain rates. This means that it will not exhibit strain harden as the way LDPE does when elongated. As the deformation rate of the polyethylene increases, LDPE demonstrates a dramatic rise in viscosity because of chain entanglement. This phenomenon is not observed with LLDPE because of the lack of long-chain branching in LLDPE that allows the chains to slide by one another upon elongation without becoming entangled. This characteristic is important for film applications because LLDPE films can be down gauged easily while maintaining high strength and toughness. The rheological properties of LLDPE are summarized as "stiff in shear" and "soft in extension".

2.6.1.2 Applications of LLDPE

LLDPE has penetrated almost all traditional markets for polyethylene; it is used for plastic bags and sheets (where it allows using lower thickness than comparable LDPE), plastic wrap, stretch wrap, pouches, toys, covers, lids, pipes, buckets and containers and covering of cables. In addition, LLDPE can be recycled into various types of products; for example, trash, can liners, lumber, landscaping ties, floor tiles, compost bins and shipping envelopes.

2.6.2 Maleic anhydride grafted polyethylene [36-37]

Maleic anhydride grafted polyethylene (PE-g-MA) can be generated from addition polymerization using peroxide as an initiator. The chemical bonding is formed between free radical chain end of polyethylene and maleic anhydride. Structure of PE-g-MA is shown in Figure 2.7. The PE-g-MA has been applied for assisted bonding of polar to non-polar substances. Besides, it can be introduced as a compatibilizer for polymer blends.

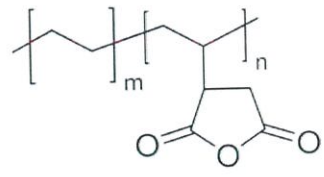

Figure 2.7 Structure of PE-g-MA [37]

Typically, PE-g-MA is introduced as a compatibilizer in PE and polar filler system. For example, an addition of PE-g-MA in the PE/$CaCO_3$ leads to good compatibility and entanglement of PE and $CaCO_3$. This is because of an interaction between $CaCO_3$ and maleic anhydride functional group.

2.6.3 Styrene ethylene-butylene styrene block copolymer [38-41]

Styrene ethylene-butylene styrene (SEBS) is a triblock copolymer which is one type of styrenic block copolymer. Figure 2.8 shows a typical structure of SEBS. The styrene end-blocks are hard polymers. The mid-block consists of rubbery polymer that is ethylene-butylene block.

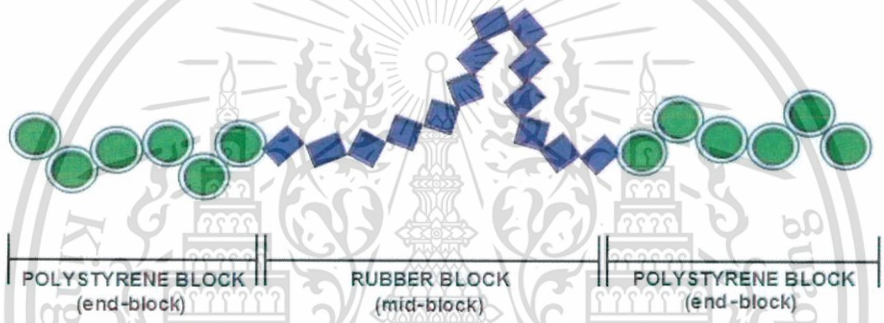

Figure 2.8 Schematic drawing of a linear styrenic triblock copolymer [39]

SEBS has two glass transition temperatures (T_g), an upper one of about 95°C for the polystyrene domains and a lower one of about -55°C for ethylene-butylene blocks. This two-phase structure gives SEBS high strength at end-use temperatures and also provides low viscosity. Moreover, it can be easily processed at elevated temperatures.

SEBS is high performance thermoplastic elastomers (TPEs) designed for use without vulcanization. It has fully saturated mid-blocks for the ultimate in stability, which is high resistance to degradation by oxygen, ozone and UV light. SEBS combines high elasticity and low temperature flexibility with resistance to water, acids and alkalis. In addition, SEBS gives the highest in tensile strength comparing to other TPEs. Because of their better thermal stability, SEBS compounds are used for more demanding applications in all market segments. One key application is a grip where the soft touch, anti-slip properties, good resistance to oil and grease are

required. Moreover, SEBS possesses major properties including transparency and easy to color, soft touch, high tear strength and elasticity, excellent surface appearance, non-slip and low hardness (down to 5 Shore A).

2.7 Zeolite

2.7.1 Structure of zeolite [42-44]

Zeolite structures consist of silica and alumina tetrahedral, that is silicon (Si^{4+}) or aluminum ions (Al^{3+}) surrounded by four oxygen ions (O^{2-}) in a tetrahedral configuration. This is called a primary unit. Each oxygen anion is bonded to two adjacent silicon or aluminum ions. When many primary units are connected together, there are many secondary building units (SBUs) formed. The common SBUs are shown in Figure 2.9. The SBUs are connected to form polyhedral units that are further linked to build up the entire framework. Structure from 4-membered rings and 6-membered rings are shown in Figure 2.10.

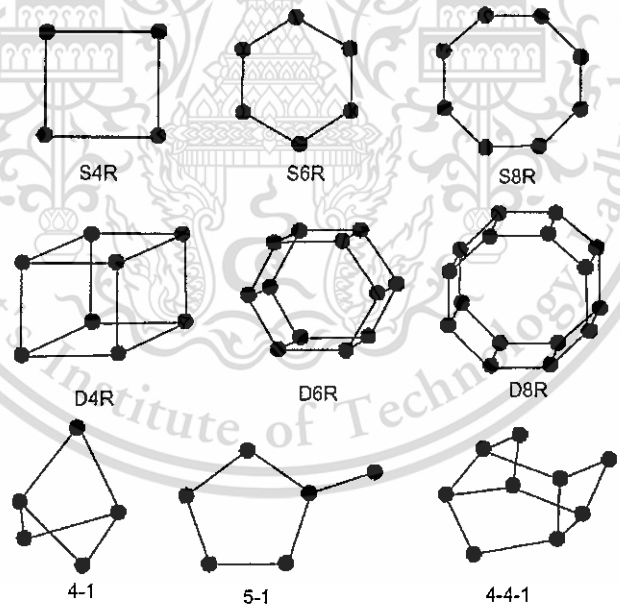

Figure 2.9 Secondary building units (SBUs) in zeolite [45]

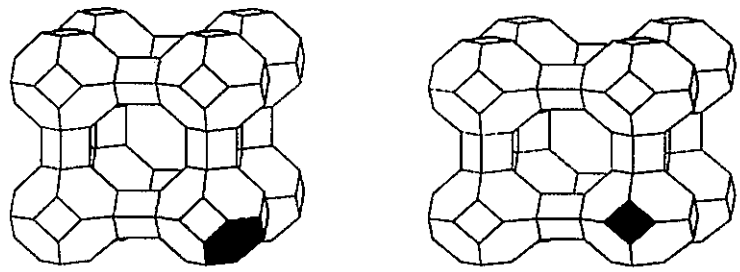

Figure 2.10 Zeolite structure of (a) 6-membered rings and (b) 4-membered rings [46]

The diameters of the pores and cavities range from 3 Å to 12 Å, which coincides with the dimensions of many hydrocarbon molecules for which they are applied as adsorbents and catalysts. The exact diameter of the pore depends on the amount of cations present in the ring.

2.7.2 Zeolite ZSM-5 [43, 47-49]

Zeolite ZSM-5 (also known as MFI) is an aluminosilicate zeolite with a high silica and low aluminium contents (high Si/Al ratio). It is composed of several pentasil units linked together by oxygen bridges to form pentasil chains as shown in Figure 2.11. A pentasil unit consists of eight five-membered rings. In these rings, the vertices are Al or Si and O that is assumed to be bonded between the vertices. The structure of ZSM-5 is a channel framework that provided by 10-membered rings, as represented in Figure 2.12.

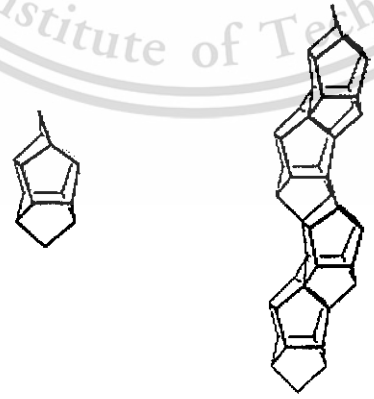

Figure 2.11 Pentasil unit and pentasil chain [50]

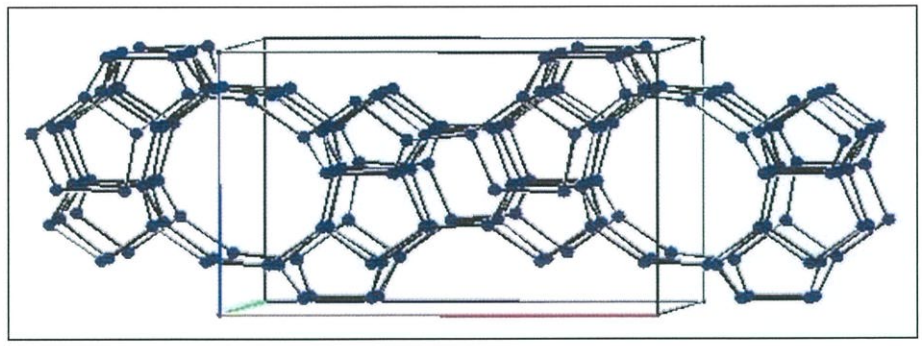

Figure 2.12 Framework structure of zeolite ZSM-5 [47]

Zeolite ZSM-5 has estimated pore size of the channel running parallel with 5.4-5.6 Å. This size is approximately in the dimensional range of aromatic molecules, so that zeolite ZSM-5 has a high shape-selectivity in catalytic reaction. Additionally, its broad range SiO_2/Al_2O_3 (30-100) makes ZSM-5 useful for various applications.

2.7.3 Zeolite as adsorbent [43, 51-52]

Zeolite is a microporous material having high surface area. The pores of zeolite are precisely uniform in size and molecular dimensions. Its porous structure can be used to sieve molecules having certain dimensions and smaller than that of the pores size. Depending on the size of these pores, molecules may be readily adsorbed, slowly adsorbed or completely excluded. The selectivity in sieving is also based on polarity of the zeolite and the sieved molecule; for instance, hydrocarbon is a hydrophobic molecule that prefers hydrophobic zeolite (high Si/Al). Due to their unique characteristics, zeolites are commercially used for drying and purifying liquids and gases, and for various industrial separation processes. Other applications of zeolite adsorption are listed in Table 2.5.

Table 2.5 Application of zeolite adsorption [53]

Application	Zeolite
Removal of water from natural gas	NaA
Adsorption of water from organic solvent	KA
Adsorption of VOC from water	Silicalite
Separation of So_x, NO_x from air	Silicalite
Separation of H_2S from natural gas	CaA
Separation of n-butane/i-butane	MFI

2.8 Silane coupling agent [54]

Silane coupling agents are silicon-based chemicals that contain two types of reactivity (inorganic and organic) in the same molecule. A typical general structure is X_3-Si-R. Where X is an organic functional group such as amino, chlorine, methacryloxy, epoxy, methoxy, ethoxy or acetoxy and R is a hydrocarbon group such as methyl, ethyl, octadecyl etc.

In general, silane coupling agent locates at an interface between an inorganic substrate (such as glass, metal or mineral) and an organic materials (such as an organic polymer, coating or adhesive) in order to bond or couple those two dissimilar materials. A simplified mechanism of the coupling is shown in Figure 2.13.

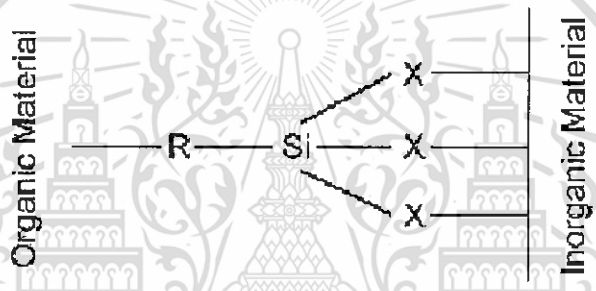

Figure 2.13 The silane coupling mechanism [55]

2.8.1 Chlorosilane [56-57]

Chlorosilane is a group of reactive, chlorine-containing silicon compounds. Each compound has at least one silicon-chlorine bond. Usually chlorosilanes are intermediates that are not only used to produce siloxane and silane but also used as protecting agent for intermediates in pharmaceutical syntheses. Most of chlorosilanes are clear liquids that react with water to form corrosive and toxic hydrogen chloride gas and hydrochloric acid.

Silicon tetrachloride ($SiCl_4$) and trichlorosilane ($HSiCl_3$) are intermediates in the production of ultrapure silicon in the semiconductor industry. Chlorosilanes obtained from crude silicon are purified by fractional distillation techniques and then reduced with hydrogen to give silicon of 99.9% purity.

Organic chlorosilanes are frequently applied as coatings for silicon and glass surfaces, and in the production of silicone (polysiloxane) polymers. In this work,

octadecyltrichlorosilane (OTS) was selected as a coupling agent and its structure is shown in Figure 2.14.

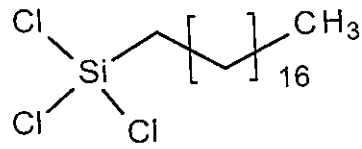

Figure 2.14 Structure of octadecyltrichlorosilane (OTS) [57]

2.8.2 Aminosilane [58]

Aminosilane is an amino-functional silane that may be utilized over a broad range of applications to give an improvement of bonding between substrates, fillers or reinforcements and resins that react via the amino group.

Aminosilane is an adhesion promoter, coupling agent and resin additive. It can improve chemical bonding of resins to inorganic fillers and reinforcing materials. Aminosilane is especially recommended for thermoplastic resins and thermosetting resins such as epoxy, polyethylene, phenolics, melamines, nylons, PVC, acrylics, polyolefins, polyurethanes and nitrile rubbers, etc. It can enhance mechanical, and physical properties; for example, flexural strength, compression strength and shear strength. In addition, it can also improve the dispersion and wettability of filler in the high molecular materials. In this work, 3-aminopropyltriethoxysilane (APS) was chosen to be a coupling agent and structure of APS is shown in Figure 2.15.

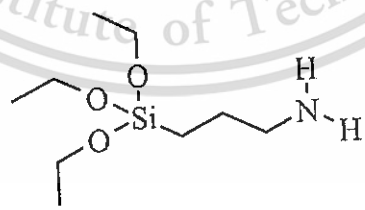

Figure 2.15 Structure of 3-aminopropyltriethoxysilane (APS) [58]

2.9 Literature reviews

Ethylene gas is a plant hormone that can accelerate the ripening process of vegetables and fruits in the climacteric group. In addition, ethylene gas causes

discoloration, odor and a decrease in nutritional value of vegetables and fruits [2]. Therefore, in order to delay the ripening process during storage and transportation, the packaging of those vegetables and fruits should be able to reduce accumulation of the ethylene gas produced.

In the past, a control of specific gases within a package can be achieved by the use of chemicals to adsorb an active gas (ethylene). Activated carbon, clay and zeolite are used to be the ethylene adsorbents [59]. Ethylene can be removed by adsorption and desorption. It was reported that potassium permanganate ($KMnO_4$) is commonly used to adsorb ethylene gas in packaging [60-61]. However, $KMnO_4$ cannot be applied directly to the food packaging, but can be only supplied in a small bag because $KMnO_4$ is toxic and shown a purple color. It can contaminate fresh produces and hence affect on human health.

Alternatively, a dispersion of minerals such as clay and zeolite into packaging films can be applied for the modified atmosphere packaging (MAP). MAP concept, low oxygen content in the package leads to a decrease in respiration rate and ethylene accumulation after harvesting. Furthermore, high carbon dioxide can inhibit the ethylene action [62].

Monprasit P. [63] developed the composite double-layered film to improve the ethylene permselectivity and tensile properties for the packaging application of fresh fruits and vegetables. The double-layered film was prepared by laminating LDPE and SEBS modified with zeolite ZSM-5. The zeolite loading is 5-30%wt of SEBS with surface rich zeolite (DB-SR) and with well dispersed zeolite (DB-WD) morphologies. The double-layered film was tested for permeation of ethylene, oxygen, carbon dioxide and water vapor. It was found that the ethylene permeability of the double-layered films (DB-SR) enhanced from 1,793 to 2,064 $cm^3.mm/m^2.day.atm$ due to a readily adsorption of ethylene gas by contained zeolite from 0 to 10%wt. This leads to a higher ethylene concentration gradient across the film which becomes a driving force for ethylene permeation. Moreover, the high dispersion of 10%wt zeolite increased the ethylene permeation up to 2,328 $cm^3.mm/m^2.day.atm$. It was also observed that there is no significant difference in ethylene permeation when zeolite contents were higher than 10%wt because the LDPE is a barrier phase. Therefore, reducing barrier property of LDPE is an interesting option to improve ethylene permeability.

Wiwattananukul R. [4] prepared the LLDPE/SEBS blend films for packaging films with improving ethylene permeability. The factors affecting properties of the LLDPE/SEBS blend films were investigated such as the mixing machine and condition, blend composition and grade of SEBS. It was found that mechanical properties and permeability of the LLDPE/SEBS blend films were similar when using either a twin-screw extruder or an internal mixer for LLDPE/SEBS compounding at the same condition (190°C, 60 rpm). A decrease in mixing speeds (from 80 to 40 rpm) in the internal mixer resulted in enlarged SEBS dispersed phase size, leading to higher ethylene permeability. An increase in SEBS content generally increased amorphous phase and hence ethylene permeability. In addition, the LLDPE/SEBS blend film at 72/28 w/w with SEBS G1657 gave dispersed phase sizes of SEBS larger than that with SEBS G1652 (Figure 2.16). This is because the ethylene-butylene in SEBS G1657 is 87%wt while that in SEBS G1652 is only 70%wt. Accordingly, the ethylene transmission rate of the film largely increased from 8,207 to 28,411 cm^3/m^2.day.atm.

Figure 2.16 SEM micrographs of cross-section area of LL72S28 (G1652) and LL72S28 (G1657) after SEBS extraction at 3,500x magnification [4]

Hongthong K., et.al. [5] prepared the LLDPE/SEBS blend film with SEBS G1657 and LLDPE/SEBS/zeolite ZSM-5 (Si/Al = 180) blend film for improving ethylene gas permeation in packaging applications. Polymer blends were compounded using an internal mixer and varied LLDPE/SEBS blend ratios at 100/0, 80/20, 75/25 and 70/30 w/w. Thereafter, the films were shaped by compression molding. Mechanical properties, thermal properties, morphology and ethylene transmission rate (ETR) were studied. Figure 2.17 shows that the blend film with a 70/30 ratio gave the

highest ETR due to the largest size of SEBS dispersed phase (Figure 2.18). In addition, ethylene permeation of the film increased when increasing zeolite ZSM-5 content (Figure 2.19). The results from SEM exhibited that zeolite could be dispersed in SEBS better than LLDPE because SEBS has polarity comparatively higher than LLDPE.

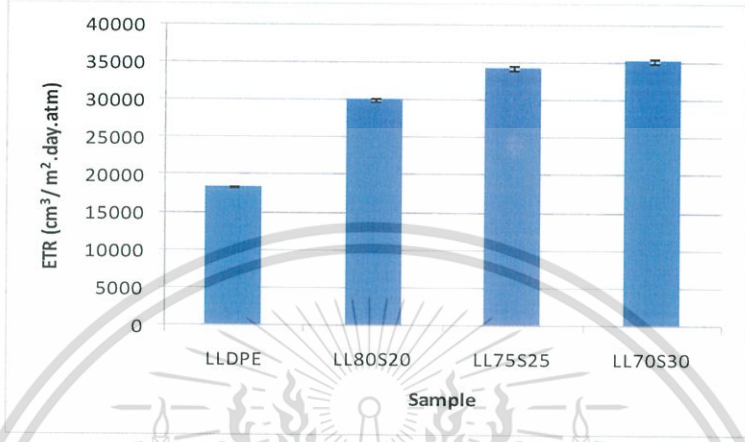

Figure 2.17 Ethylene transmission rate of the LLDPE/SEBS blend film with various SEBS loadings [5]

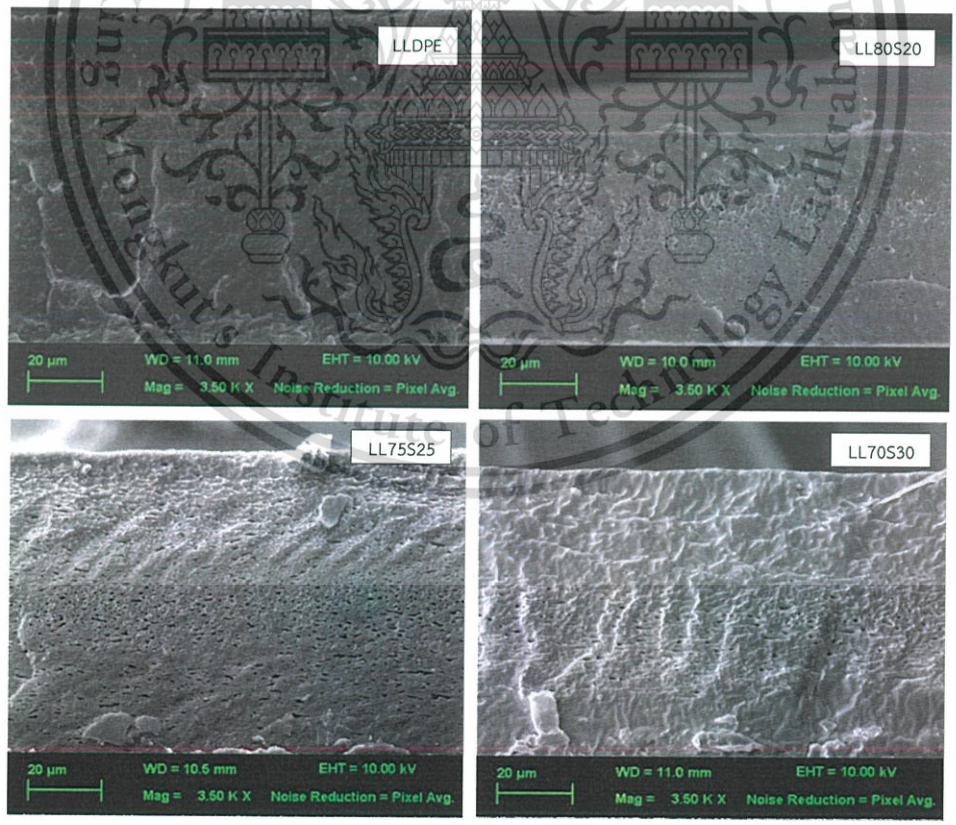

Figure 2.18 SEM micrographs of cross-section area of LLDPE/SEBS blend film with various SEBS loadings after SEBS extraction at 3,500x magnification [5]

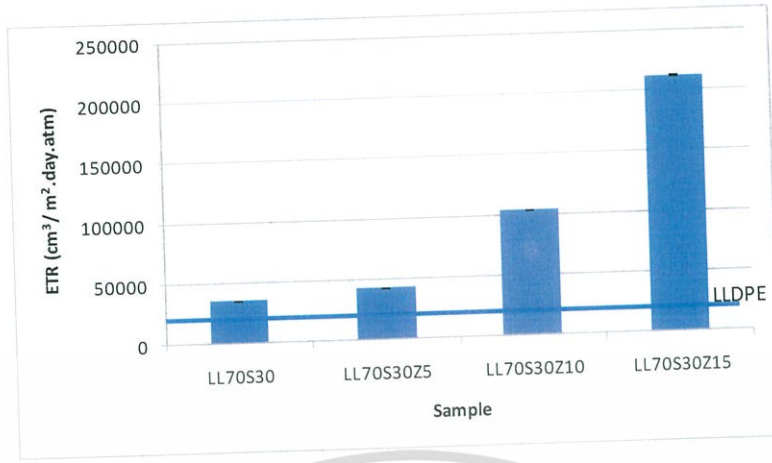

Figure 2.19 Ethylene transmission rate of the LLDPE/SEBS/zeolite ZSM-5 blend film at 0-15%wt loadings [5]

Sirikittikul D. et.al [64] prepared chemical modification of zeolite beta (BEA) with a series of organosilane compounds $[R(CH_3)_nSiX_{(3-n)}]$, where X is a chloro or alkoxy group with n=0 and 2, and R is an alkyl chains varying from CH_3 to $C_{18}H_{37}$. The hydrophobic characteristic of the unmodified and surface grafted BEA as determined by preferential dispersion in the biphasic water/n-heptane medium was examined. The polymer matrix was an elastomeric block copolymer of styrene-b-(ethylene-ran-butylene)-b-styrene (G1652). The membranes were prepared by casting the mixture on glass plates and the BEA particles was adjusted to 10%wt of the dry polymer. The results suggest that the alkyl chain introduced on the BEA surface was sufficiently hydrophobilized on the surface, independent of the chain length. The hydrophobic particle surface promoted homogeneous distribution and particles/polymer adhesion, which would significantly improve the permselectivity of the mixed matrix membranes developed. Accordingly, the membranes containing the BEA grafted with long chain length i.e. $C_{16}H_{33}$ and $C_{18}H_{37}$ showed higher CO_2 permeability than those containing the BEA grafted with shorter chain length. The membranes having the BEA grafted with C_3H_7 to $C_{18}H_{37}$ showed a great improvement of CO_2 permeability, while O_2 and C_2H_4 permeabilities significantly unchanged.

Sahassanon T. [6] reported on LLDPE/SEBS/Zeolite Y blends for selective ethylene permeation of packaging film. The LLDPE/SEBS blend film at 70/30 weight ratio was successfully improved ethylene gas permeation when zeolite Y was added. The LLDPE/SEBS films with 5 %wt filler loading (Zeolite Y, calcium carbonate and

silica) were prepared for comparing with the LLDPE/SEBS blend film. It was found that the 5%wt filler-filled film gave tensile strength and %elongation at break lower than the blend film without filler. This is due to the poor compatibility between polymers and solid particles. When comparing of the filler-filled films, the LLDPE/SEBS blend film with 5%wt silica gave the lowest tensile properties because silica has very poor dispersion and distribution in the film. The 5%wt zeolite Y-filled film gave ETR higher than the 5%wt calcium carbonate-filled film because zeolite Y is porous material and selective with ethylene gas. In addition, the surface of zeolite Y was modified for lower polarity or higher hydrophobicity using organosilanes two types: ethyltrichlorosilane (ETS) and octadecyltrichlorosilane (OTS). The LLDPE/SEBS film incorporated with ETS or OTS-modified zeolite Y revealed a better dispersion of modified zeolite Y, as compared with that containing unmodified zeolite Y. This is because the modified zeolite Y became hydrophobic, resulting in a better compatibility with LLDPE and SEBS, and so a greater tensile strength of the film (Figure 2.20). Moreover, the modified zeolite Y-filled film possessed greater ethylene permeability because a better zeolite dispersion could reduce diffusion pathway of ethylene gas. Using the different chain lengths of alkyl silane in modification of zeolite Y, it was found that the LLDPE/SEBS blend film incorporated modified zeolite Y with a long alkyl chain length ($C_{18}H_{37}$) exhibited tensile strength and ethylene permeability higher than that with the short chain length (C_2H_5).

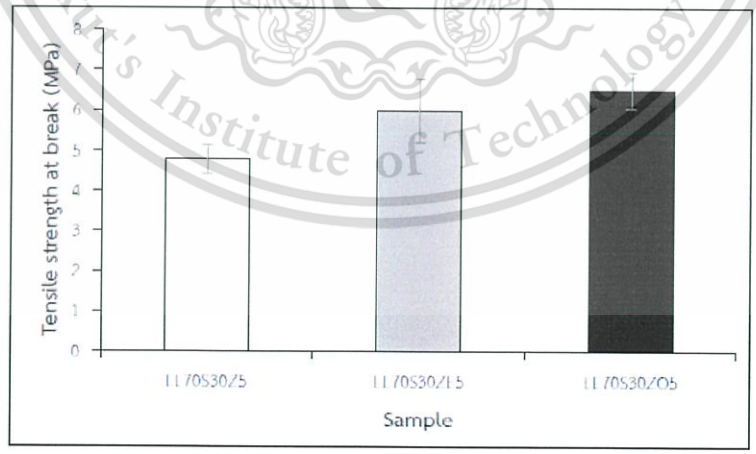

Figure 2.20 Tensile strength at break of LLDPE/SEBS films with 5%wt modified and unmodified zeolite Y [6]

Qiao B. et.al [65] modified silica surface with 3-aminopropyltriethoxysilane (APS). The chemical states of the unmodified and APS-modified silica were analyzed by XPS. It was found that binding energies of Si 2p and O 1s in unmodified silica were 103.6 eV and 532.8 eV, respectively, while binding energies of Si 2p and O 1s in APS-modified silica were shifted to 102.8 eV and 532.1 eV, respectively. A decrease in binding energy indicated that the chemical bond on the surface was changed from Si-O-H to Si-O-Si. Surface modified silica could be used as filler in rubber and plastic to increase tensile strength and abrasion resistance and to improve rheological behavior.

Shokri E. et.al [66] prepared neat and compatibilized high density polyethylene (HDPE) and ethylene vinyl acetate (EVA) blend membranes via thermally induced phase separation method. PE-g-MA compatibilizer was used to improve HDPE/EVA blend compatibility and the special effects of PE-g-MA on the HDPE/EVA membrane structure and performance were investigated. It was found that the mechanical strength of compatibilized blend membrane was improved. This phenomenon was mainly due to the effect of co-crystallization of HDPE and EVA molecules in which, the addition of compatibilizer efficiently improved the blend compatibility, resulting in suitably operational characteristics of membrane. As a result, the fabrication of HDPE/PE-g-MA/EVA blend membrane showed a promising improvement in membrane material to prepare efficient, high permeable, good mechanical resistant, less fouling and very cheap polymer membrane.

From the previous researches, the LLDPE/SEBS G1657 blend film at 70/30 weight ratio gave an acceptable tensile strength and the highest ethylene transmission rate (ETR) due to the largest size of SEBS dispersed phase. Moreover, zeolite was filled in polymer blend for increasing ethylene permeability. So the LLDPE/SEBS blend film at 70/30 weight ratio with zeolite ZSM-5 (Si/Al = 15-infinity) was studied. Zeolite ZSM-5 has polarity lower than zeolite Y (Si/Al = 1.5-3) so that zeolite ZSM-5 is more selective for ethylene adsorption. However, zeolite ZSM-5 surface is relatively polar, as compared to the polymers, leading to poor compatibility between zeolite and polymers. Therefore, zeolite ZSM-5 surface was functionalized with OTS and APS/PE-g-MA for improving zeolite surface to be hydrophobic. When hydrophobicity of zeolite is increased, a better compatibility with polymer should be obtained. Thus more zeolite particles could be dispersed in

LLDPE phase and this would reduce gas barrier property of LLDPE in the blend. As previous reports, the ethylene permeation of the film was higher when increasing of zeolite loading, the effect of zeolite content (5-15%wt) in the LLDPE/SEBS films were examined.

Chapter 3

Research methodology

3.1 Chemicals and materials

1. Linear low density polyethylene (LLDPE): DOW™ Butene 1220G1, The Dow Chemical Co., Ltd.

Table 3.1 Specification of LLDPE DOW™ Butene 1220G1 [67]

Property	Value
Melt flow index (190°C, 2.16 kg), g/10 min	2.0
Density, g/cm^3	0.919
Dart drop impact (D1709), g	175
Tear resistance (D1922)	
Machine direction (MD), g	107
Transverse direction (TD), g	218

2. Poly(styrene-ethylene/butylene-styrene) (SEBS): Kraton®G1657, Kraton Performance Polymers, Inc.

Table 3.2 Specification of SEBS Kraton® G1657 [68]

Property	Value
Styrene content, %wt	12.3 to 14.3
Melt flow rate (230°C, 5 kg), g/10 min	22.0
Specific gravity	0.900
Viscosity (Solution in toluene 20%wt and 25°C), cP	1200 to 1800
Elongation at break, %	750
Tensile strength, psi	3400
300% Modulus, psi	350
Hardness shore A, 10 s	47

3. Zeolite ZSM-5: CBV 28014, Zeolyst International, Inc.

Table 3.3 Specification of zeolite ZSM-5 [69]

Property	Data
SiO_2/Al_2O_3	280
Nominal cation form	Ammonium
Na_2O weight, %wt	0.05
Surface area (BET), m^2/g	400
Specific gravity	> 1

4. Maleic anhydride grafted linear low density polyethylene (LLDPE-g-MA): SCONA® TSPE 1112 GALL, BYK Additives and Instruments

Table 3.4 Specification of LLDPE-g-MA [70]

Property	Value
Maleic anhydride content, %wt	2.0
Melt flow index (190°C, 5 kg), g/10 min	5.0
Drying loss (3 h, 110°C), %wt	0.5

5. Octadecyltrichlorosilane (OTS) (>90%): Sigma-Aldrich Co., Ltd.
6. 3-aminopropyltriethoxysilane (APS) (99%): Thermo Fisher Scientific Inc.
7. Toluene (Analytical grade): Thermo Fisher Scientific Inc.
8. Xylene (Analytical grade): Thermo Fisher Scientific Inc.
9. Ethanol (Analytical grade): Thermo Fisher Scientific Inc.
10. Ethanol (Commercial grade): Thermo Fisher Scientific Inc.
11. Methanol (Analytical grade): Thermo Fisher Scientific Inc.
12. Tetrahydrofuran (THF) (Analytical grade): Thermo Fisher Scientific Inc.
13. Air zero (Purity 99.9%): Praxair (Thailand) Co., Ltd.
14. Nitrogen gas (Purity 99.99%): Praxair (Thailand) Co., Ltd.
15. Nitrogen gas (Purity 99.5%): Praxair (Thailand) Co., Ltd.
16. Helium gas (Purity 99.9%): Praxair (Thailand) Co., Ltd.
17. Carbon dioxide, (Purity 99.9%): Thai Industrial Gases Co., Ltd.
18. Ethylene (C_2H_4) gas, (Purity 99.9%): Thai Industrial Gases Co., Ltd.

19. Standard Carbon dioxide: Thai Industrial Gases Co., Ltd.
20. Liquid nitrogen
21. Distilled water

3.2 Apparatus

1. Internal mixer (PL2000/PL2001): C. Melchers & Co. (Thailand) Ltd.
2. Plastic grinder (Bosco A600): Bosco Engineering Co., Ltd.
3. Compression molding machine (MGLP 20 AT): Machgroup (1992) Co., Ltd.
4. Universal testing machine (LR 5K): LLOYD Instrument Ltd.
5. Field emission scanning electron microscope (JSM-7001F): JEOL Co.,Ltd.
6. Differential scanning calorimeter (DSC 204 F1 Phoenix): Netzsch Co., Ltd.
7. Thermogravimetric analyzer (TG 209): Netzsch Co., Ltd.
8. X-ray photoelectron spectrophotometer (AXIS ULTRA): Kratos Analytical Ltd.
9. Dynamic mechanical analyzer (Rheogel-E4000): UBM Co., Ltd.
10. Cone-and-plate rheometer (AR 2000ex): TA Instruments Ltd.
11. Permeation rig
12. Permeation cell
13. Thermal conductivity detector: Valco Instruments Co., Inc.
14. Hotplate and thermocouple
15. Magnetic stirrer (ST 1200): Scilution Co., Ltd.
16. Ultrasonic bath (KLSC09): Labquip International Co., Ltd.
17. Centrifuge (1000 serie): Centurion Scientific Ltd.
18. Water aspirator with suction flask and buchner funnel
19. Nylon filter
20. Micrometer
21. Laboratory glassware
22. Tube furnace: Vecstar Ltd.
23. Oven (UN 500): Memmert (Germany) Co., Ltd.

3.3 Zeolite ZSM-5 modification

3.3.1 Preparation of modified zeolite ZSM-5

- Modification with OTS [7]

2 g of the zeolite ZSM-5 was charged in a 250 ml erlenmeyer flask containing 40 ml of toluene before placing in an ultrasonic bath for 1 h in order to disperse zeolite. A 400 µl of OTS was dissolved in 100 ml of toluene in another erlenmeyer flask. Then the prepared organic solution was added in the zeolite suspension flask. The mixture was stirred using a magnetic stirrer at room temperature for 24 h. The toluene was separated from the modified zeolite ZSM-5 using a centrifuge with a speed of 3500 rpm. The OTS-modified zeolite ZSM-5 was washed several times with ethanol to eliminate the acid residue that was generated after reaction and then was collected by suction filtration with nylon filter (0.22 µm pore size). Finally, it was dried overnight in an oven at 100°C.

- Modification with APS/PE-g-MA

2 g of the zeolite ZSM-5 was charged in a 50 ml evaporating dish. The zeolite was impregnated with a 300 µl of APS in 1 ml of toluene. The mixture was calcined in a tube furnace at 190°C for 12 h under the nitrogen atmosphere. The APS-modified zeolite ZSM-5 was washed two times with hot toluene and then was collected by suction filtration with nylon filter. Finally, it was dried overnight in an oven at 100°C.

Next, 0.1 g of PE-g-MA and 2 g of the APS-modified zeolite ZSM-5 were charged in a 250 ml round bottom flask containing 100 ml of xylene before placing in an oil bath. The mixture was refluxed at 130°C for 24 h under the nitrogen atmosphere. The APS/PE-g-MA-modified zeolite ZSM-5 was precipitated in methanol and then collected by suction filtration with nylon filter. Finally, it was dried overnight in an oven at 100°C.

3.3.2 Characterization of modified zeolite ZSM-5

Binding energy of unmodified and modified zeolite ZSM-5 were conducted using the X-ray photoelectron spectroscopy (XPS). The monochromatic AlKα was used as a source (anode HT = 15 kV). The XPS peaks were referenced to the binding energy of C 1s, O 1s, Si 2p and N 1s peaks at about 285, 533, 103 and 399 eV, respectively. The sample was attached onto a stub with a carbon tape. It was placed in a chamber and the internal pressure was decreased down to 1×10^{-8} torr at room temperature. The quantitative spectrum was collected. The correction of the background due to a carbon substrate was also performed.

3.4 Preparation of polymer blends

The LLDPE/SEBS blends with and without zeolite ZSM-5 were prepared using an internal mixer. The composition of LLDPE/SEBS/zeolite ZSM-5 is listed in Table 3.5. Examples of compound formula are presented in Table 3.6.

Table 3.5 Composition of LLDPE/SEBS/zeolite ZSM-5 blends (LLDPE:SEBS = 70:30)

Formula	Zeolite content (%)	Weight content (g)		
		LLDPE	SEBS	Zeolite
LL70S30	0	28.0	12.0	-
LL70S30Z5	5	26.6	11.4	2.0
LL70S30Z10	10	25.2	10.8	4.0
LL70S30Z15	15	23.8	10.2	6.0
LL70S30ZO5	5	26.6	11.4	2.0
LL70S30ZO10	10	25.2	10.8	4.0
LL70S30ZO15	15	23.8	10.2	6.0
LL70S30ZA5P (60 rpm)	5	26.6	11.4	2.0
LL70S30ZA5P (100 rpm)	5	26.6	11.4	2.0

Table 3.6 Examples of compound formula

Formula	Zeolite	Rotor speed (rpm)
LL70S30	-	60
LL70S30ZX	Unmodified zeolite	60
LL70S30ZOX	OTS-modified zeolite	60
LL70S30ZAXP (60 rpm)	APS/PE-g-MA-modified zeolite	60
LL70S30ZAXP (100 rpm)	APS/PE-g-MA-modified zeolite	100

Note X is designated for the content of zeolite by weight percentage.

P is designated for PE-g-MA 5% of zeolite.

Mixing procedure as follows:

1. LL70S30Z5; LLDPE 26.6 g and zeolite 2.0 g were mixed using an internal mixer at 170°C with a rotor speed of 60 rpm for 20 min.
2. SEBS 11.4 g was filled in the mixer.

3. The mixture of LLDPE/SEBS/zeolite was continuously mixed at 190°C with rotor speed of 60 rpm for 20 min. Then, the polymer blends were crushed with a grinder.

4. LL70S30Z10 and LL70S30Z15 were mixed as the same method with zeolite contents at 10%wt and 15%wt, respectively.

5. LLDPE/SEBS/modified zeolite was mixed following step 1-3.

Remarks: The LL70S30 was prepared using only step 3 with 20 min mixing time.

The LL70S30ZAXP (100 rpm) was compounded using a rotor speed of 100 rpm

3.5 Films preparation

LLDPE/SEBS blend films with and without zeolite were prepared using a compression molding machine. In order to gain uniform thickness, the film was prepared using 2-step compression. First, the compound was compressed to be a sheet with 2 mm thick. Then, the sheet was cut, weighed and compressed to obtain a thin film. The thickness of the films was controlled by charged weight of the blends. The films were prepared into 2 thickness ranges (without a mold spacer):

1. Film for permeation test: film thickness is about 40-60 μm with a diameter 7 cm by weighing sheet of polymer blend about 0.2 g.

2. Film for mechanical test: film thickness is about 60-80 μm with a diameter 10 cm by weighing sheet of polymer blend about 0.7 g.

The compression molding condition is shown as follows (without a spacer):

Mold size	20×20×1 cm^3
Pressure of pressing	1800 psi
Temperature of hot press	190°C
Time of preheating mold	5 min
Time of preheating polymer or sheet	5 min
Time of hot press	5 min
Temperature of cold press	18°C
Time of cold press	5 min

3.6 Characterization

3.6.1 Determination of filler content

The filler content was determined by Netzsch TG 209 thermo-gravimetric analyzer (TGA). Approximately 5-10 mg of a sample was placed in a platinum pan hanging from a microbalance. Nitrogen gas was introduced as a carrier gas from 25°C to 550°C and then air zero was used from 550°C to 700°C at a heating rate of 20°C/min.

3.6.2 Rheological test

Rheological properties of polymer blends were determined using a cone and plate rheometer (AR 2000 EX). Cone and plate geometry was used with a plate radius of 25 mm and a cone angle of 4°. The gap between the cone and plate was set at 103 μm. The sample was heated at 150, 190 and 230°C to measure the rheological properties in the molten state. The shear rate was applied in a range of 0.01-100 s^{-1}.

3.6.3 Dynamic mechanical test

Dynamic mechanical analyzer (DMA, UBM-E4000-DVE) was used to analyze storage modulus, loss modulus and tan δ of samples in dimension of 20 mm long, 5 mm wide and 1 mm thick. DMA was measured in the tension mode at a constant frequency of 10 Hz and heating rate of 2°C/min from -100°C to 120°C.

3.6.4 Determination of morphology

The morphology of LLDPE/SEBS blends with unmodified and modified zeolite ZSM-5 was determined by FE-SEM. To examine filler dispersion, the blend samples were cut to a size of 1×3 cm^2 and soaked in liquid nitrogen for 1 h and then cryogenically cracked. After that the samples were coated with gold by ion sputtering. Field emission scanning electron micrographs were taken at a magnification of 2,000.

In addition, to investigate SEBS dispersion in the blends, THF solvent was used to extract SEBS dispersed phase. The cracked specimens were immersed in a 100 ml beaker having 20 ml of THF solvent and the beaker then was put in an ultrasonic bath (50/60 Hz) for 1.5 h. Thereafter, the extracted specimens were dried at room temperature for 12 h before placing in the oven at 40°C for 48 h. Finally, the samples were gold coated before examining with FE-SEM at a 2,000 magnification.

3.6.5 Determination of melting temperature (T_m), crystallization temperature (T_c) and %crystallinity

The T_m, T_c and %crystallinity of all samples were evaluated by a DSC 204 F1 Phoenix. Approximately 5-10 mg of a sample was placed in aluminum pan. The sample was heated from room temperature to 160°C with a heating rate of 10°C/min in N_2 atmosphere, then cooled down to room temperature with a cooling rate of 10°C/min.

3.6.6 Tensile property test

Tensile properties of the films were examined using a universal testing machine. The tensile properties including tensile strength at break, %elongation at break and Young's modulus were measured according to ASTM D882. The film specimens were cut into a size of 10x80 mm^2 and the tensile testing conditions as follows:

Load cell	100 N
Test speed	100 mm/min
Gauge length	30 mm

3.6.7 Permeation testing

The film size of 6x6 cm^2 was placed in the membrane cell that has the gas permeation area of 5x5 cm^2. Membrane cell consists of two pieces of polypropylene (PP) plates sandwiched with two seal (O-ring) plates and two metal plates as shown in Figure 3.1. The plates were tightened by four screws.

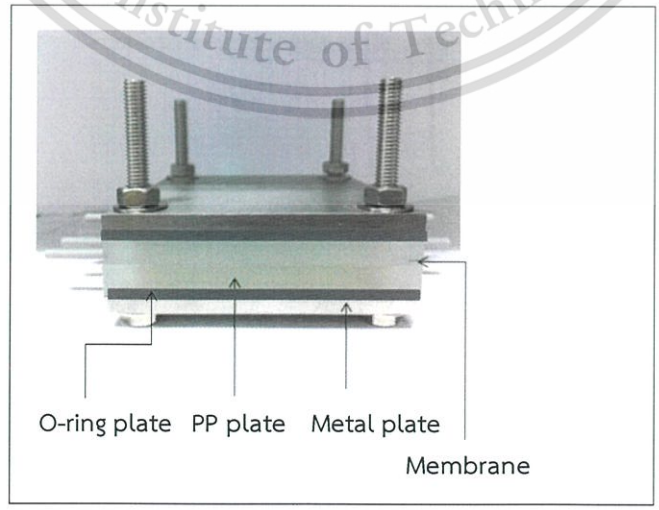

Figure 3.1 Membrane cell of the permeation test

Feed gas (C_2H_4 or CO_2) was flowed into the upper plate (feed side) while carrier gas (Helium) was flowed into the lower plate (permeate side) of the membrane cell with an opposite flow direction. The flow rates of the feed gas and the carrier gas were 30 ml/min. These gases separately controlled using mass flow controllers. As the feed gas flows across the film surface, some of the gas could diffuse through the film to the permeating side. The permeated gas was swept by the carrier gas into the permeate outlet and analyzed by the thermal conductivity detector (TCD). On the other hand, some of gas that could not diffuse through the film and then it was passed to the retentate outlet and vented as shown in Figure 3.2. Diagram of the permeation rig is illustrated in Figure 3.3.

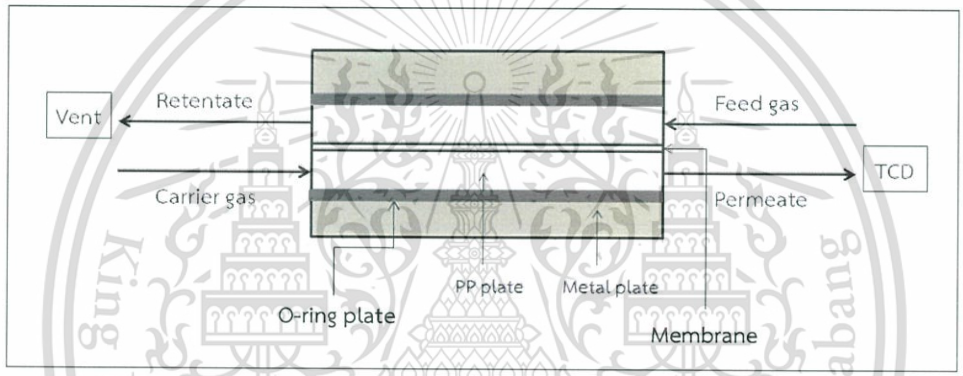

Figure 3.2 Diagram of the permeation test

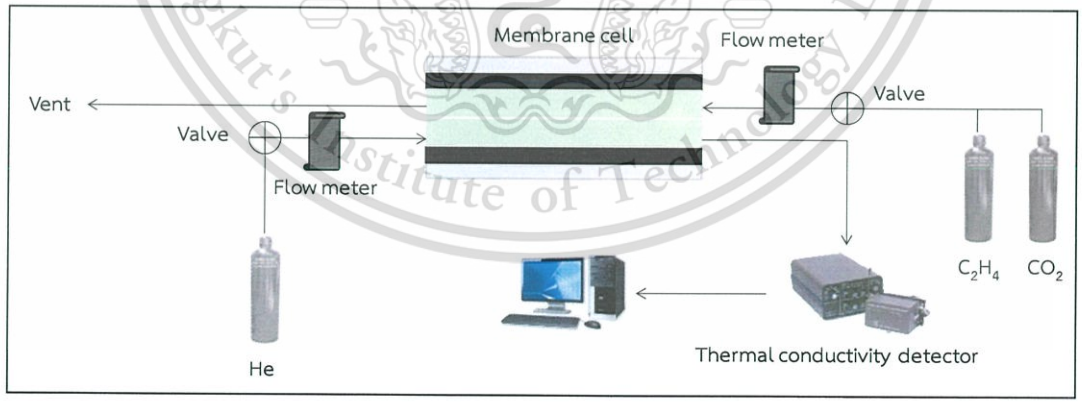

Figure 3.3 Diagram of the permeation rig

Gas permeability of the LLDPE/SEBS blend films with and without zeolite ZSM-5 can be calculated from area under a TCD signal (peak area) that was calibrated with standard gas in the equation 3.1.

Ethylene transmission rate (ETR) = $J / (A_F \times \Delta p_i)$ (3.1)

When J = Transmission rate of ethylene (ml/min)

A_F = Surface area of the film (m^2)

Δp_i = Differential partial pressure (atm)

Feed gas flowed into the system can be calculated in the equation 3.2.

$$J = 10^{-3} \times C_E \times F_x \quad (3.2)$$

When C_E = Concentration of the ethylene in permeated gas (ppm)

F_x = Flow rate of the permeated gas (ml/min)

Concentration of the ethylene in permeated gas can be calculated in the equation 3.3.

$$C_E = C_S \times (A_E / A_S) \quad (3.3)$$

When C_S = Concentration of the standard ethylene (ppm)

A_E = Peak area of the permeated ethylene (V.s)

A_S = Peak area of the standard ethylene (V.s)

Chapter 4
Results and Discussion

This research developed the high ethylene gas permeation film for packaging application. Linear low density polyethylene (LLDPE) and styrene-(ethylene/butylene) -styrene block copolymer (SEBS) were selected as materials for preparing the blend films at a LLDPE:SEBS weight ratio of 70:30. The zeolite ZSM-5 was functionalized with octadecyltrichlorosilane (OTS) and 3-aminopropyltriethoxysilane (APS)/PE-g-MA for increasing compatibility between zeolite and polymers. Factors affecting mechanical properties and permeability of the films were divided in 2 parts; zeolite surface modification and zeolite loading (5-15%wt). The films were characterized for thermal and morphological properties and examined for rheological, dynamic mechanical and ethylene gas permeation properties.

4.1 Effect of modification of zeolite ZSM-5

Effect of modification of zeolite on the properties of the blend films was investigated by preparing the blends with 5%wt zeolite loading. Zeolite was functionalized with OTS and APS/PE-g-MA to reduce the polarity and hence improved the compatibility with polymers.

4.1.1 Characterization of modified zeolite ZSM-5

4.1.1.1 Binding energy of chemical bonds in modified zeolite

The zeolite samples with and without modification were analyzed by XPS. Signals from XPS describe binding energy and intensity of chemical bonds in the sample. The spectra of C 1s, O 1s, Si 2p and N 1s are shown in Figure 4.1. The C 1s signal of the OTS-modified zeolite shows higher intensity than that of the APS-modified zeolite (Figure 4.1 (a)). This is because the number of C atoms of OTS (C-18) is higher than that of APS (C-3). The C 1s signal of the unmodified zeolite is the lowest intensity due to none exist of carbon on the zeolite surface. The C 1s binding energy of the OTS-modified zeolite is observed at 284.60 eV, while binding energy of the APS-modified zeolite shift from 284.60 eV (unmodified zeolite) to 285.00 eV. This is because the electronegativity (EN) of C-N bond is greater than that of C-H bond.

The spectra of zeolite samples show O 1s and Si 2p signals at binding energies of 532.67 and 101.50 eV, respectively related to the Si-O bond (Figures 4.1 (b) and (c)). The modified zeolite shows a lower intensity, as compared with the unmodified zeolite. Because the silanol groups (Si-O-H) on zeolite surface was replaced by alkyl group (Si-O-Si-C) after surface modification. The intensity of OTS-modified zeolite is lower than that of APS-modified zeolite. This indicates that the OTS is more active than APS because electronegativity (EN) of Cl atom in OTS is greater than that of ethoxy group in APS. Reaction of zeolite modification with OTS is depicted in Figure 4.2.

The APS-modified zeolite shows at binding energies of 399.30 and 401.50 eV, related to N-H and C-N bonds, respectively (Figure 4.1 (d)). The APS-modified zeolite shows the highest intensity, as compared with those of the unmodified and OTS-modified zeolite because of amine groups on zeolite surface (Figure 4.3). N 1s signal of the unmodified one was similar to that of the OTS-modified one. This is because amine group is not present in these two samples.

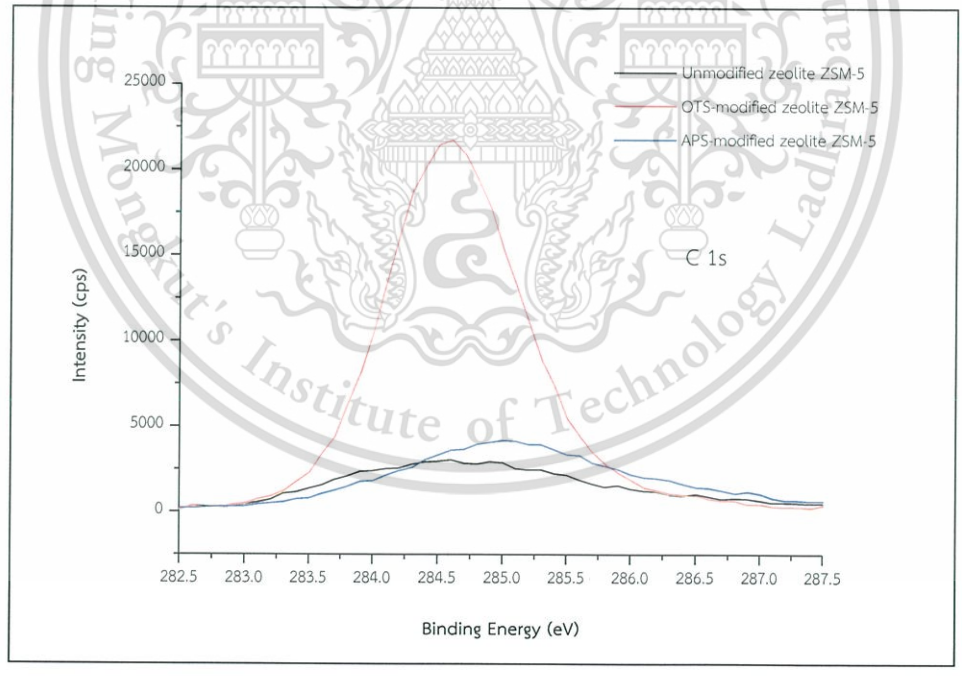

(a) C 1s

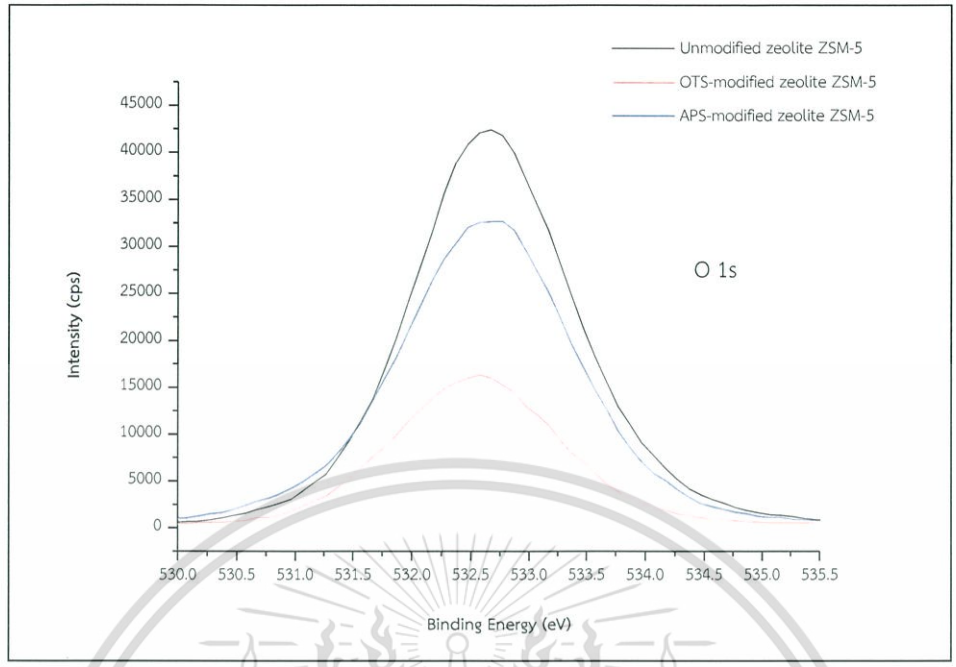

(b) O 1s

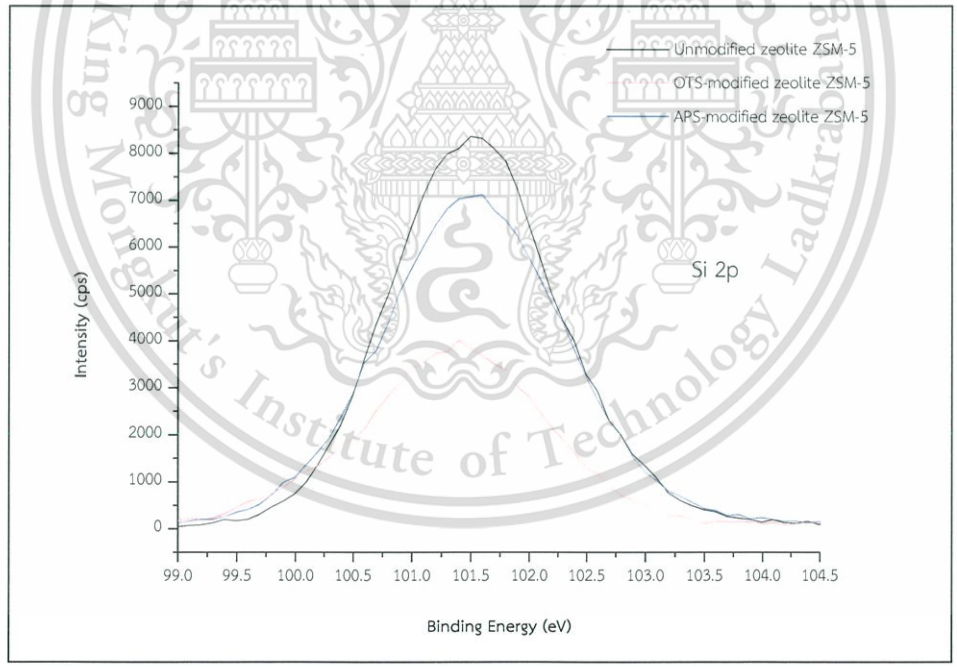

(c) Si 2p

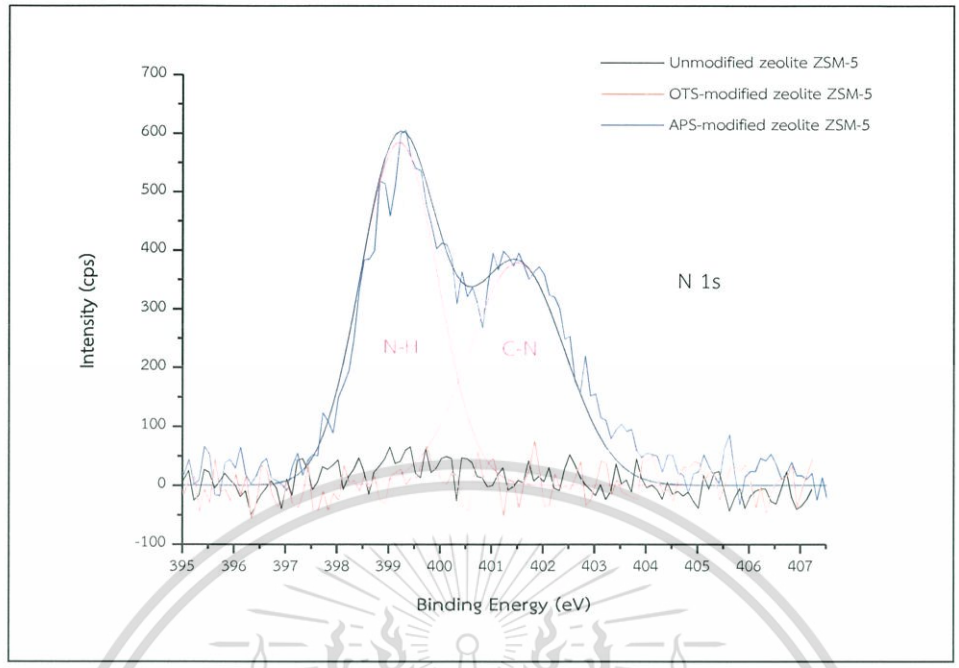

(d) N 1s

Figure 4.1 XPS spectra of the zeolite ZSM-5 with and without modification

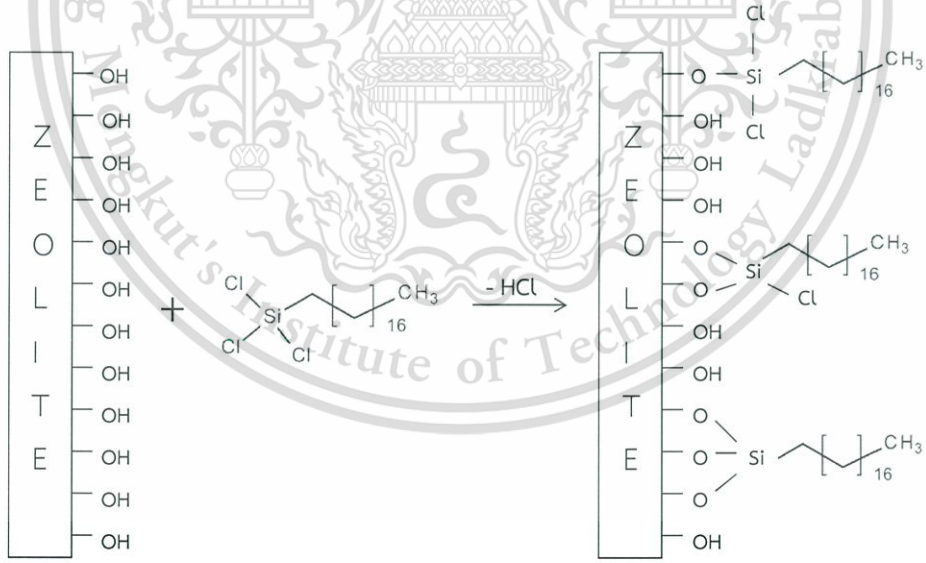

Zeolite OTS-modified zeolite

Figure 4.2 Reaction of zeolite modification with OTS

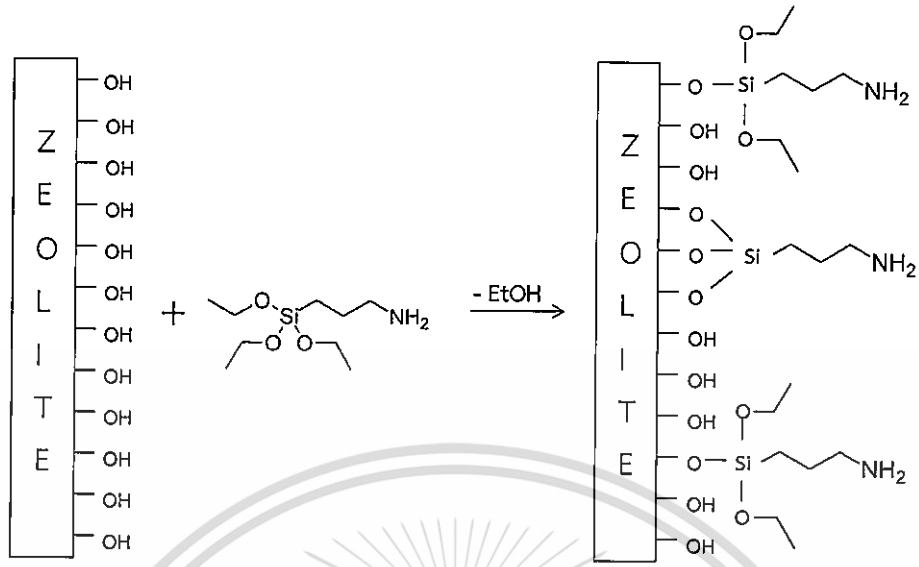

Zeolite APS-modified zeolite

Figure 4.3 Reaction of zeolite modification with APS

The surface of zeolite was successfully functionalized with OTS and APS. After modification with OTS, the zeolite surface was changed from silanol group to alkyl group that could lead to a better compatibility with polymers. On the other hand, APS-modified zeolite was changed from silanol group to amine group (Figure 4.3) that may improve interaction with PE-g-MA (Figure 4.4). The PE-g-MA could provide better compatibility between zeolite and polymers.

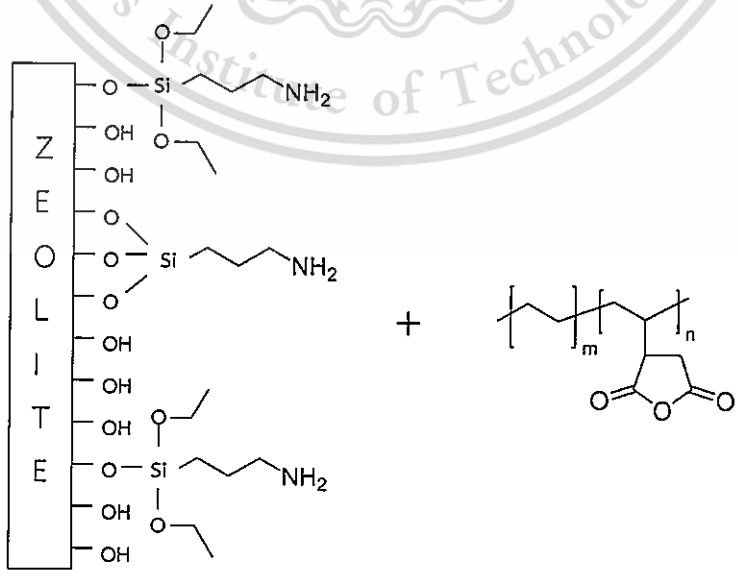

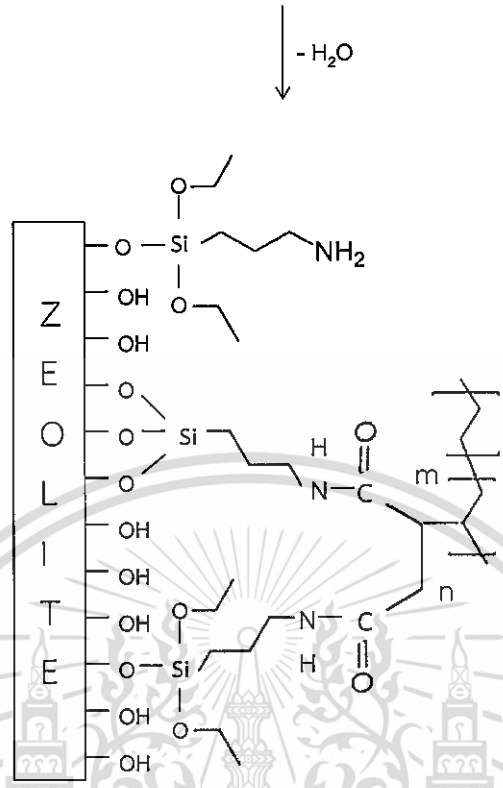

Figure 4.4 Reaction of APS-modified zeolite and PE-g-MA

4.1.1.2 Content of modifiers on zeolite surface

To determine exactly how much of modifying agent was presented on the zeolite, thermogravimetric analysis (TGA) was performed to quantify the amount of silane anchored on the external surface. TGA thermograms of OTS and APS/PE-g-MA-modified zeolite are shown in appendix D (Figures A.1 and A.2, respectively). It was found that OTS-modified zeolite has 2.09% weight loss at 257.2°C and APS/PE-g-MA-modified zeolite has 2.41% weight loss at 243.2°C. These losses are contributed to the decomposition of organosilane. Since the decomposition temperatures of OTS and APS in the modified zeolites are higher than their boiling points (223°C for OTS and 217°C for APS), it indicates that strong chemical bonds have formed between silane and zeolite [71]. Another weight loss (7.12% at 283.2°C) of APS/PE-g-MA-modified zeolite belongs to PE-g-MA, which added for improving compatibility between APS/PE-g-MA-modified zeolite and polymers.

4.1.1.3 Hydrophobicity of modified zeolite ZSM-5

The hydrophobicity of organosilane functionalized zeolite was studied. Figure 4.5 presents an experiment where the unmodified, OTS and APS/PE-g-MA modified zeolite are suspended in water. The unmodified zeolite is entirely submerged in water due to its high polar structure. After surface modification either with OTS or APS/PE-g-MA, the surface polarity of zeolite was decreased. The modified zeolite became more hydrophobic and therefore, it was able to stay repelled from aqueous phase.

Figure 4.5 Hydrophobicity of unmodified and modified zeolite ZSM-5

4.1.2 Characterization and test of films

4.1.2.1 Content of zeolite in the films

The zeolite content in LLDPE/SEBS/zeolite blend films was determined by TGA (thermogram in appendix A) and given in Table 4.1. The actual and the target zeolite contents were similar due to the use of closed-mixing process.

Table 4.1 The zeolite content in LLDPE/SEBS/zeolite ZSM-5 blend films

Sample	Target zeolite content (%)	Actual zeolite content (%)
LL70S30	0.00	0.00
LL70S30Z5	5.00	5.28
LL70S30ZO5	5.00	4.29
LL70S30ZA5P	5.00	4.74

4.1.2.2 Morphology of films

FE-SEM micrographs at the magnification of 2,000x of the cross-section area of the LLDPE/SEBS blend without zeolite and the LLDPE/SEBS blends with unmodified and modified zeolite before SEBS extraction are demonstrated in Figure 4.6 (a) and Figures 4.6 (b-d), respectively.

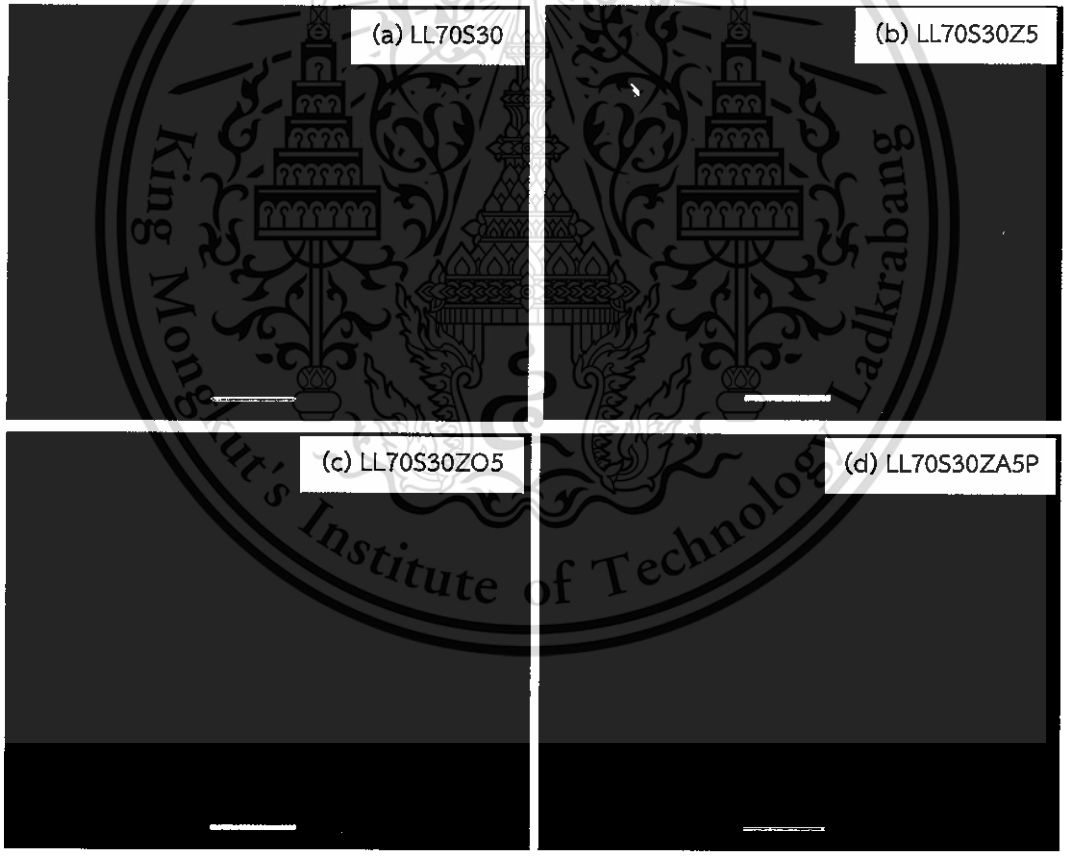

Figure 4.6 FE-SEM micrographs of cross-section area of the LLDPE/SEBS blends with and without 5%wt zeolite at 2,000x magnification

It was found that the smooth surface is revealed in LLDPE/SEBS (LL70S30) film, while the white particles present zeolite (1-2 μm) in the LL70S30Z5, LL70S30ZO5 and LL70S30ZA5P blends. However, a good distribution and dispersion of zeolite in LL70S30Z5 and LL70S30ZO5 blends were achieved. This may be because of low zeolite content (5%wt) and therefore the unmodified and OTS-modified zeolite could still be easily dispersed. On the other hand, APS/PE-g-MA-modified zeolite shows good distribution but poor dispersion in LL70S30ZA5P blend. This is suggested that APS/PE-g-MA-modified zeolite is poor compatibility with polymers.

The cross-section area of the LLDPE/SEBS (LL70S30) blend with and without modified zeolite (5%wt) after SEBS extraction are shown in Figure 4.7 (a-d).

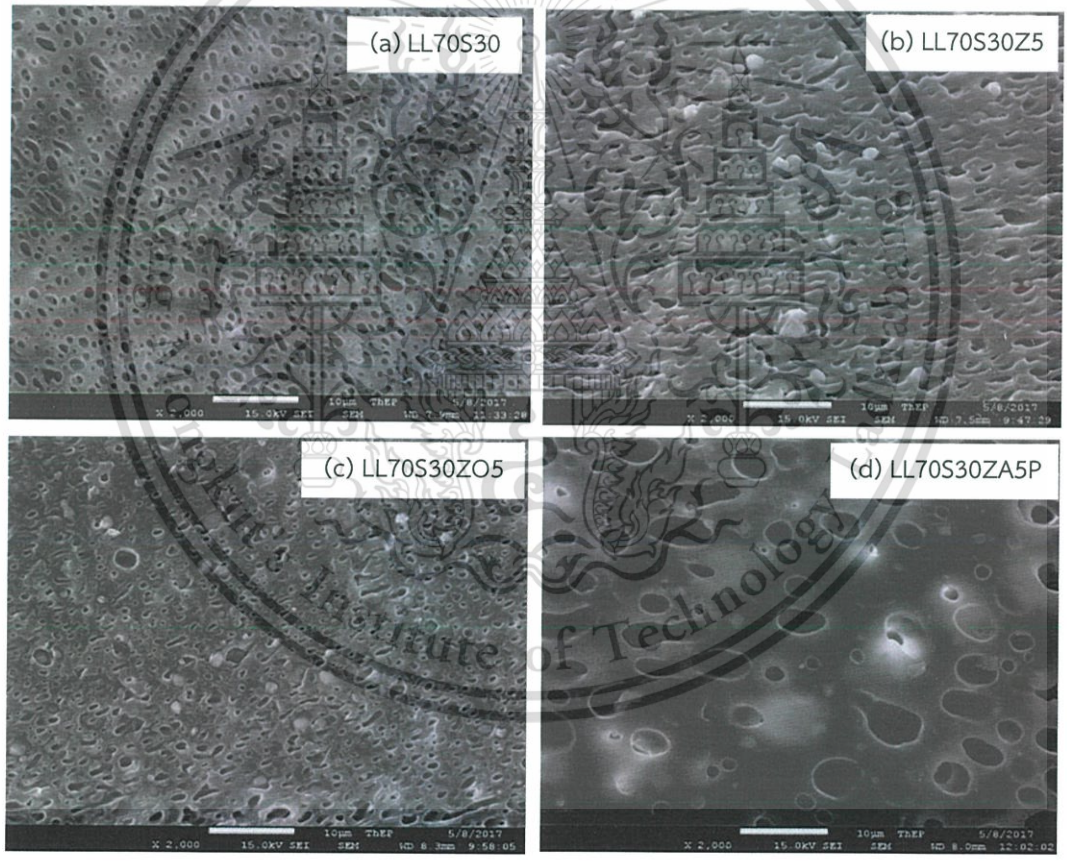

Figure 4.7 FE-SEM micrographs of cross-section area of the LLDPE/SEBS blends with and without 5%wt zeolite after SEBS extraction at 2,000x magnification

It was found that the black holes and white particles represent extracted SEBS and zeolite, respectively. LL70S30 and LL70S30Z5 blends illustrated spherical

size of SEBS dispersed in LLDPE. The dispersed phase size of SEBS in LL70S30ZO5 blend is slightly decreased, as compared to that in LL70S30 and LL70S30Z5 blends. This is owing to a better compatibility of LLDPE and SEBS. In addition, the white particles were observed in LLDPE phase. It is advised that modified zeolite exhibited good dispersion in LLDPE. However, the amount of modified zeolite is lesser than that was observed from SEM (Figure 4.6). It is indicated that some zeolite was extracted with SEBS. This is because the zeolite has good affinity with styrene segment in SEBS and this agrees with previous work [63]. In contrast, LL70S30ZA5P blend illustrated larger phase size of SEBS than other blends. This is suggested that PE-g-MA in APS/PE-g-MA-modified zeolite-filled film reduces compatibility between LLDPE and SEBS, resulting in coalescence of SEBS.

4.1.2.3 Thermal properties of films

The films incorporated with 5%wt zeolite with and without modification were examined by DSC in order to indicate T_m, T_c and peak area of T_m (ΔH_f) (thermograms presented in appendix B). %Crystallinity of LLDPE in LLDPE/SEBS/zeolite blend films with and without zeolite modification is calculated in appendix B and listed in Table 4.2.

Table 4.2 T_m, T_c and %crystallinity of LLDPE in LLDPE/SEBS/zeolite ZSM-5 blend films with and without zeolite modification

Sample	Melting temperature, T_m (°C)	Crystallization temperature, T_c (°C)	Crystallinity, X_c (%)
LLDPE	120.2	104.0	27
LL70S30	116.9	101.6	25
LL70S30Z5	117.6	102.5	25
LL70S30ZO5	117.9	103.2	26
LL70S30Z5AP	116.2	103.0	24

It was found that T_m, T_c and %crystallinity of LLDPE in all the samples were 116.2-117.9°C, 101.6-103.2°C and 24-26%, respectively. This result is similar to that of the previous work [5]. The solubility parameter (δ) of SEBS and LLDPE are 8.5 $(cal/cm^3)^{1/2}$ and 7.9 $(cal/cm^3)^{1/2}$, respectively. It implies that SEBS has relative polarity higher than LLDPE. Unmodified and modified zeolite, containing aluminosilicate

framework, are preferentially dispersed in SEBS phase rather than LLDPE phase. Therefore, the addition of zeolite did not interfere the crystallization of LLDPE in the films.

4.1.2.4 Tensile properties of films

Tensile strength, %elongation at break and Young's modulus of LLDPE/SEBS (70/30 ratio) blend films with unmodified, OTS-modified and APS/PE-g-MA-modified zeolite are exhibited in Figures 4.8-4.10, respectively. It was found that the unmodified (LL70S30Z5) and OTS-modified zeolite-filled LLDE/SEBS films (LL70S30ZO5) gave tensile strength and %elongation at break higher than that of the LLDPE/SEBS blend film (LL70S30) and Thai Industrial Standard (TIS 711-1987, 7 MPa) [72]. This is due to the good affinity between zeolite and styrene segment in SEBS, which coincides with the previous work [63]. In addition, OTS-modified zeolite is hydrophobic particles, which could be dispersed in LLDPE (matrix), leading to a better interaction between polymers matrix and zeolite. Young's modulus of all those films was not different because these blends had low content (5%wt) of zeolite which was mostly dispersed in SEBS.

On the other hand, tensile properties of APS/PE-g-MA-modified zeolite-filled LLDE/SEBS films (LL70S30ZA5P) and LLDPE/SEBS blend films were similar. This is suggested that large spherical size of dispersed SEBS (Figure 4.7 (d)) generated from incompatibility between LLDPE and SEBS and resulted in comparable tensile strength, %elongation at break and Young's modulus.

When comparing modifiers type of zeolite, the zeolite modification with long alkyl chain (OTS) was more hydrophobicity. It can be seen that the OTS-modified zeolite-filled film gave the tensile strength and %elongation at break higher than the APS/PE-g-MA-modified zeolite-filled film because of a better compatibility between polymers and OTS-modified zeolite.

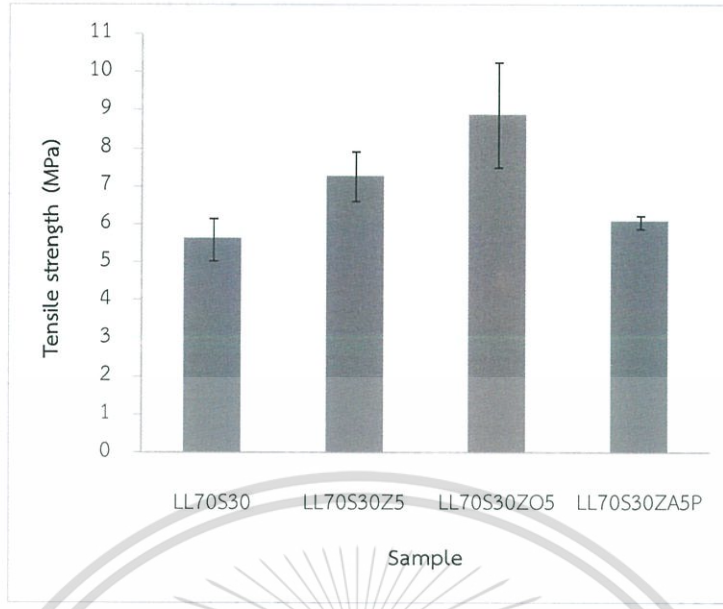

Figure 4.8 Tensile strength of LLDPE/SEBS films with and without 5%wt zeolite

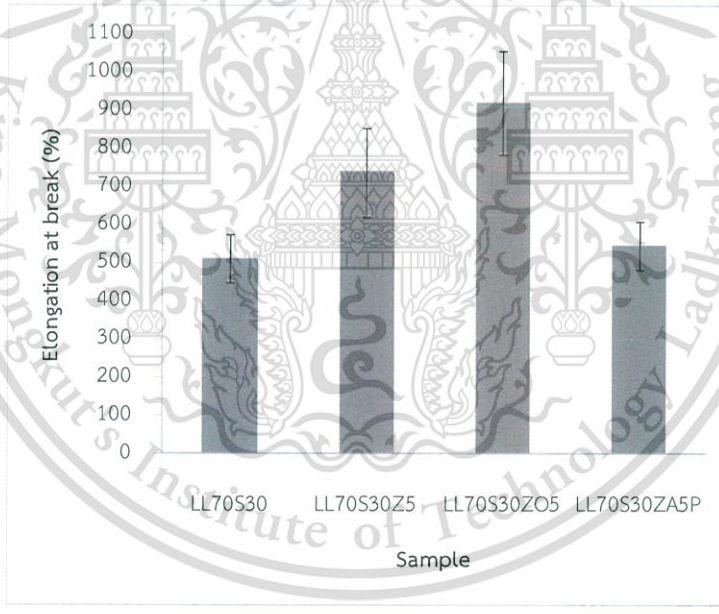

Figure 4.9 Elongation at break of LLDPE/SEBS films with and without 5%wt zeolite

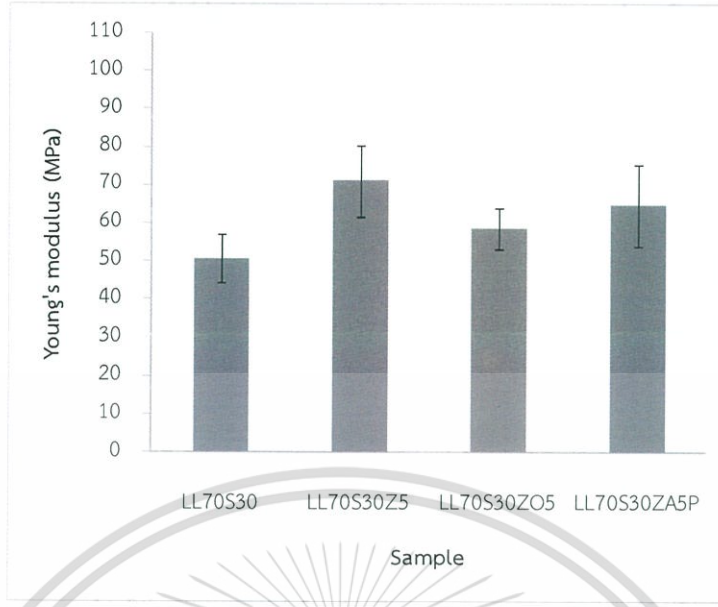

Figure 4.10 Young's modulus of LLDPE/SEBS films with and without 5%wt zeolite

4.1.2.5 Gas permeation of films

The ethylene and carbon dioxide gas permeabilities of the LL70S30, LL70S30Z5, LL70S30ZO5 and LL70S30ZA5P films are demonstrated in Figures 4.11. Calculation of ethylene and carbon dioxide transmission rates (ETR and CO_2TR) and ethylene and carbon dioxide signals are shown in Appendix D and E, respectively. LLDPE is semi-crystalline that has arranged chain in crystalline phase, causing low gas permeability. Consequently, gas can diffuse through amorphous SEBS better than LLDPE. This is because an amorphous polymer (SEBS) has high elasticity and free volume as compared to LLDPE. It was found that the LL70S30Z5 film had a high ETR (4,674 cm^3/m^2.day.atm) in comparison with LL70S30 film (2,523 cm^3/m^2.day.atm), as seen in Figure 4.11. This is because zeolite ZSM-5 has porous and continuous channel structure which is selective with ethylene gas. The zeolite can adsorb ethylene gas, resulting in high ethylene concentration gradient that leads to simplify ethylene permeation. Moreover, the addition of zeolite in polymer (LLDPE/SEBS) can shorten diffusion pathway of ethylene gas in the film as illustrated in Figure 4.12.

The ETR of LLDPE/SEBS/modified zeolite films were higher than that of LLDPE/SEBS/unmodified zeolite films (LL70S30Z5). The ETR of the LL70S30ZO5 and LL70S30ZA5P film were 5,878 and 4,789 cm^3/m^2.day.atm, respectively. The addition of modified zeolite in LLDPE/SEBS blend can increase ethylene permeability of the

film because the modification of zeolite reduces polarity of the zeolite surface. In addition, the modifying agent type affected on ethylene gas permeation. It can be seen that the LL70S30ZO5 film incorporated with modified zeolite with long chain alkyl silane (OTS) exhibited higher ETR, as compared to that of the modified zeolite with a short chain alkyl silane (APS) and PE-g-MA. This is because long chain hydrocarbon of OTS improves hydrophobicity on zeolite surface and leads to a better compatibility between polymers and zeolite. This is corresponding to an increase in tensile strength and %elongation at break (Figures 4.8 and 4.9). The film with APS/PE-g-MA-modified zeolite ZSM-5 exhibited in large dispersed phase size of SEBS (Figure 4.7 (d)), due to an incompatibility between LLDPE and SEBS.

CO_2TR of the LLDPE/SEBS blend films with and without 5%wt zeolite is shown in Figure 4.11. CO_2TR values of LL70S30, LL70S30Z5, LL70S30ZO5 and LL70S30ZA5P were 215, 312, 312 and 273 cm^3/m^2.day.atm, respectively. These CO_2TR values were in the same range and this is suggested that LLDPE/SEBS/modified zeolite-filled films were specifically selective with C_2H_4 gas (hydrophobic gas). Thus, these films were not selective with CO_2 gas.

Figure 4.11 Ethylene and carbon dioxide transmission rate of LLDPE/SEBS films with and without 5%wt zeolite

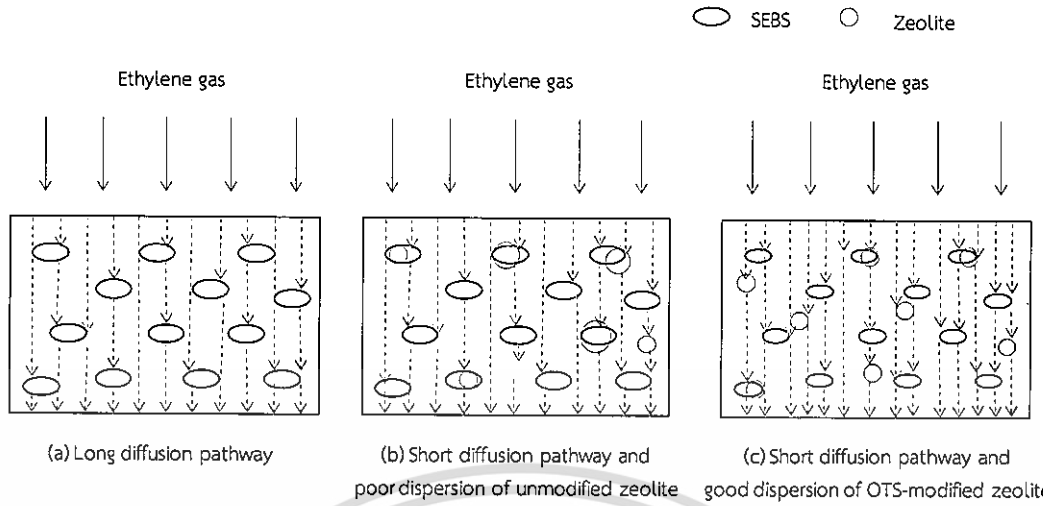

Figure 4.12 Diffusion pathway of ethylene gas: (a) Long diffusion pathway of LLDPE/SEBS film (b) Short diffusion pathway and poor dispersion of unmodified zeolite in LLDPE/SEBS film and (c) Short diffusion pathway and good dispersion of OTS-modified zeolite in LLDPE/SEBS film

4.1.3 Effect of rotor speed on LL70S30ZA5P film

From section 4.1.2, tensile properties and ETR of the LLDPE/SEBS/APS/PE-g-MA-modified zeolite film were lower than those of LLDPE/SEBS/OTS-modified zeolite film. In addition, large dispersed phase size of SEBS in the film with APS/PE-g-MA modifiers was obtained (Figure 4.7 (d)). This suggests an incompatibility between LLDPE and SEBS. Therefore, the effect of shear stress in compounding process via rotor speed on properties of the LL70S30ZA5P film was examined.

4.1.3.1 Morphology of films

FE-SEM micrographs of the cross-section area of the LL70S30ZA5P blends at rotor speeds 60 and 100 rpm before and after SEBS extraction are shown in Figure 4.13. It was found that a dispersion of APS/PE-g-MA-modified zeolite in LL70S30ZA5P blend at rotor speed 100 rpm is better than that at rotor speed 60 rpm (Figures 4.13 (a) and (b)). In addition, the morphology of dispersed SEBS in LL70S30ZA5P blend at rotor speed 60 rpm is spherical, while that at rotor speed 100 rpm are spherical and cylindrical (Figures 4.13 (c) and (d)). This is indicated that increasing shear force caused an elongated SEBS. The higher rotor speed, the smaller dispersed phase size

was obtained. The small dispersed phase size indicates that compatibility of polymer blend is increased.

Figure 4.13 FE-SEM micrographs of cross-section area of the LL70S30ZA5P blends at rotor speeds 60 and 100 rpm before and after SEBS extraction at 2,000x magnification

4.1.3.2 Thermal properties of films

Thermal properties of APS/PE-g-MA-modified zeolite-filled film (LL70S30ZA5P) at rotor speeds 60 and 100 rpm are presented in Table 4.3. It was found that the zeolite content in LL70S30ZA5P at rotor speeds 60 and 100 rpm were similar. T_m, T_c and percentage of crystallinity of LLDPE in the films were 116-119°C, 102-103°C and 23-24%, respectively. This is suggested that these blends had low content of zeolite (5%wt), leading to non-interference in the crystallization of LLDPE in the films.

Table 4.3 Thermal properties of LL70S30ZA5P films at rotor speeds 60 and 100 rpm

Property	Measuring instrument	Results	
		60 rpm	100 rpm
Zeolite content, %	TGA	4.74	4.20
Melting temperature (T_m), °C	DSC	116.2	118.7
Crystallization temperature (T_c), °C	DSC	103.0	102.9
Crystallinity (X_c), %	DSC	24	23

4.1.3.3 Tensile properties of films

Tensile properties of APS/PE-g-MA-modified zeolite ZSM-5-filled film (LL70S30ZA5P) at rotor speeds 60 and 100 rpm are depicted in Figures 4.14-4.16. It was found that the LL70S30ZA5P film at rotor speed 100 rpm possessed tensile strength and %elongation at break higher than LL70S30ZA5P film at rotor speed 60 rpm. Thus, high shear force in a mixer leads to better zeolite dispersion and compatibility of the zeolite and polymers. However, Young's modulus of LL70S30ZA5P film was not affected by rotor speed as seen in Figure 4.17. This is because these films had similar zeolite content at about 5%wt as shown in Table 4.3, section 4.1.3.2.

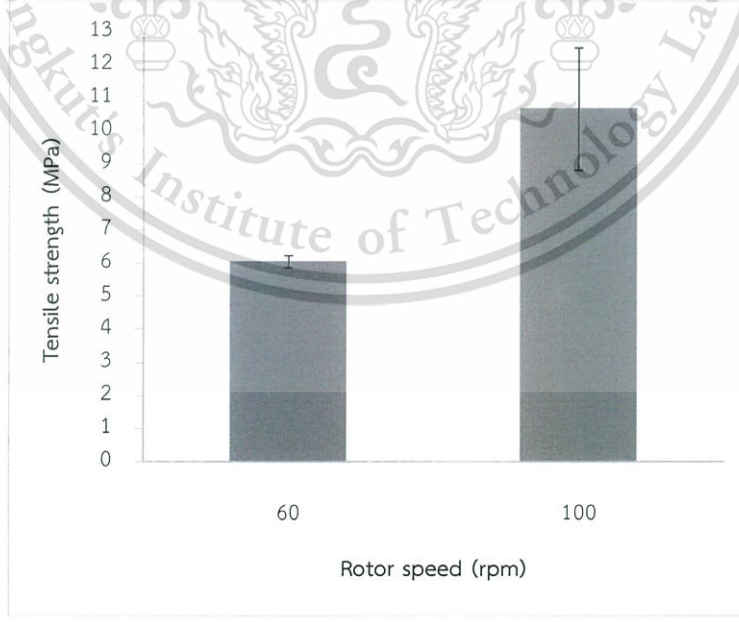

Figure 4.14 Tensile strength of LL70S30ZA5P films at rotor speeds 60 and 100 rpm

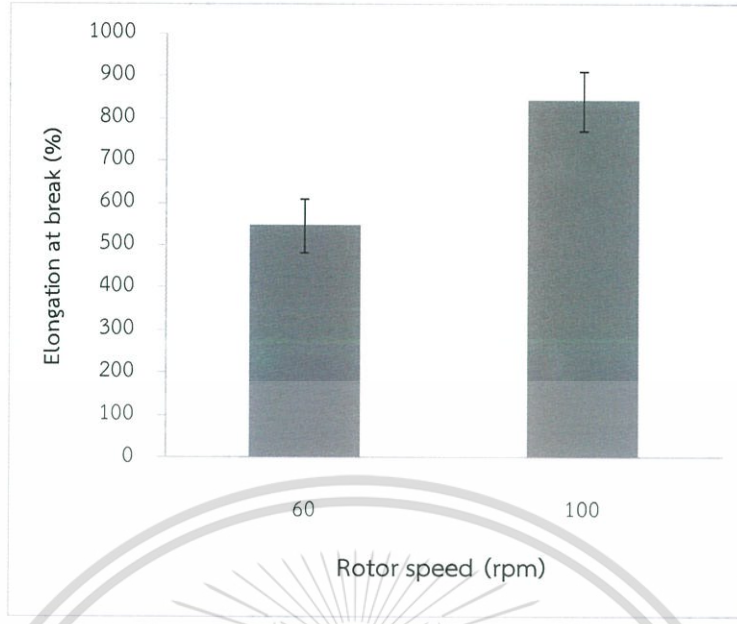

Figure 4.15 Elongation at break of LL70S30ZA5P films at rotor speeds 60 and 100 rpm

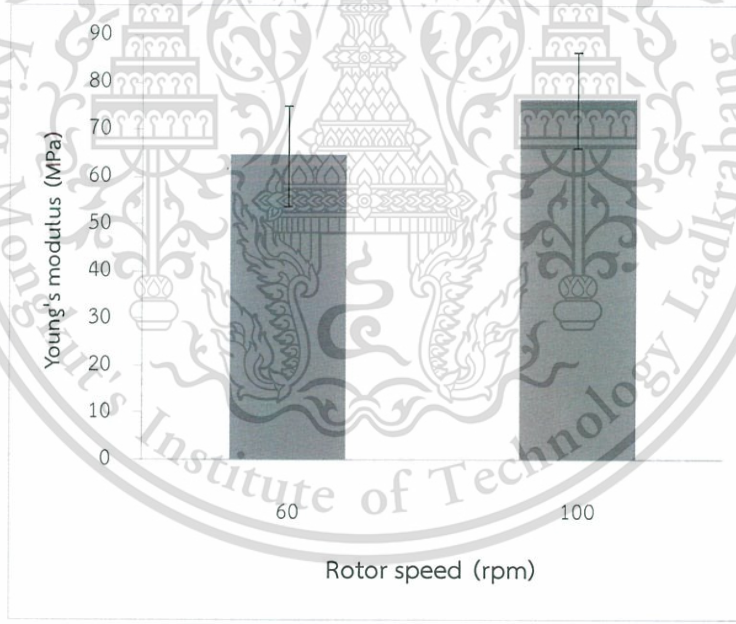

Figure 4.16 Young's modulus of LL70S30ZA5P films at rotor speeds 60 and 100 rpm

4.1.3.4 Gas permeation of films

The ETR and CO_2TR of LL70S30ZA5P films at rotor speeds 60 and 100 rpm are shown in Figure 4.17. It was found that the LL70S30ZA5P film at rotor speed 100 rpm (5,635 cm^3/m^2.day.atm) possessed ETR higher than LL70S30ZA5P film at rotor speed

60 rpm (4,789 cm^3/m^2.day.atm). Compatibility and dispersion of zeolite in the polymers were enhanced with increasing rotor speed as mentioned in the section 4.1.2.4. CO_2TR of the LLDPE/SEBS blend film at rotor speed 60 and 100 rpm are 273 and 351 cm^3/m^2.day.atm, respectively. This is because these films specifically selective with C_2H_4 gas, which is hydrophobic gas, better than CO_2 gas that is hydrophilic gas.

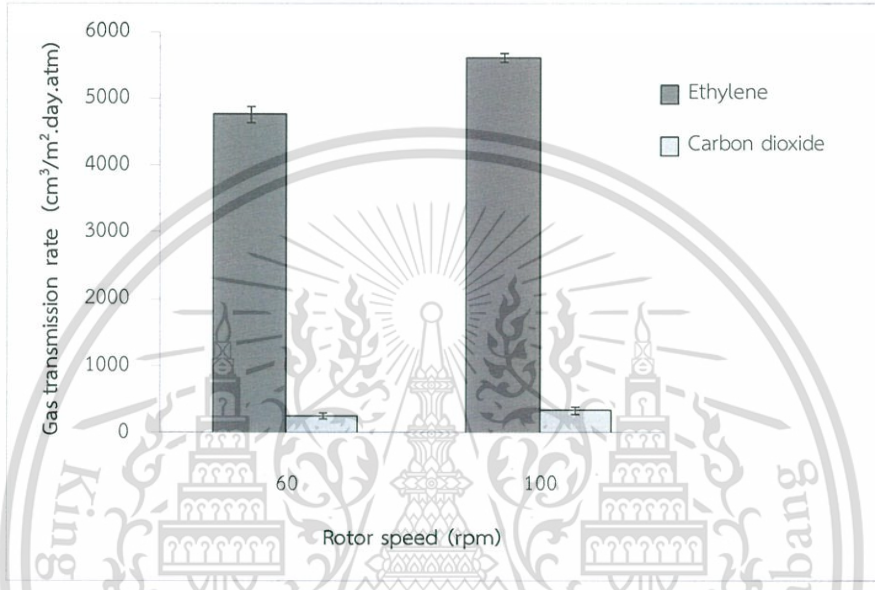

Figure 4.17 Ethylene and carbon dioxide transmission rate of LL70S30ZA5P films at rotor speeds 60 and 100 rpm

4.2 Effect of zeolite loading

In the previous part, the effect of modification of zeolite was studied. It was found that the ETR of OTS-modified zeolite-filled film was higher than APS/PE-g-MA-modified zeolite-filled film. This is due to OTS improving a better compatibility between zeolite and polymers. Therefore, the effect of zeolite loading in the LLDPE/SEBS blend film with unmodified and OTS-modified zeolite was further investigated.

4.2.1 Content of zeolite in the films

The zeolite content in LLDPE/SEBS blend film with unmodified and OTS-modified zeolite were determined by TGA (thermogram in appendix A). The zeolite

content is depicted in Table 4.4. It can be noticed that target zeolite content in the film and actual zeolite content were similar.

Table 4.4 The zeolite content in LLDPE/SEBS/zeolite ZSM-5 blend films

Sample	Target zeolite content (%)	Actual zeolite content (%)
LL70S30	0.00	0.00
LL70S30Z5	5.00	5.28
LL70S30Z10	10.00	9.54
LL70S30Z15	15.00	14.28
LL70S30ZO5	5.00	4.29
LL70S30ZO10	10.00	7.56
LL70S30ZO15	15.00	14.59

4.2.2 Morphology of films

FE-SEM micrographs of LLDPE/SEBS blends with various zeolite loadings before and after SEBS extraction are shown in Figures 4.18 and 4.19, respectively. A good dispersion of 5%wt of unmodified and OTS-modified zeolite was found in the blends. However, the particles of unmodified zeolite tended to agglomerate at high loadings (10-15%wt) as illustrated in Figure 4.18 (c) and (e), and the agglomerate may lead to the blends with interfacial-void and/or defects. Because zeolite had polarity higher than that of polymers, the low compatibility between zeolite and polymers was observed. Moreover, a better dispersion of OTS-modified zeolite in the LLDPE/ SEBS blends was achieved, as compared with that of unmodified zeolite in the blend at the same loading. This is because the polarity on surface modified zeolite was reduced, leading to the good compatibility and dispersion with LLDPE. In addition, Figure 4.19 illustrates that the dispersed SEBS size are bigger with zeolite loading.

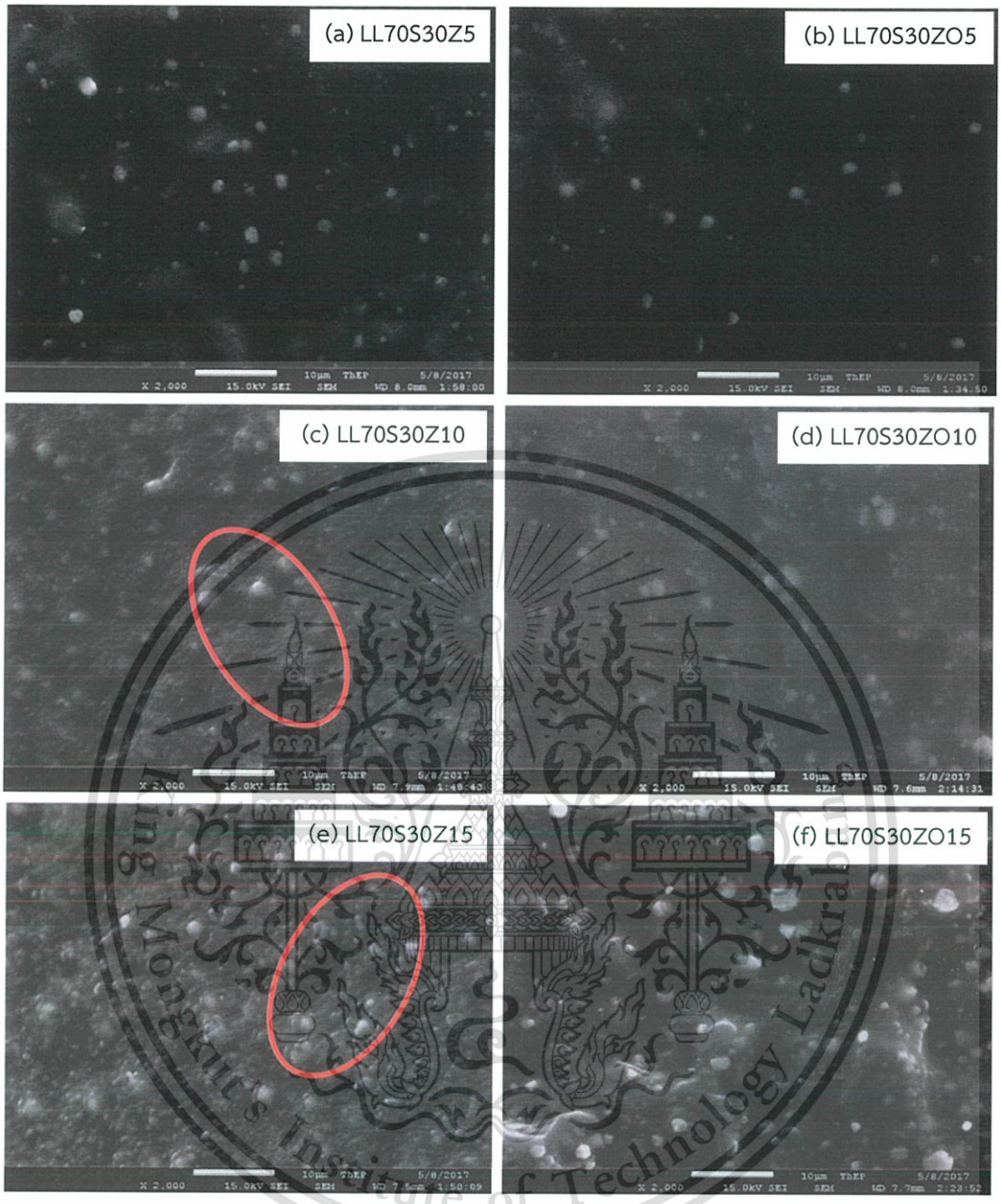

Figure 4.18 FE-SEM micrographs of cross-section area of LLDPE/SEBS blends with various zeolite loadings at 2,000x magnification

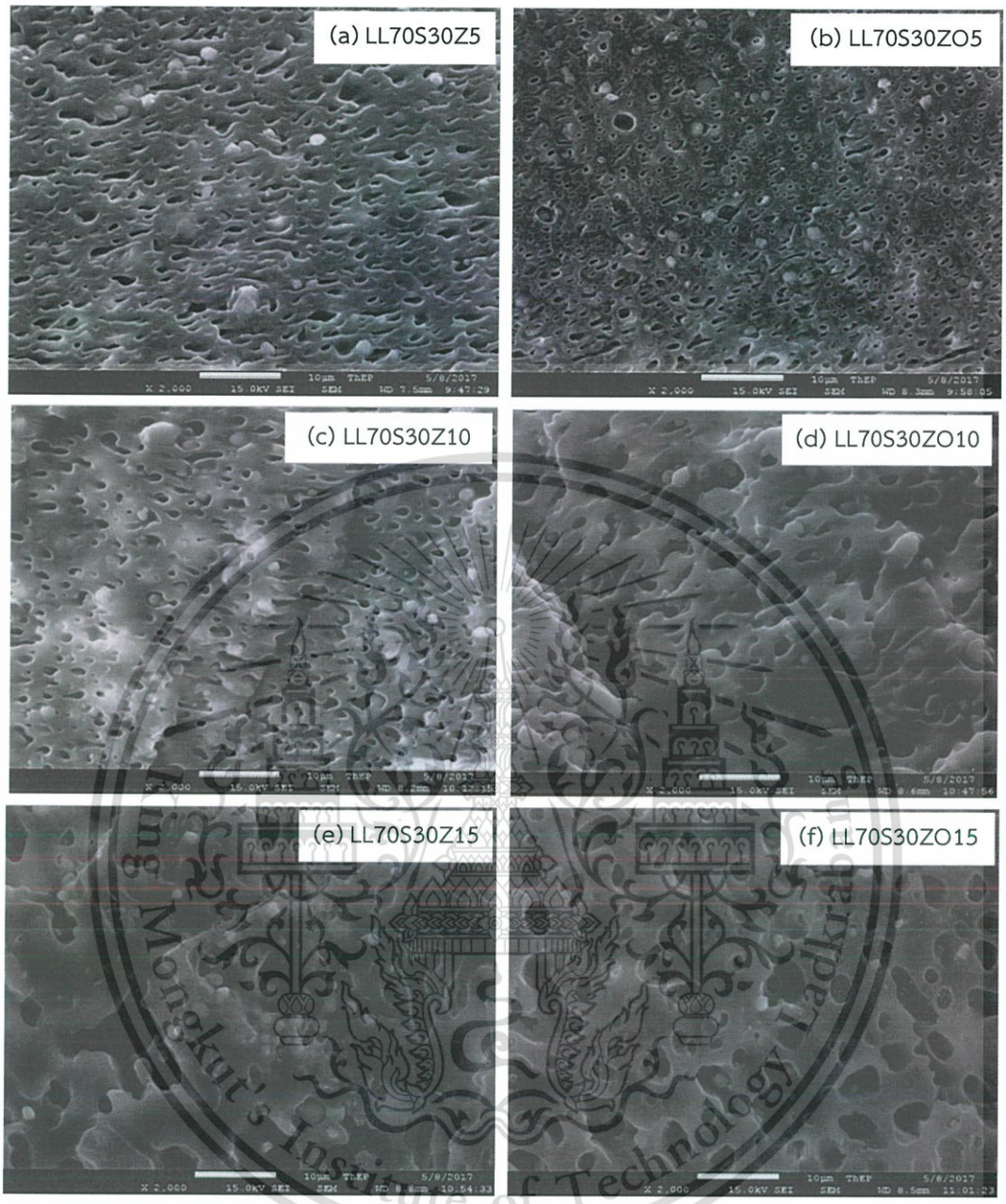

Figure 4.19 FE-SEM micrographs of cross-section area of LLDPE/SEBS blends with various zeolite loadings after SEBS extraction at 2,000x magnification

4.2.3 Thermal properties of films

The LLDPE/SEBS blend films incorporated with zeolite and OTS-modified zeolite at 5-15%wt loadings were examined for thermal properties using DSC (Table 4.5). It was observed that T_m, T_c and percentage of crystallinity of LLDPE in all the samples were in the same range (115-121°C, 101-105°C and 23-26%, respectively). This is because SEBS has slightly higher polarity, as compared with LLDPE. Hence,

unmodified and OTS-modified zeolite can be dispersed in SEBS phase better than in LLDPE phase as mentioned in section 4.1.2.2. Therefore, the zeolite particles did not impede the crystallization of LLDPE phase.

Table 4.5 T_m, T_c and %crystallinity of the LLDPE/SEBS/zeolite ZSM-5 blend films with various zeolite loadings

Sample	Melting temperature, T_m (°C)	Crystallization temperature, T_c (°C)	Crystallinity, X_c (%)
LLDPE	120.2	104.0	27
LL70S30	116.9	101.6	25
LL70S30Z5	117.6	102.5	25
LL70S30Z10	116.0	104.3	22
LL70S30Z15	115.0	102.2	23
LL70S30ZO5	117.9	103.2	26
LL70S30ZO10	120.8	103.3	25
LL70S30ZO15	116.2	104.4	24

4.2.4 Rheological properties

To deeply understand processability and compatibility of polymer, the sample was heated at 150, 190 and 230°C to measure the rheological properties in the molten state. The master curve of angular frequency dependence of oscillatory shear modulus at 150°C was generated. The storage modulus (G′) and loss modulus (G″) are normally used to describe elastic and viscous of polymer blends, respectively. G′ and G″ of all the blends increase with increasing angular frequency (ω).

The master curve of both moduli of LLDPE, SEBS and LLDPE/SEBS blend at 70/30 ratio (LL70S30) are illustrated in Figure 4.20. It was found that the G′ and G″ of SEBS is the highest, as compared with LLDPE and LL70S30. This is because SEBS consists of ethylene/butylene 87%wt and styrene 13%wt, which is attached to elastomeric (ethylene/butylene) chain and performs physical crosslink to the rubber. The difficult movement of SEBS chain causes high modulus and long-time relaxation behavior [73].

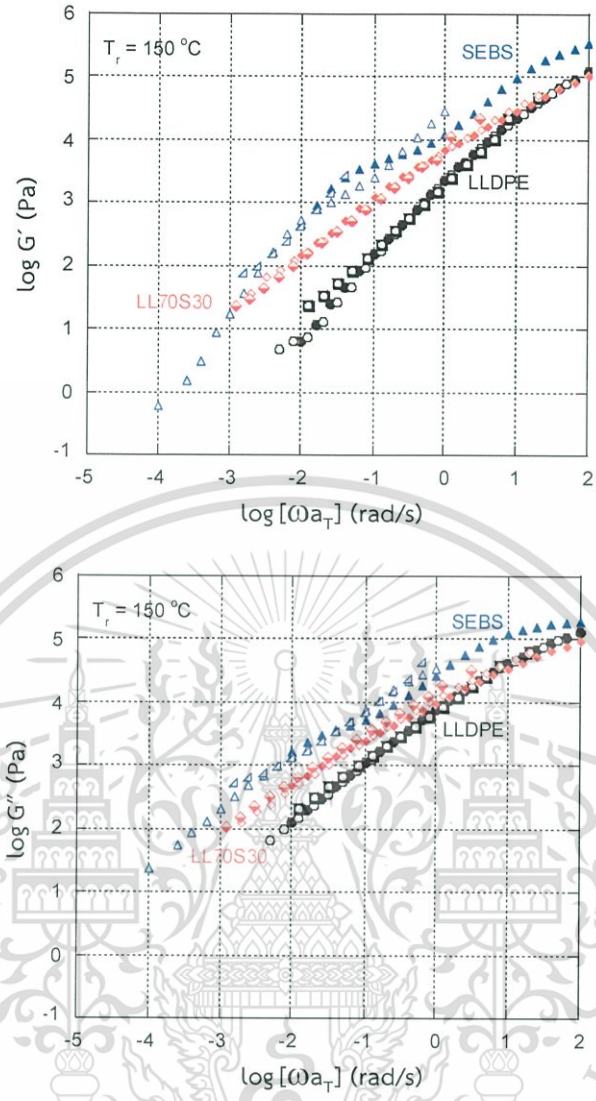

Figure 4.20 Master curves of frequency dependence of storage modulus (G′) and loss modulus (G″) of LLDPE, SEBS and LL70S30 blend at 150°C

The master curves in Figures 4.21 and 4.22 show both moduli of the LLDPE/SEBS/unmodified zeolite and LLDPE/SEBS/OTS-modified zeolite blends, respectively. It was found that the G′ and G″ behavior of the blends did not affect by the presence of unmodified zeolite at 5 and 10%wt zeolite loadings. In contrast, the G′ and G″ of LLDPE/SEBS blend with 15%wt unmodified zeolite loading were increased because high polar zeolite surface could create an agglomeration, resulting in high viscosity of LL70S30Z15. However, the G′ and G″ behavior of the OTS-modified zeolite-filled blends with various zeolite loadings (0-15%wt) were significantly

unchanged because of a better compatibility and a weak interaction between OTS-modified zeolite and polymers.

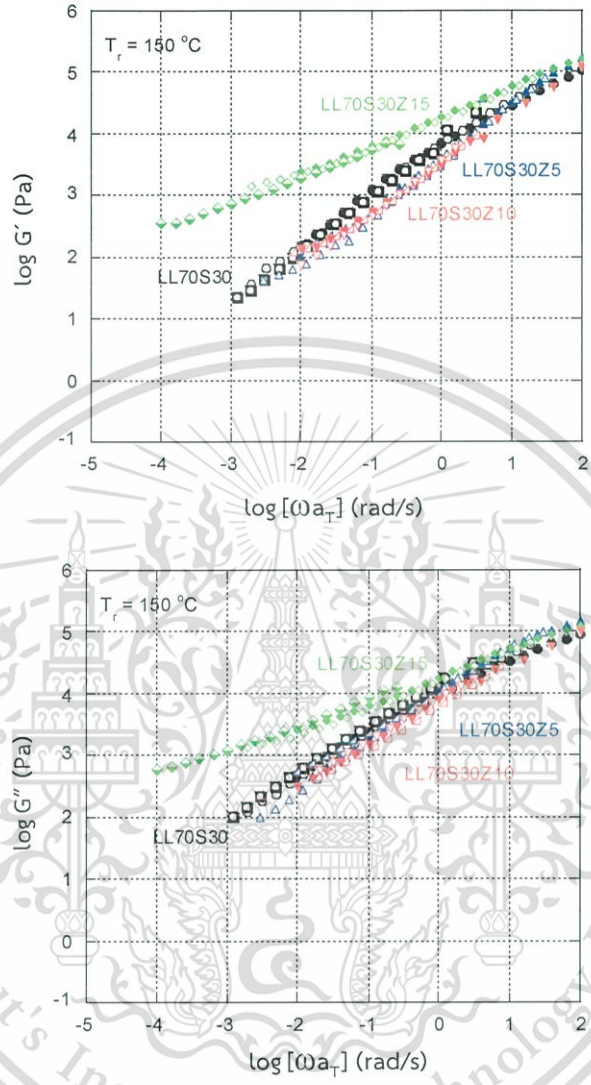

Figure 4.21 Master curves of frequency dependence of storage modulus (G') and loss modulus (G") of LL70S30, LL70S30Z5, LL70S30Z10 and LL70S30Z15 blends at 150°C

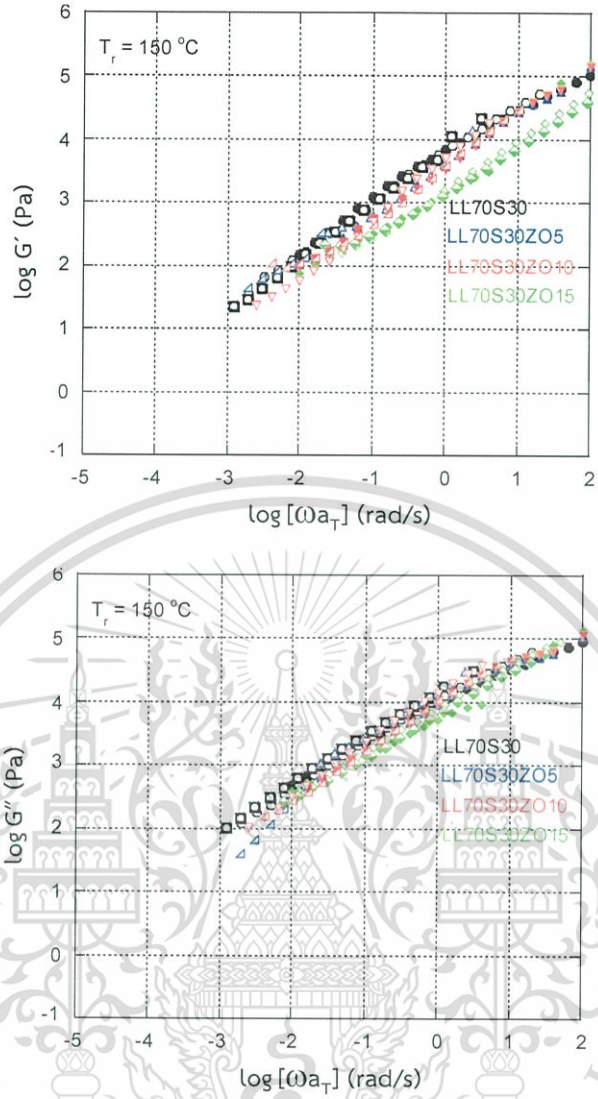

Figure 4.22 Master curves of frequency dependence of storage modulus (G′) and loss modulus (G″) of LL70S30, LL70S30ZO5, LL70S30ZO10 and LL70S30ZO15 blends at 150°C

4.2.5 Dynamic mechanical properties

To study an interaction between polymers and zeolite, dynamic mechanical properties (DMA) of polymer blends was used to analyze storage modulus (E′) and loss modulus (E″). The ratio of loss modulus and storage modulus (E″/E′) was designated as tan δ, which can inform glass transition temperature (T_g) of materials.

E′, E″ and tan δ of LLDPE, SEBS and LLDPE/SEBS blends (LL70S30) are illustrated in Figure 4.23. It can be seen that the α relaxation of the LLDPE crystalline part is represented by the tan δ peak at the highest temperature, i.e., 80.0°C. The

appearance of the β relaxation peak, which is related to the side or short chains of LLDPE, is -20.0°C [74]. T_g of SEBS was observed at -43°C belonging to ethylene/ butylene segment. The amplitude of tan δ of elastomer (SEBS) was higher than semi-crystalline (LLDPE). This suggests that SEBS can be moved and relaxed easier than LLDPE that has chain arrangement. Therefore, rubbery plateau of SEBS in E′ graph is the lowest because SEBS has the highest flexibility. Moreover, E′ and E″ of LL70S30 have rheological trend between LLDPE and SEBS but T_g of LL70S30 blend and parent polymers are not different because of immiscibility of the LLDPE/SEBS blend.

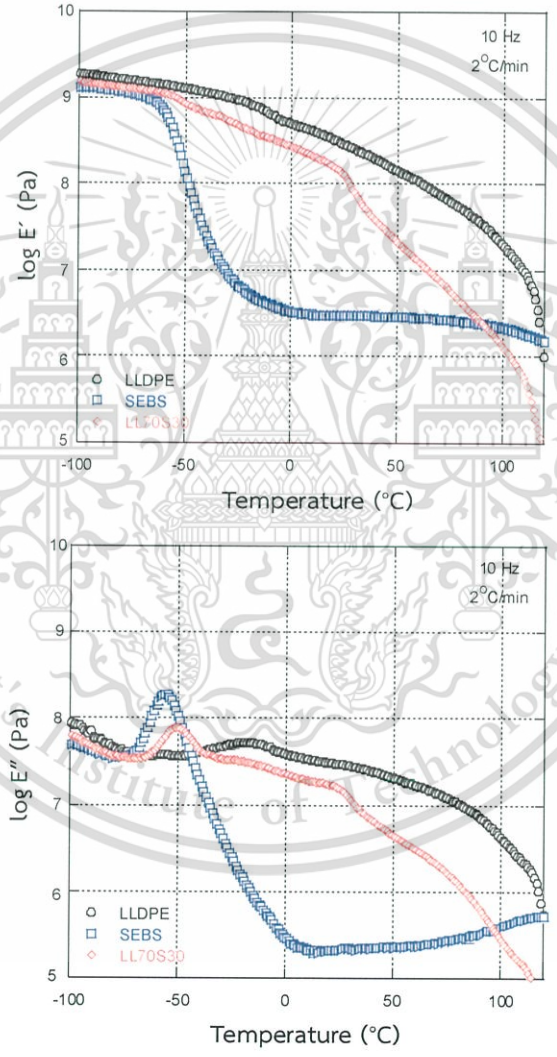

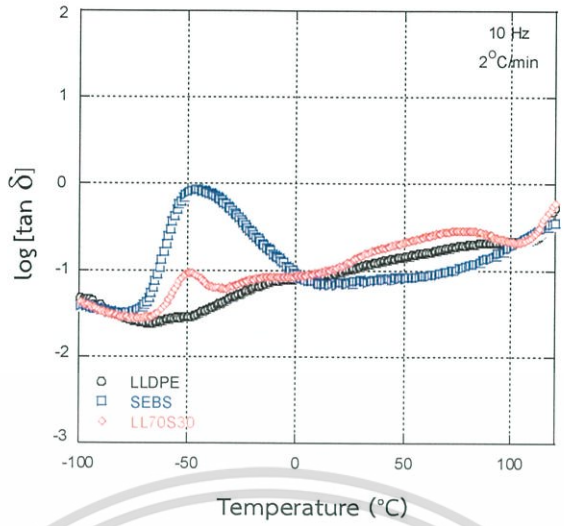

Figure 4.23 Temperature dependence of DMA for storage modulus (E′), loss modulus (E″) and tan δ of LLDPE, SEBS and LL70S30 blend

Figures 4.24 and 4.25 demonstrate the temperature dependence of LLDPE/SEBS blends with unmodified and modified zeolite, respectively. The presence of zeolite (either unmodified or OTS-modified) in LLDPE/SEBS blend hardly affected the dynamic mechanical properties of the blend in the solid state. T_g of ethylene/ butylene of SEBS was -46.3°C (from tan δ peak in Table 4.6) and that of ethylene/ butylene moiety in all the blends was invariable. This indicates that the addition of either unmodified or OTS-modified zeolite did not strongly affect the movement of the ethylene/butylene chains in SEBS because of the weak interaction between zeolite and polymers.

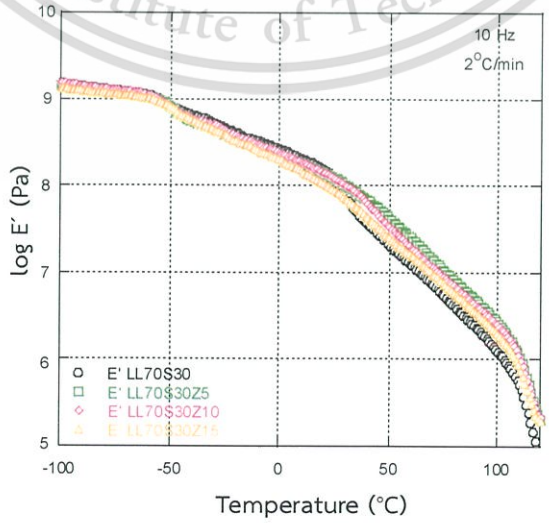

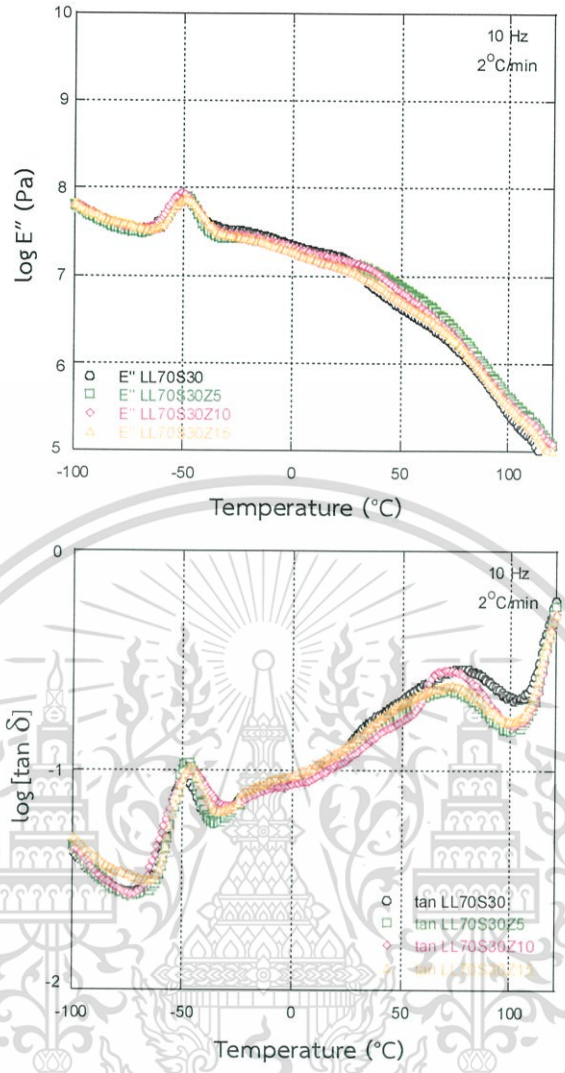

Figure 4.24 Temperature dependence of DMA for storage modulus (E'), loss modulus (E'') and tan δ of LL70S30, LL70S30Z5, LL70S30Z10 and LL70S30Z15 blends

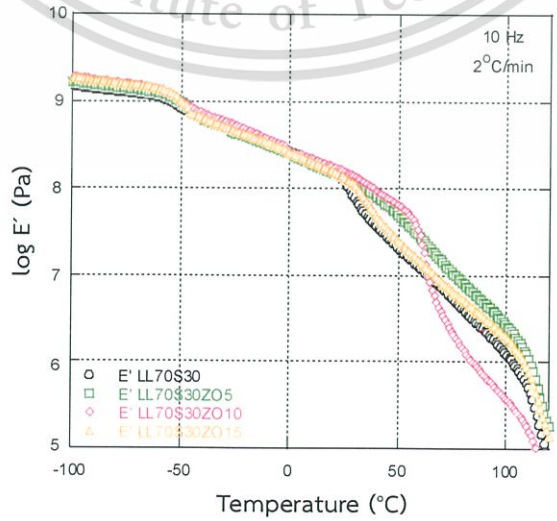

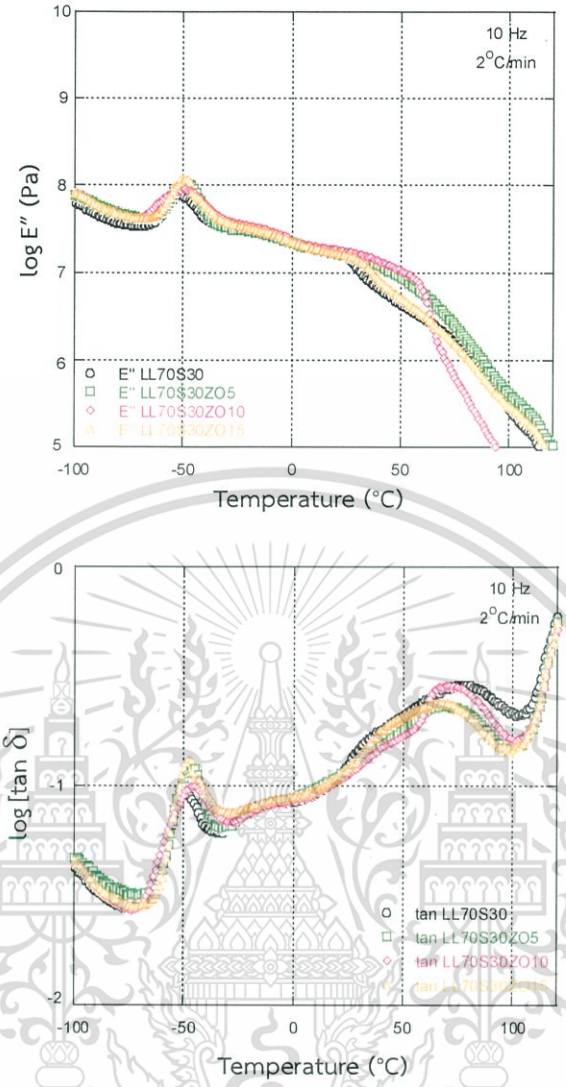

Figure 4.25 Temperature dependence of DMA for storage modulus (E′), loss modulus (E″) and tan δ of LL70S30, LL70S30ZO5, LL70S30ZO10 and LL70S30ZO15 blends

Table 4.6 T_g (from tan δ peaks) of the polymer in the blend

Sample	T_g of ethylene/butylene (°C)	T_g of LLDPE (°C)	
		α peak	β peak
LLDPE	-	80.0	-20.0
SEBS	-46.3	-	-
LL70S30	-49.1	74.8	-20.0
LL70S30Z5	-48.3	72.8	-20.0
LL70S30Z10	-49.3	71.8	-20.0
LL70S30Z15	-47.3	72.9	-20.0
LL70S30ZO5	-46.3	69.7	-20.0
LL70S30ZO10	-46.3	70.8	-20.0
LL70S30ZO15	-47.3	67.7	-20.0

4.2.6 Tensile properties of films

Tensile strength, %elongation at break and Young's modulus of the zeolite-filled films with 5-15%wt zeolite loading are illustrated in Figures 4.26-4.28. Tensile strength of unmodified and OTS-modified zeolite-filled film was enhanced with increasing zeolite loading. This is because the zeolite is good affinity between styrene segment in SEBS and zeolite. In addition, tensile strength of the OTS-modified zeolite-filled film was higher than unmodified zeolite-filled film. This indicates that hydrophobic zeolite is achieved after surface modification, leading to better compatibility and dispersion of OTS-modified zeolite in the blends.

Besides, %elongation at break of unmodified zeolite-filled films was decreased with increasing zeolite loading owing to agglomeration of zeolite, whereas %elongation at break of OTS-modified zeolite-filled films was significantly unchanged with zeolite loading. This is because surface modification of zeolite has better compatibility with polymers, resulting in well dispersed of zeolite (seen in FE-SEM Figure 4.18). Young's modulus values of all the zeolite-filled films were in the same range because most zeolite particles were dispersed in SEBS for all blends.

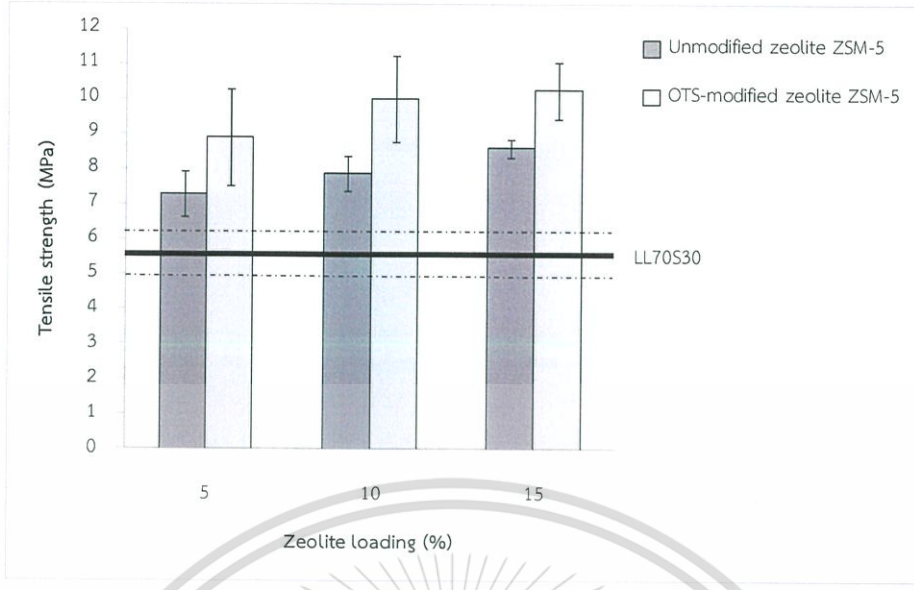

Figure 4.26 Tensile strength of LLDPE/SEBS films with various zeolite loadings

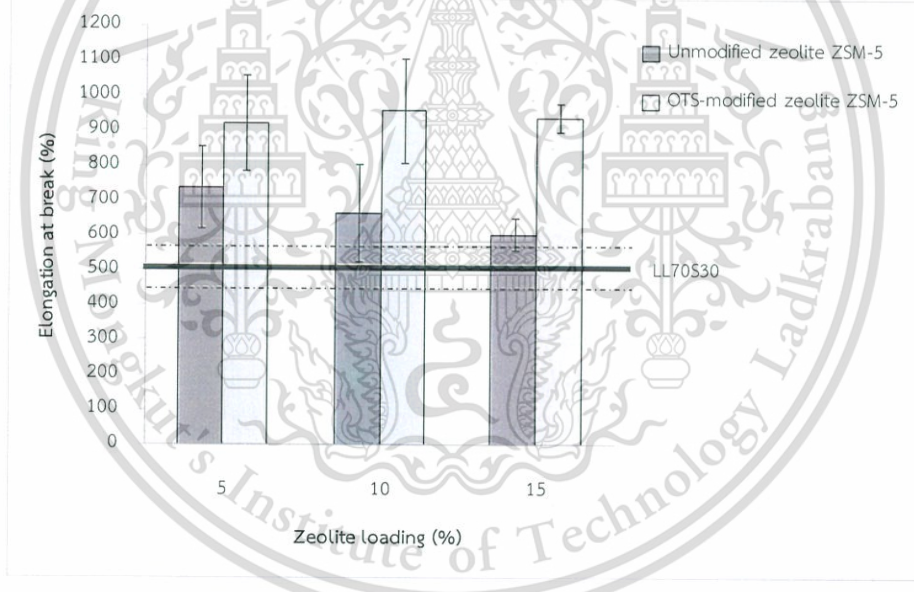

Figure 4.27 Elongation at break of LLDPE/SEBS films with various zeolite loadings

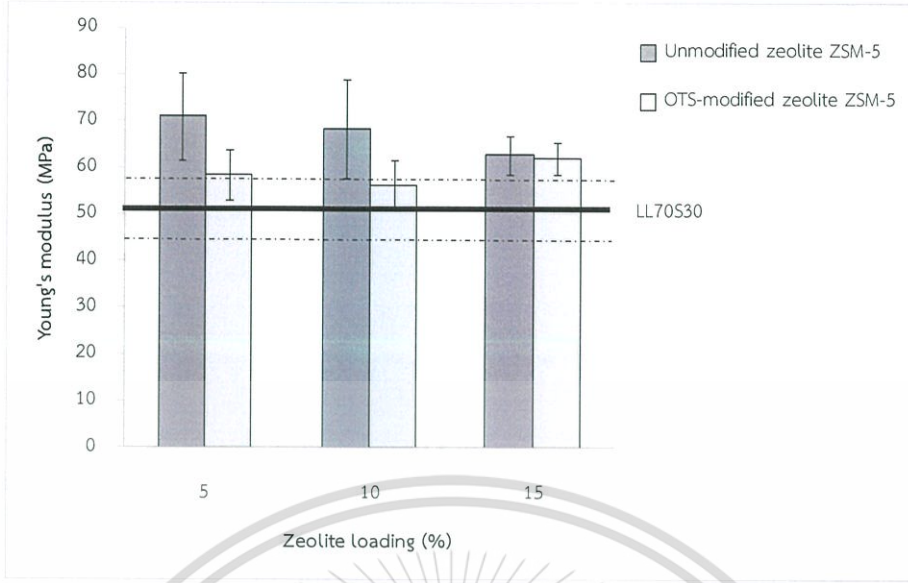

Figure 4.28 Young's modulus of LLDPE/SEBS films with various zeolite loadings

4.2.7 Gas permeation of films

Ethylene gas permeability of the zeolite-filled films with various zeolite loadings is exhibited in Figure 4.29 (Polynomials curve). It can be seen that the ETR of unmodified zeolite-filled films is increased when content of zeolite is increased. This is because the zeolites adsorb ethylene gas, leading to shortens diffusion pathway of ethylene gas. Moreover, zeolite causes high ethylene concentration gradient because zeolite has selective with ethylene gas.

The ETR of OTS-modified zeolite-filled films are slightly increased when increasing zeolite content. The ETR of the film with 5%wt of OTS-modified zeolite was higher than that of the film with 5%wt unmodified zeolite due to a better dispersion of OTS-modified zeolite in the film (Figure 4.12). However, OTS-modified zeolite-filled films at 10 and 15%wt zeolite loadings had ETR lower than unmodified zeolite-filled films at the same loadings.

Typically, zeolite is not selective with CO_2 gas. Hence, permeation of CO_2 gas in the film with unmodified and modified zeolite was measured in order to understand gas permeation of the films. The CO_2TR of the LLDPE/SEBS with various contents of unmodified and OTS-modified zeolites are presented in Figure 4.30. It can be noted that the unmodified zeolite-filled film with 5%wt gave similar CO_2TR to the OTS-modified zeolite-filled film. In contrast, LLDPE/SEBS films with 10 and 15%wt of unmodified zeolite exhibited remarkable increase trend for CO_2 permeation. In

addition, the blend with unmodified zeolite has poor compatibility between zeolite and polymers as observed from morphology (Figure 4.18). It could suggest that significant increase in CO_2 permeability was due to the presence of interfacial-void, leading to high diffusion but non-selective of ethylene gas.

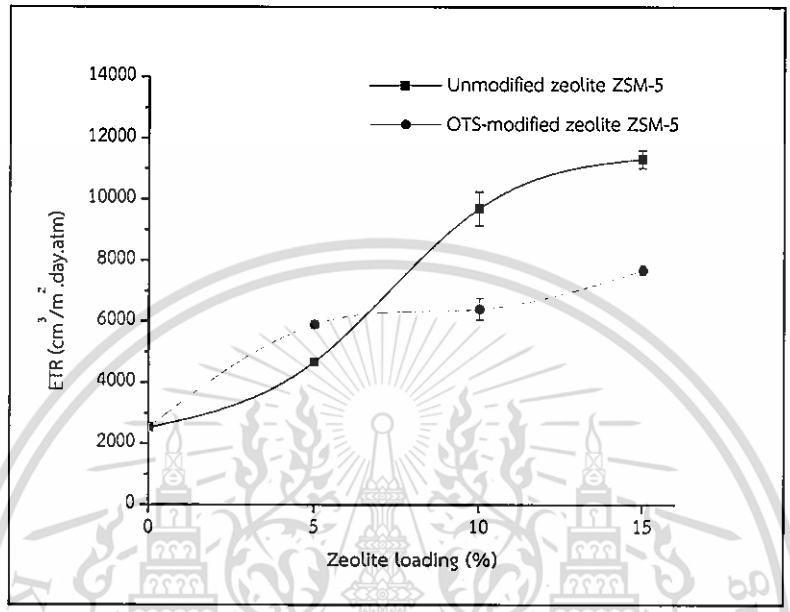

Figure 4.29 Ethylene transmission rate of the LLDPE/SEBS films with various zeolite loadings

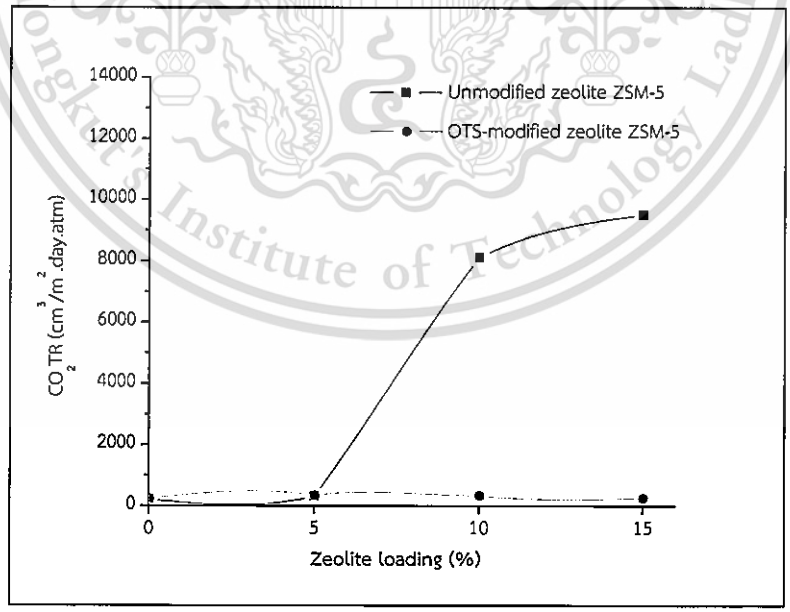

Figure 4.30 Carbon dioxide transmission rate of the LLDPE/SEBS films with various zeolite loadings

Comparing result in the literature, it can be seen that developed composite films in this work provide relatively high flux of ethylene as presented in Table 4.7.

Table 4.7 Flux of ethylene obtained in the present work compared to those described in literature

Membranes type	Pressure (bar)	Thickness (μm)	Flux of ethylene ($cm^3/m^2.day$)	References
Polymer of intrinsic microporosity (PIM-1)	2	100±10	~940	[75]
Polymer of intrinsic microporosity with hydroxyl functionalities (PIM-6FDA-OH)	2	90±10	~4,400	[76]
Composite hollow fiber membranes: Polypropylene (PP)/ Ethylene propylene diene terpolymer (EPDM)	3	N/A	~650,000	[77]
Composite hollow fiber membranes: Poly(ethylene oxide) (PEO)/poly(butylene terephthalate) (PBT)	1	125±25	~124	[78]
LLDPE/SEBS/OTS-modified zeolite ZSM-5	1	50±8	~7,700	This work

Chapter 5
Conclusions and Suggestions

5.1 Conclusions

The LLDPE/SEBS blend film (70/30 weight ratio) with zeolite exhibited relatively high ethylene permeability. This is because the zeolite has porous structures and continuous channel which is selective with ethylene gas. It was found that the unmodified zeolite-filled film had a high ethylene transmission rate (ETR) in comparison with LLDPE/SEBS blend film. However, unmodified zeolite-filled film had poor compatibility between zeolite and the blend.

In order to improve the compatibility between zeolite and polymer, surface modification of zeolite was carried out to reduce zeolite surface polarity, hence increase its hydrophobicity. However, the incorporation of 5%wt APS/PE-g-MA-modified zeolite in the LLDPE/SEBS blend film resulted in larger dispersed SEBS phase size, as compared to that in the LLDPE/SEBS blend film without zeolite or with unmodified zeolite. This is because PE-g-MA in APS/PE-g-MA-modified zeolite had entanglement with LLDPE more than that of SEBS, resulting in coalescence of SEBS. Therefore, APS/PE-g-MA-modified zeolite reduced compatibility between LLDPE and SEBS. The better compatibility of polymers in the APS/PE-g-MA-modified zeolite-filled film can be obtained when increasing the rotor speed from 60 to 100 rpm. Subsequently, the ETR, tensile strength and %elongation at break of this film were improved, as compared to APS/PE-g-MA-modified zeolite-filled film at 60 rpm and unmodified zeolite-filled film.

Alternatively, the zeolite surface was modified with OTS. ETR of OTS-modified zeolite-filled film was significantly improved, as compared to all the zeolite-filled film at 5%wt zeolite content. This is due to the long chain alkyl silane of OTS that increased hydrophobicity of the modified zeolite surface. Therefore, good distribution and dispersion of modified zeolite in the film were achieved because the zeolite had selective with ethylene gas, shortens diffusion pathway for ethylene gas and high virtual ethylene concentration gradient.

The tensile strength of unmodified and OTS-modified zeolite-filled film were enhanced with an increasing the zeolite loading (higher than Thai Industrial Standard,

7 MPa). This is because of a good affinity between styrene segment in SEBS and zeolite. Additionally, the ETR of unmodified and OTS-modified zeolite-filled film were enhanced with an increasing the zeolite loading. As discussed, zeolite had shortens diffusion pathway for ethylene gas and high virtual ethylene concentration gradient, resulting in facilitated ethylene permeation. However, the unmodified zeolite-filled film at high zeolite loadings (10-15%wt) exhibited remarkable increase in carbon dioxide permeation due to the presence of interfacial-void, leading to high diffusion but non-selective of ethylene gas.

Finally, it could be concluded that LLDPE/SEBS/zeolite ZSM-5 films with high permselectivity for ETR and with acceptable tensile properties could be achieved when using OTS-modified zeolite at least 10%wt loading.

5.2 Suggestions for future studies

1) Film production processing methods as used in an industry such as melt casting and blow film processes could be studied.

2) Shelf-life test of fresh vegetables and fruits should be evaluated using the developed film.

3) Other properties of films such as brightness and color could be further investigated.

References

[1] Karnjanaworawanit B. 2015. **Extend the Life of Fruits and Vegetables.** [Online]. Available: http://www.mtec.or.th/index.php?option=com_content&task=view&id=1389&Itemid=176.

[2] Thailand Institute of Scientific and Technological Research. 2015. **Ripening of Fruits.** [Online]. Available: http://www.tistrfoodprocess.net/Fruit/fruit_home/fruit_home2.html#top.

[3] Peacock A.J. 2000. **Handbook of Polyethylene Structure, Properties and Applications.** New York : Marcel Dekker.

[4] Wiwattananukul R. 2013. "Study on LLDPE/SEBS Blend for Improving Ethylene Permeability of Packaging Film." M.Sc. Thesis, King Mongkut's Institute of Technology Ladkrabang.

[5] Hongthong K., Makphon K. and Rungroang C. 2013. "Study on LLDPE/SEBS/ Zeolite ZSM-5 Blends for Improving Ethylene Permeation of Packaging Film." B.Sc. Special Project, King Mongkut's Institute of Technology Ladkrabang.

[6] Sahassanon T., Rukchonlatee S., Sooknoi T. and Ritvirulh C. 2015. "Improvement of Ethylene Permeation in LLDPE/SEBS Film with Zeolite Y." *The Proceedings of Pure and Applied Chemistry International Conference 2015* (PACCON 2015), January 21-23, Bangkok, Thailand, pp. 432-435.

[7] Paula A., Huang Y., Borja M.A.G. and Resasco D.E. 2013. "Silylated Hydrophobic Zeolites with Enhanced Tolerance to Hot Liquid Water." *Journal of Catalysis.* 308 : 82-97.

[8] Tsuyoshi W., Yosuke N., Shingo K. and Katasunori Y. 2013. "Development of Amine-Modified Solid Sorbents for Postcombustion CO_2 Capture." *Energy Procedia.* 37 : 199-204.

[9] Saltveit M.E. 1999. "Effect of Ethylene on Quality of Fresh Fruits and Vegetables." *Postharvest Biology and Technology.* 15(3) : 279-292.

[10] Vemeiren L., Devliegher L.F., Van Beest M., De Kruijf N. and Debevere J. 1999. "Development in the Packaging of Foods." *Trend in Food Science and Technology.* 10 : 77-86.

[11] Yahia E.M. 2009. **Modified and Controlled Atmosphere for the Storage,**

Transpiration and Packaging of Horticultural Commodities. New York : CRC Press.

[12] Jongen W. 2002. **Fruit and Vegetable Processing.** New York : Woodhead Publishing Ltd and CRC Press.

[13] Irtwange S.V. 2006. "Application of Modified Atmosphere Packaging and Related Technology in Postharvest Handling of Fresh Fruits and Vegetables." *Agricultural Engineering International: the CIGR Ejournal Invited Overview.* 3(4) : 178-187.

[14] Watson J.A., Treadwell D., Sargent S.A., Brecht J.K. and Pelletier W. 2004. "Postharvest Storage, Packaging and Handling of Specialty Crops: A Guide for Florida Small Farm Producers." Book Net, University of Florida.

[15] FAO. 1989. **Prevention of Post-Harvest Food Losses Fruits, Vegetables and Root Crops.** Rome : Food and Agriculture Organization of The United Nations.

[16] Chris B.W. and Jacqueline F.N. 2012. "Production Guide for Storage of Organic Fruits and Vegetables." Department of Horticulture, Cornell University.

[17] Blakistone. 1999. **Principles and Applications of Modified Atmosphere Packaging of Foods.** Washington, DC : Aspen Publishers.

[18] Mangaraj S., Goawami T.K. and Mahajan P.V. 2009. "Application of Plastic Films for Modified Atmosphere Packaging of Fruits and Vegetables." *Food Engineering Reviews.* 1(2) : 133-158.

[19] Zagory D. and Kader A.A. 1998. "Modified Atmosphere Packaging of Fresh Product." *Food Technology.* 42(9) : 70-77.

[20] Kader A.A., Zagory D. and Kerbel E.L. 1989. "Modified Atmosphere Packaging of Fruits and Vegetables." *Food Science and Nutrution.* 28(1) : 1-30.

[21] Campbell A. and Potter L. 2011. "Active Modification of Atmospheres in Packages." *Modified Atmosphere Packaging for Fresh-Cut Fruits and Vegetables.* 1(2) : 141-146.

[22] Suwandi M.S. and Anhar S. 1987. **Membrane Technology: Proceedings of the Fourth ASEAN (Training) Workshop on Membrane Technology Held at National University of Malaysia in April 15-25.** Bangi : Asean Working Group on Food Waste Materials.

[23] Baker R.W. 2004. **Membrane Technology and Applications.** New York : John

Wiley and Sons.

[24] Rowan University. 2005. **Membrane Gas Separation.** [Online]. Available: http://users.rowan.edu/~savelski/uol/gas.html.

[25] Apisittinet S. 2007. "Study on Ethylene Gas Permeability of Zeolite-LDPE and Zeolite SEBS Composite Film." M.Sc. Thesis, King Mongkut's Institute of Technology Ladkrabang.

[26] Comyn J. 1985. "Polymer Permeability." London : Elsevier Applied Science Publishers.

[27] Young S. 2004. **Gas and Liquid Diffusion in Membranes.** [Online]. Available: http://www.psrc.usm.edu/mauritz/diffuse.html.

[28] Thomas S., Grohens Y. and Jyotishkumar P. 2014. **Characterization of Polymer Blends: Miscibility, Morphology, and Interfaces.** Weinheim : Wiley-VCH Verlag.

[29] Charles E. and Carraher Jr. 2012. **Introduction to Polymer Chemistry.** 3rd ed. London : Taylor and Francis group.

[30] Grulke A.E. 1994. **Polymer Process Engineering.** New Jersey : Prentice-Hall.

[31] Lohse D.J. and Datta S. 1996. **Polymeric Compatibilizers : Uses and Benefits in Polymer Blends.** New York : Hanser Publishers.

[32] Wikipedia. 2015. **Linear Low-Density Polyethylene.** [Online]. Available: https://en.wikipedia.org/wiki/Linear_low-density_polyethylene.

[33] Polymer Science Learning Center. 2016. **Polyethylene.** [Online]. Available: http://www.pslc.ws/macrog/pe.htm

[34] Lepoutre P. 2015. **The Manufacture of Polyethylene.** Guangdong : Transpak Industries.

[35] A Recognized Student Organization at Texas A and M University. 2014. **Branching in Polyethylenes.** [Online]. Available: http://plastics.tamu.edu/classresourcebranching-Polyethylenes.

[36] Liang G., Xu J., Bao S. and Xu W. 2003. "Polyethylene/Maleic Anhydride Grafted Polyethylene/Organic-Montmorillonite Nanocomposites. I. Preparation, Microstructure, and Mechanical Properties." *Journal of Applied Polymer Science*. 91(6) : 3974-3980.

[37] Susan P.J., Susan S.Y. and Ariane V. 2012. "Polymeric Materials Including a

Glycosaminoglycan Networked with a Polyolefin-Containing Polymer." Book Net, Colorado State University Research Foundation.

[38] Legge N.R., Holden G. and Schroeder H.E. 1987. **Thermoplastic Elastomers.** New York : Hanser Publishers.

[39] Eastman Chemical Company. 2015. **Block Copolymer.** [Online]. Available: http://www.eastman.com/Markets/Tackifier_Center/Block_Copolymer.htm.

[40] Specialchem and Omnexus. 2015. **Block Copolymers Based on Styrene and Butadiene (TPE-S or SBS, SEBS).** [Online]. Available: http://www.omnexus.com/plastics-channels/rubber-replacement/performances.aspx?id=types.

[41] Kraton Polymer LLC. 2006. **An Introduction to Kraton Polymer.** [Online]. Available: http://www.kraton.com/content/includes/An%20Intro%20To%20Kraton.pdf.

[42] Dyer A. 1988. **An Introduction to Zeolite Molecular Sieves.** New York : John Wiley and Sons.

[43] Auerbach S.M., Carrado K.A. and Dutta P.K. 2003. **Handbook of Zeolite Science and Technology.** New York : Basel.

[44] Donk S.V. 2002. **Adsorbtion, Diffusion and Reaction Studies of Hydrocarbons on Zeolite Catalysts.** [Online]. Available: http://igitur-archive.library.uu.nl/dissertations/2002-1209-125604/c1.pdf.

[45] Meier W.M. 1968. **Zeolite Structures In: Molecular Sieves.** London : Society of Chemical Industry.

[46] Szostak R. 1989. **Molecular Sieves: Principles of Synthesis and Identification.** Connecticut : International Thomson Publishing.

[47] Wikipedia. 2015. **ZSM-5.** [Online]. Available: http://en.wikipedia.org/wiki/ZSM-5.

[48] Roy A.H., Broudy R.R., Auebach S.M. and Vinning W.J. 2009. **Teaching Materials that Matter: An Interactive, Multi-media Module on Zeolite in General Chemistry.** [Online]. Available: http://samson.chem.umass.edu/~auerbach/pub_pdf/pap24.pdf.

[49] University of California San Diego. 2008. **ZSM-5 Catalyst.** [Online]. Available: http://chemelab.ucsd.edu/methanol/memos/ZSM-5.html.

[50] Saremi P. 2015. **Adsorption of Bio-Based Butanol and Butyric Acid Solution by Using ZSM-5.** [Online]. Available: https://pure.ltu.se/ws/files/34419081/LTU-EX-2011-34332120.pdf.

[51] Lenntech. 2015. **Zeolite Application.** [Online]. Available: http://www.lenntech.com/zeolites-applications.htm.

[52] Wilmot J. 2015. **Zeolite Adsorbents.** [Online]. Available: http://www.cefic.be/Templates/shwAssocDetails.asp?NID=473&HID=429&ID=177.

[53] Auerbach S.M., Carrado K.A. and Dutta P.K. 2003. **Handbook of Zeolite Science and Technology.** New York : Basel.

[54] A Meryer Chemical Technology Shanghai Company. 2005. **Silane Coupling Agents.** Shanghai : Gelest.

[55] Power Chemical Corporation. 2015. **SiSiB Silane Coupling Agent.** [Online]. Available: http://www.powerchemical.net/coupling1.htm.

[56] Power Chemical Corporation. 2015. **Products–Chloro Silanes.** [Online]. Available: http://www.powerchemical.net/silanes/chlorosilanes.html.

[57] Wikipedia. 2015. **Chlorosilane.** [Online]. Available: https://en.wikipedia.org/wiki/Chlorosilane.

[58] Power Chemical Corporation. 2015. **Products–Regular Commercial Amino Silanes.** [Online]. Available: http://www.powerchemical.net/silanes/aminosilanes.html.

[59] Vemeiren L., Devliegher L.F., Beest M.V., Kruijf N.D. and Debevere J. 1999. "Development in the Packaging of Foods." *Trend in Food Science and Technology*. 10 : 77-86.

[60] Rooney M.L. 1995. **Active Food Packaging.** London : Blackie Academic and Professional.

[61] Suslow T. 1997. "Performance of Zeolite Based Products in Ethylene Removal." *Perishables Handling Quarterly.* 92 : 32-33.

[62] Reed D. 2009. **Senescence and Post-Harvest Storage.** [Online]. Available: http://generalhorticulture.tamu.edu/HORT604/LectureSupplMex07/SenescencePostHarvest.pdf.

[63] Monprasit P., Ritvirulh C., Sooknoi T., Rukchonlatee S., Fuongfuchat A. and Sirikittikul D. 2011. "Selective Ethylene-Permeable Zeolite Composite Double-Layered Film for Novel Modified Atmosphere Packaging." *Polymer Engineering and Science*. 51(7) : 1264-1272.

[64] Sirikittikul D., Fuongfuchat A. and Booncharoen W. 2008. "Chemical Modification

of Zeolite Beta Surface and Its Effect on Gas Permeation of Mixed Matrix Membrane." *Polymers Advanced Technologies*. 20 : 802-810.

[65] Qiao B., Wang T.J., Gao H. and Jin Y. 2015. "High Density Silanization of Nano-Silica Particle Using 3-Aminopropyltriethoxysilane (APTES)." *Applied Surface Science*. 351 : 646–654.

[66] Shokri E., Yegani R., Heidari S. and Shoeyb Z. 2015. "Effect of PE-g-MA Compatibilizer on the Structure and Performance of HDPE/EVA Blend Membranes Frabricated via TIPS Method." *Chemical Engineering Research and Design*. 100 : 237-247.

[67] Dow Chemical. 2015. **Dow Plastic – Film Grade.** [Online]. Available: http://www.universalpolymer.com/images/column_1247455937/DowDatasheet.pdf.

[68] Kraton Polymer LLC. 2006. **Data Document Kraton® G1657M Polymer.** [Online]. Available: http://docs.kraton.com/pdfDocuments/20090925144339859648l5.pdf.

[69] Zeolyst International. 2006. **Data Sheet of ZSM-5 Type Zeolite Product (MFI).** [Online]. Available: http://www.zeolyst.com/html/zsm5.asp.

[70] BYK Additives and Instruments. 2015. **SCONA TSPE 1112 GALL.** [Online]. Available:file:///C:/Users/Admin/Downloads/TDS_SCONA_TSPE_1112_GALL_EN.pdf.

[71] Han X., Wang L., Li J., Zhan X., Chen J. and Yang J. 2011. "Tuning the Hydrophobicity of ZSM-5 Zeolites by Surface Silanization using Alkyltrichlorosilane." *Applied Surface Science*, 257(22) : 9525-9531.

[72] Thailand Industrial Standards Institute. 1987. "Standard for Polyethylene Plastic Film for Agriculture." Bangkok : Thailand Industrial Standards Institute.

[73] Bigg D.M. 1988. "Mechanical Property Enhancement of Semicrystalline Polymers." *Journal of Engineering and Science*. 28(13) : 830-841.

[74] Dahlan H.M., Zaman M.D.K. and Ibrahim A. 2002. "The Morphology and Thermal Properties of Liquid Natural Rubber (LNR)-Compatibilized 60/40 NR/LLDPE Blends." *Polymer Testing*. 21 : 905-911.

[75] Salinas O., Ma X., Litwiller E. and Pinnau I. 2016. "Ethylene/Ethane Permeation,

Diffusion and Gas Sorption Properties of Carbon Molecular Sieve Membranes Derived from the Prototype Ladder Polymer of Intrinsic Microporosity (PIM-1)." *Journal of Membrane Science.* 504 : 133-140.

[76] Salinas O., Ma X., Litwiller E. and Pinnau I. 2016. "High-Performance Carbon Molecular Sieve Membranes for Ethylene/Ethane Separation Derived from an Intrinsically Microporous Polyimide." *Journal of Membrane Science.* 500 : 115-123.

[77] Nymeijer D.C., Visser T.A. and Wessling M. 2004. "Composite Hollow Fiber Gas–Liquid Membrane Contactors for Olefin/Paraffin Separation." *Separation and Purification Technology* 37 : 209–220.

[78] Nymeijer K., Visser T., Assen R. and Wessling M. 2004. "Olefin-Selective Membranes in Gas-Liquid Membrane Contactors for Olefin/Paraffin Separation." *Industrial and Engineering Chemistry Research.* 43 : 720-727.

[79] Billmeyer F.W. 1984. **Textbook of Polymer Science.** New York : John Wiley and Sons Inc.

Appendices

Appendix A

TGA

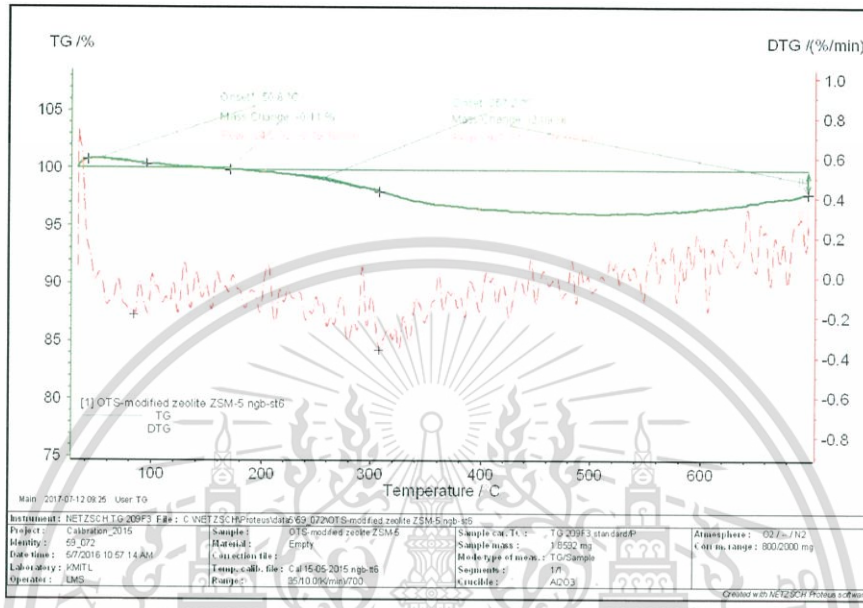

Figure A.1 TGA thermogram of OTS-modified zeolite ZSM-5

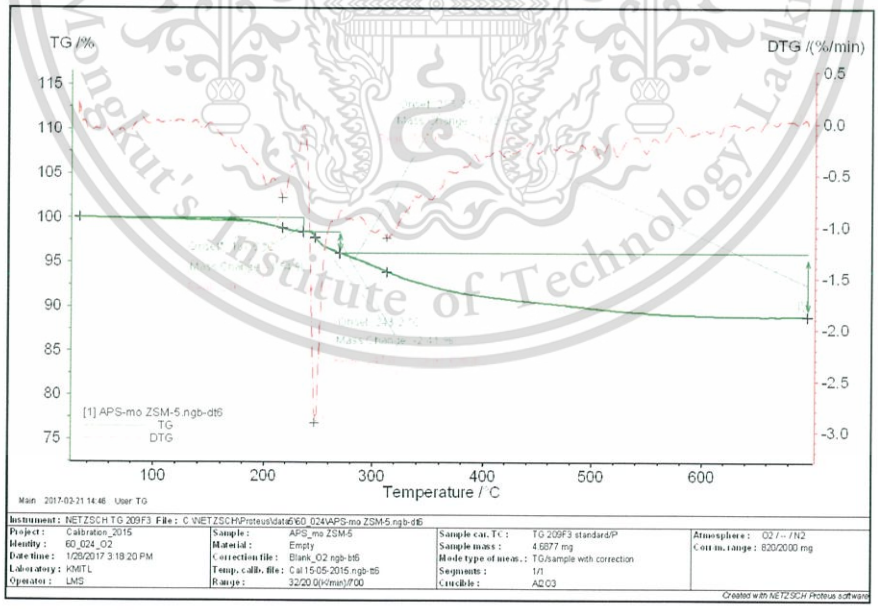

Figure A.2 TGA thermogram of APS/PE-g-MA-modified zeolite ZSM-5

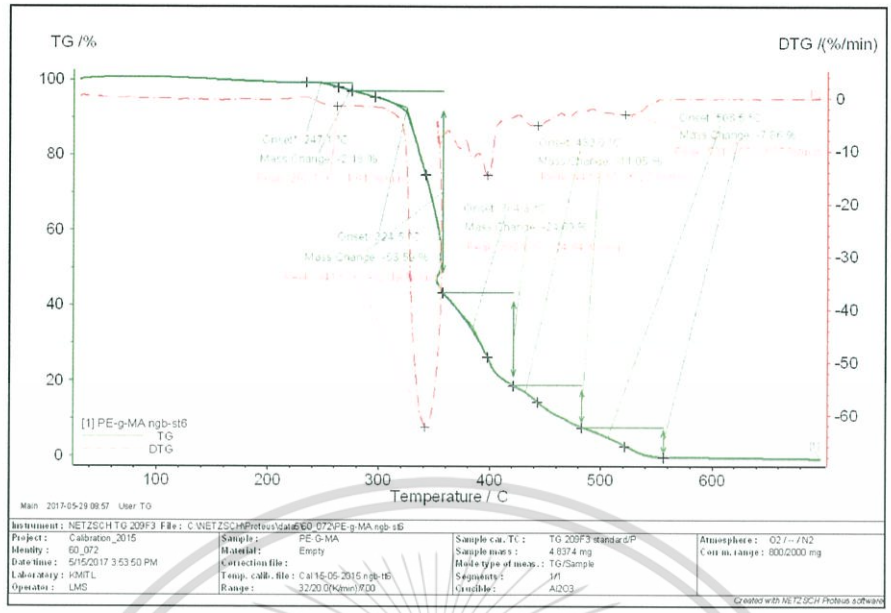

Figure A.3 TGA thermogram of PE-g-MA

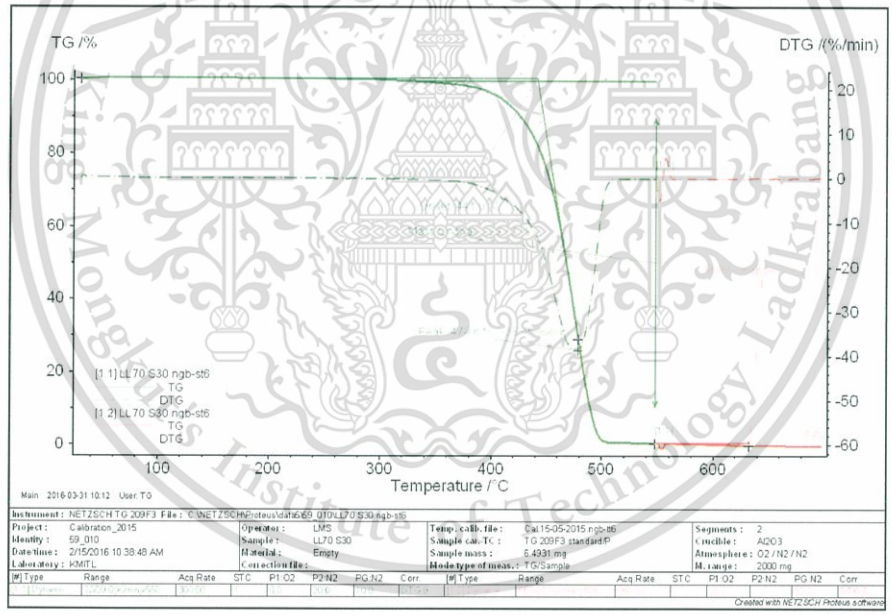

Figure A.4 TGA thermogram of LL70S30 film

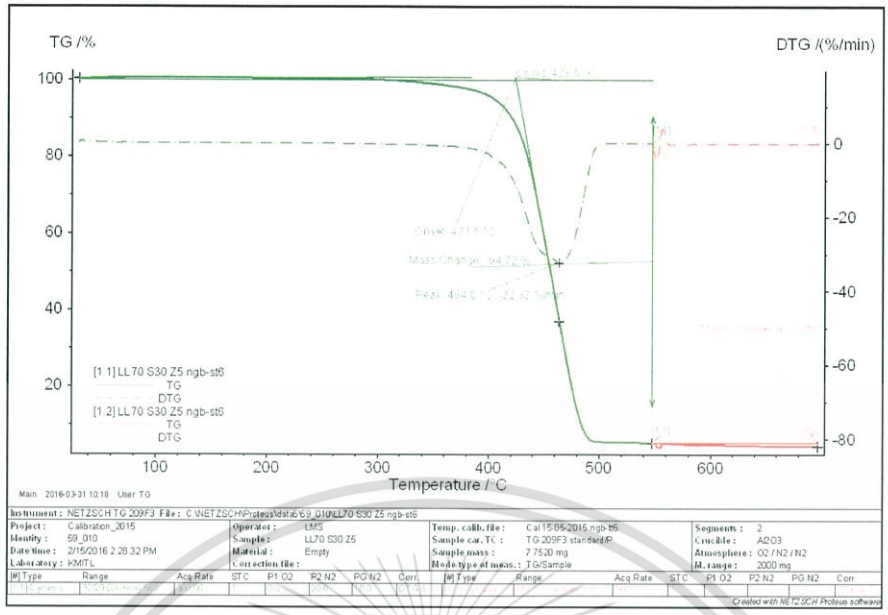

Figure A.5 TGA thermogram of LL70S30Z5 film

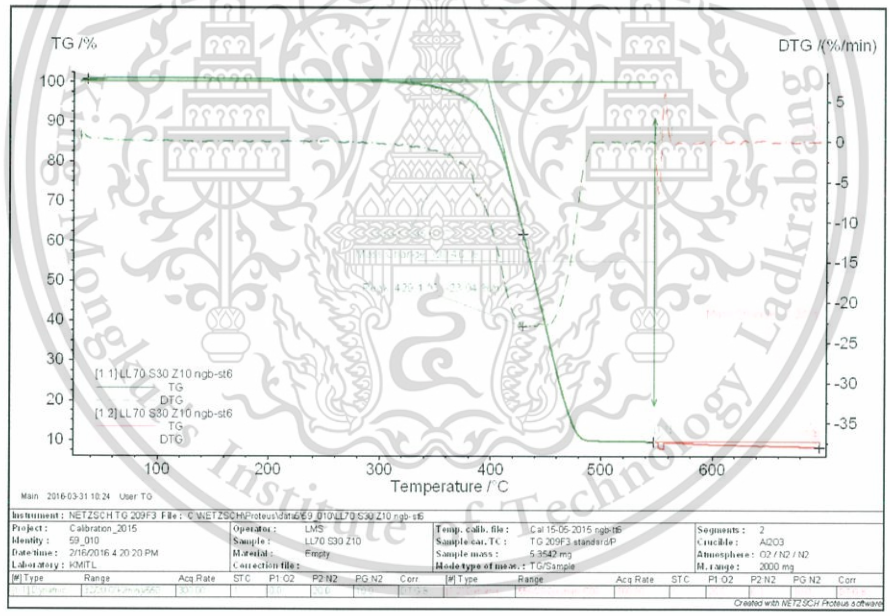

Figure A.6 TGA thermogram of LL70S30Z10 film

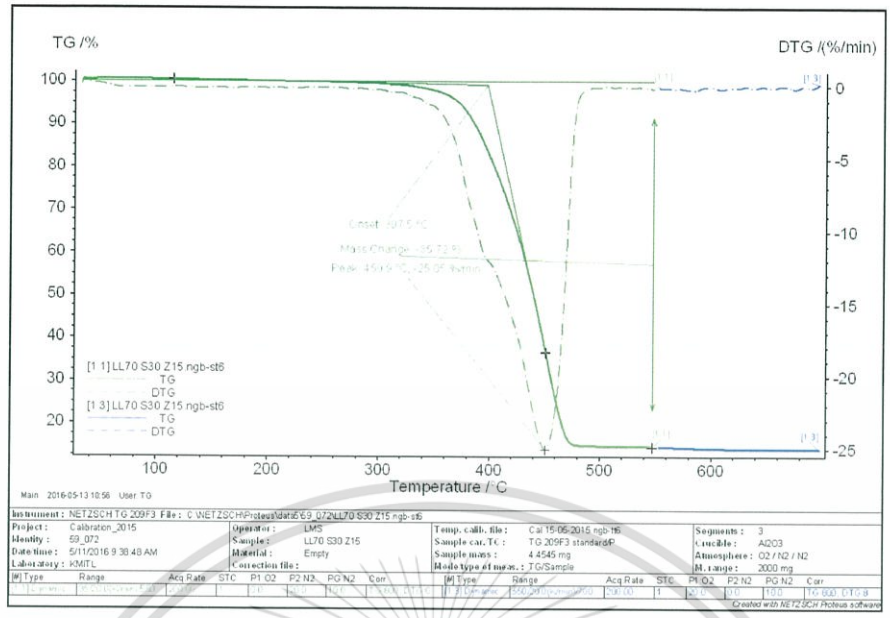

Figure A.7 TGA thermogram of LL70S30Z15 film

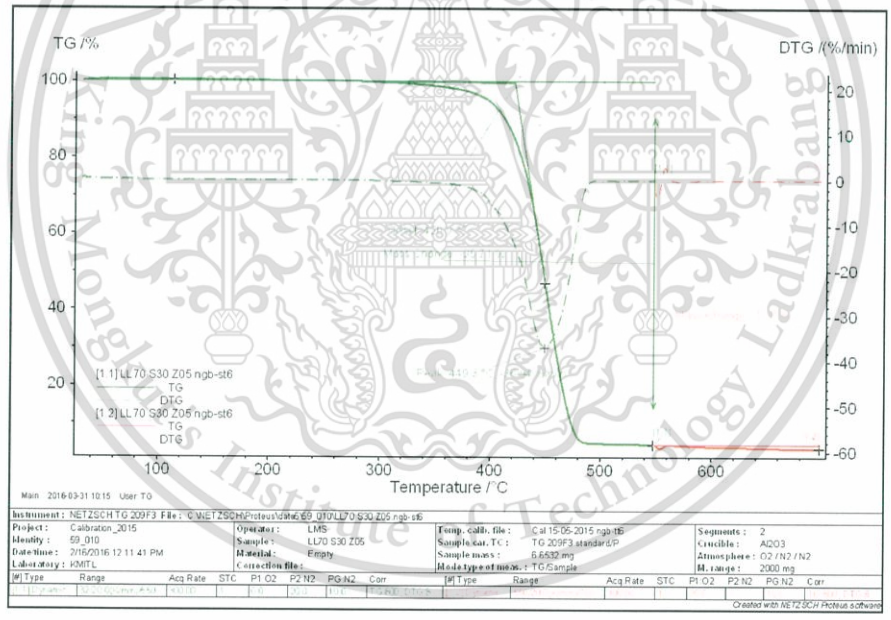

Figure A.8 TGA thermogram of LL70S30ZO5 film

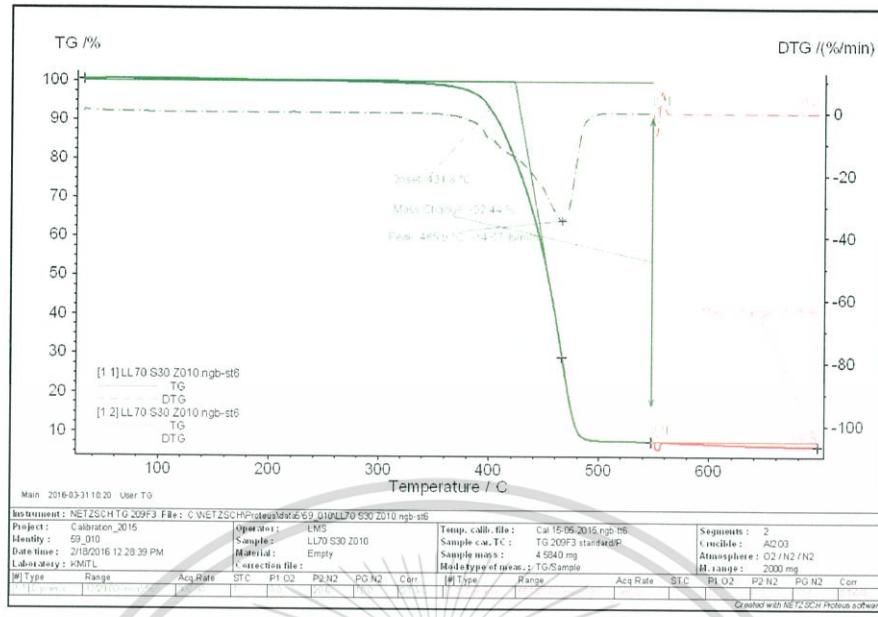

Figure A.9 TGA thermogram of LL70S30ZO10 film

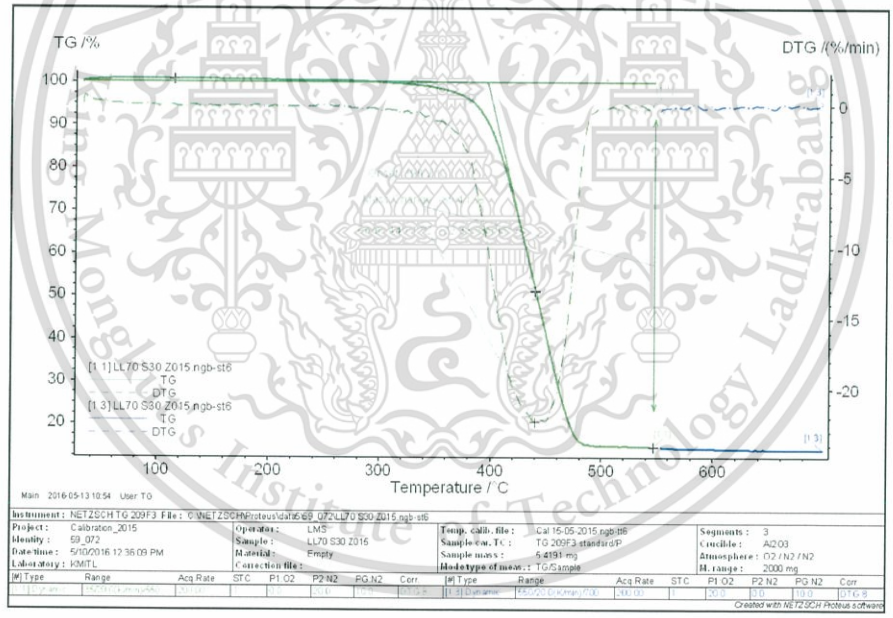

Figure A.10 TGA thermogram of LL70S30ZO15 film

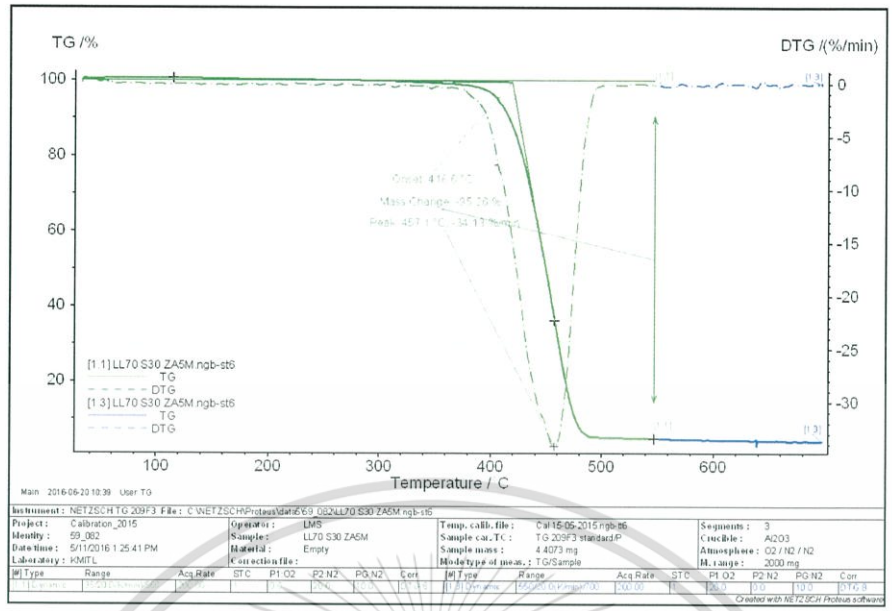

Figure A.11 TGA thermogram of LL70S30ZA5P film (60 rpm)

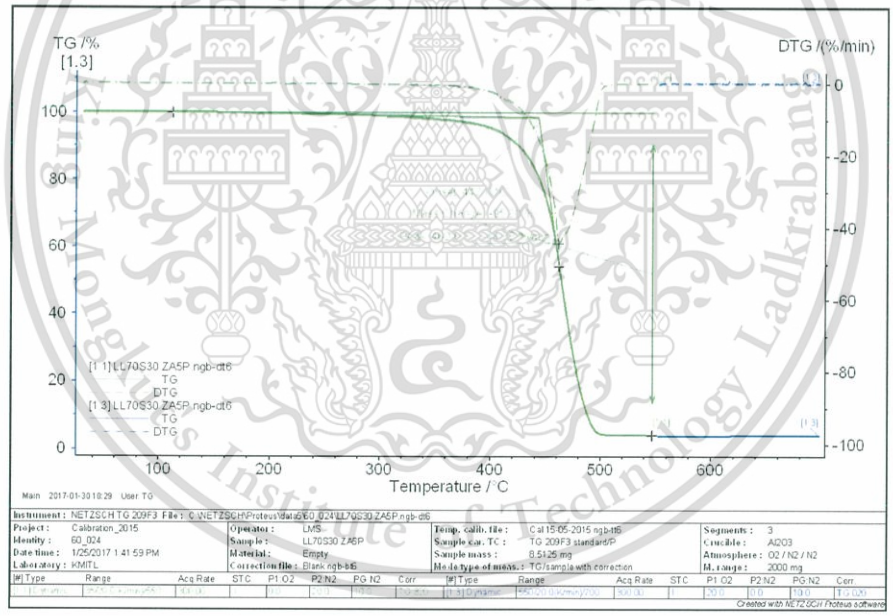

Figure A.12 TGA thermogram of LL70S30ZA5P film (100 rpm)

Appendix B

DSC

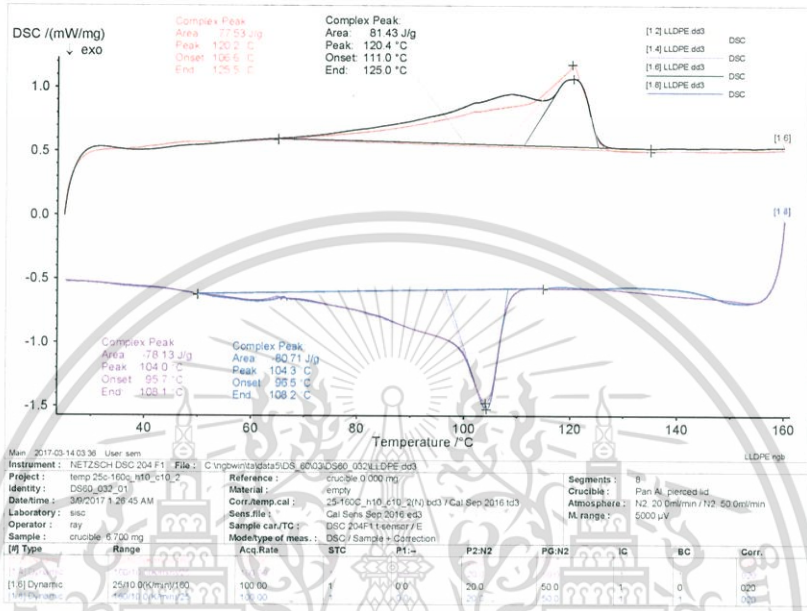

Figure B.1 DSC thermogram of LLDPE film

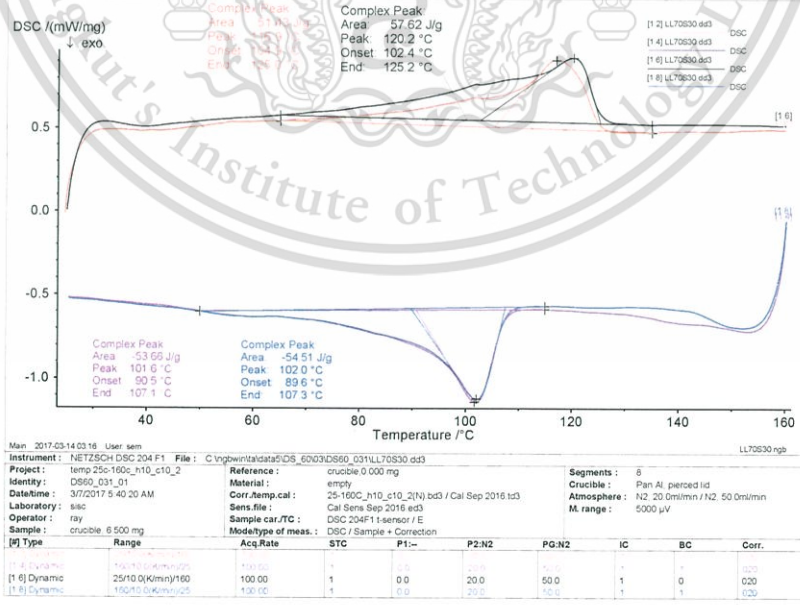

Figure B.2 DSC thermogram of LL70S30 film

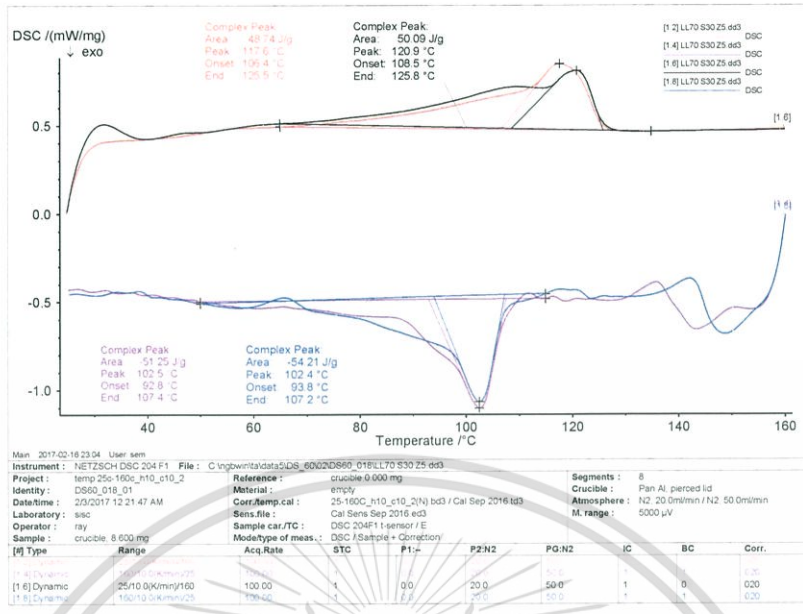

Figure B.3 DSC thermogram of LL70S30Z5 film

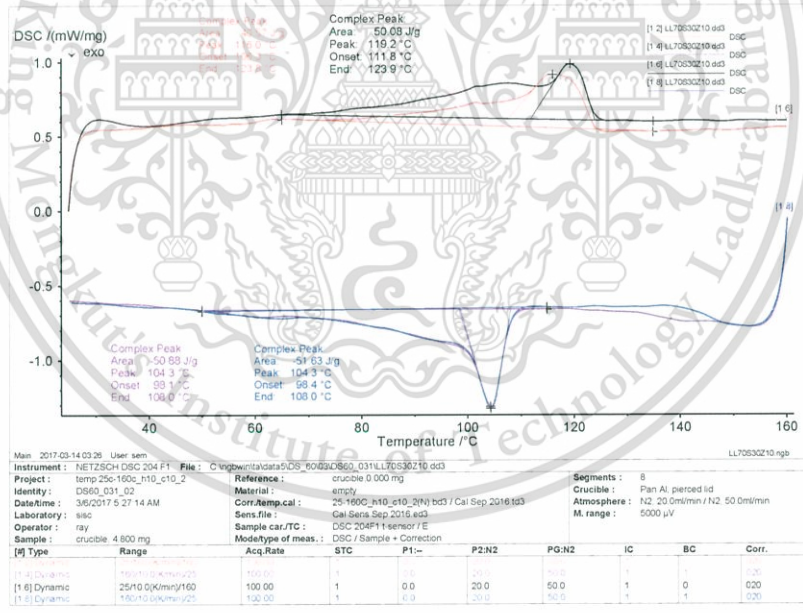

Figure B.4 DSC thermogram of LL70S30Z10 film

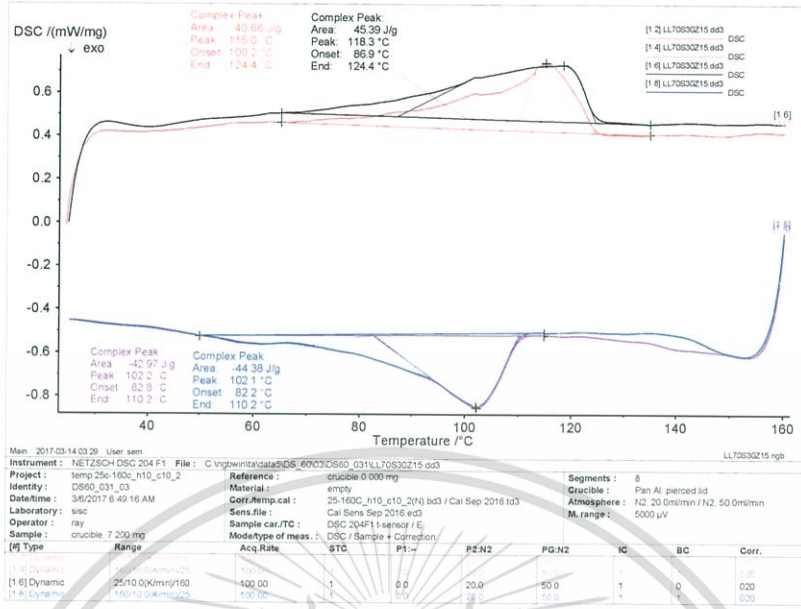

Figure B.5 DSC thermogram of LL70S30Z15 film

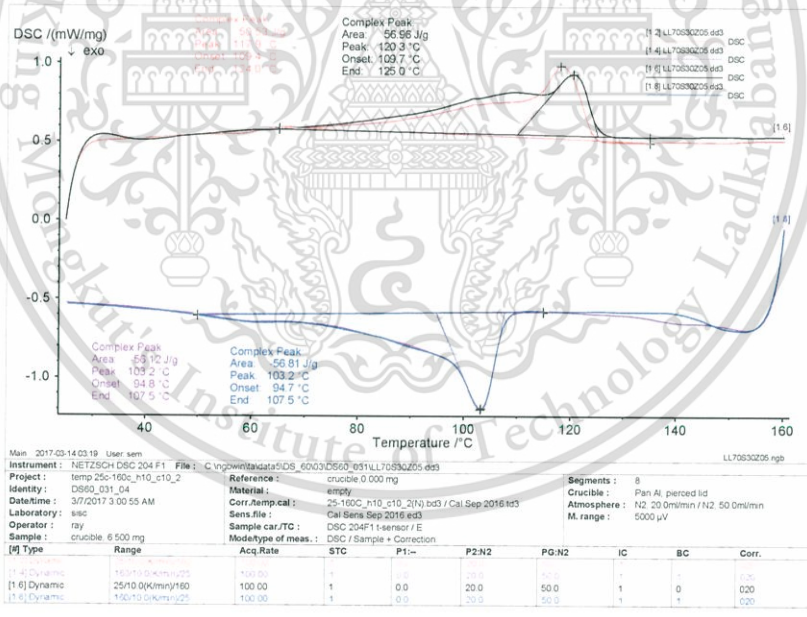

Figure B.6 DSC thermogram of LL70S30ZO5 film

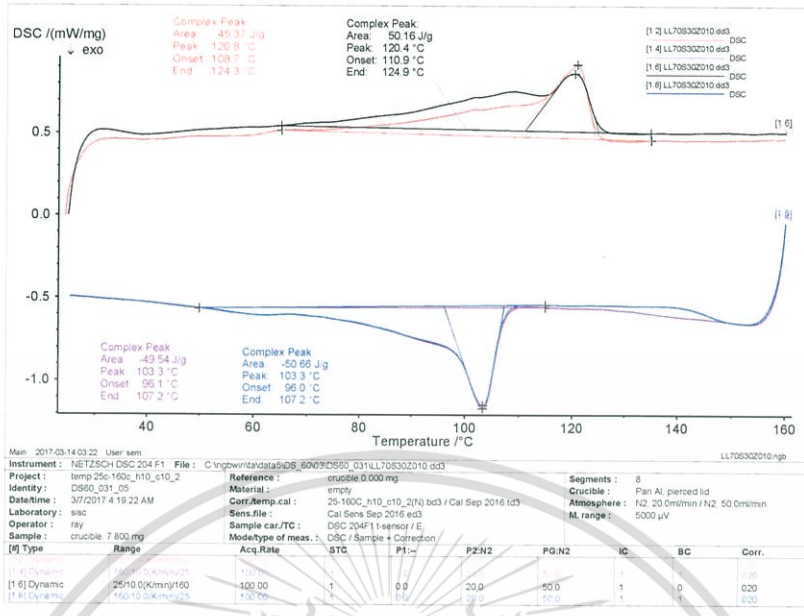

Figure B.7 DSC thermogram of LL70S30ZO10 film

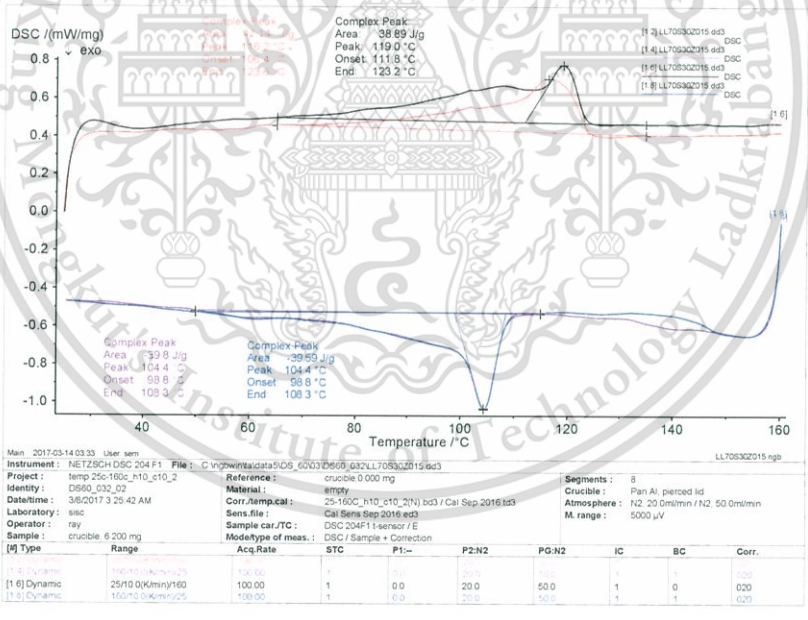

Figure B.8 DSC thermogram of LL70S30ZO15 film

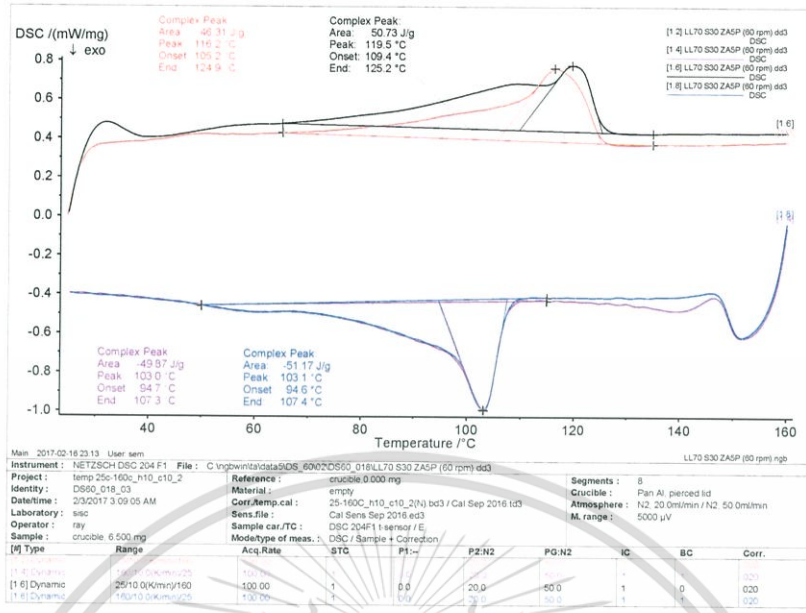

Figure B.9 DSC thermogram of LL70S30ZA5P film (60 rpm)

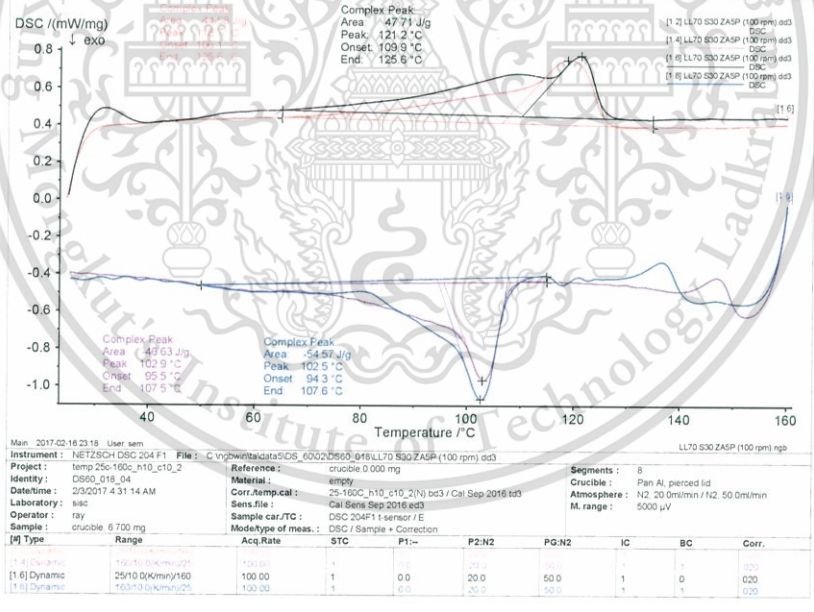

Figure B.10 DSC thermogram of LL70S30ZA5P film (100 rpm)

Table B.1 %Crystallinity of LLDPE

Sample	LLDPE in film (%wt)	ΔH_f (J/g)	Crystallinity, X_c (%)
LLDPE	100.0	77.53	27
LL70S30	70.0	51.43	25
LL70S30Z5	66.5	48.74	25
LL70S30Z10	63.0	40.57	22
LL70S30Z15	59.5	40.66	23
LL70S30ZO5	66.5	50.53	26
LL70S30ZO10	63.0	45.37	25
LL70S30ZO15	59.5	42.14	24
LL70S30Z5AP (60 rpm)	66.5	46.31	24
LL70S30Z5AP (100 rpm)	66.5	44.58	23

ΔH_f° (J/g) = 293 J/g (100% crystallinity of LLDPE) [79]

$$\%\text{Crystallinity} = \frac{\Delta H_f}{\Delta H_f^\circ} \times \frac{100}{\text{LLDPE in film (\%wt)}} \times 100$$

Example: %Crystallinity of LLDPE in LL70S30 film

$$= \frac{51.43}{293} \times \frac{100}{70} \times 100$$

$$= 25.08\%$$

$$\approx 25\%$$

Appendix C

Tensile properties

Table C.1 Tensile properties of the films

Sample	Thickness (μm)	Tensile strength at break (MPa)	Elongation at break (%)	Young's modulus (MPa)
LL70S30	70.0±8.8	5.6±0.5	514±62.7	50.8±6.2
LL70S30Z5	70.0±7.8	7.3±0.6	741±118.1	71.2±9.4
LL70S30Z10	72.0±8.6	7.9±0.5	667±140.9	68.6±10.6
LL70S30Z15	79.3±10.3	8.6±0.3	605±45.7	62.9±4.1
LL70S30ZO5	73.1±9.5	8.9±1.4	924±135.6	58.6±5.4
LL70S30ZO10	76.0±7.4	10.0±1.2	960±149.0	56.4±5.2
LL70S30ZO15	73.3±9.8	10.3±0.8	939±41.5	62.1±3.5
LL70S30ZA5P (60 rpm)	74.7±9.9	6.1±0.2	548±63.2	64.9±10.7
LL70S30ZA5P (100 rpm)	65.7±5.1	10.7±1.9	844±71.6	76.6±10.2

Appendix D

Ethylene permeation

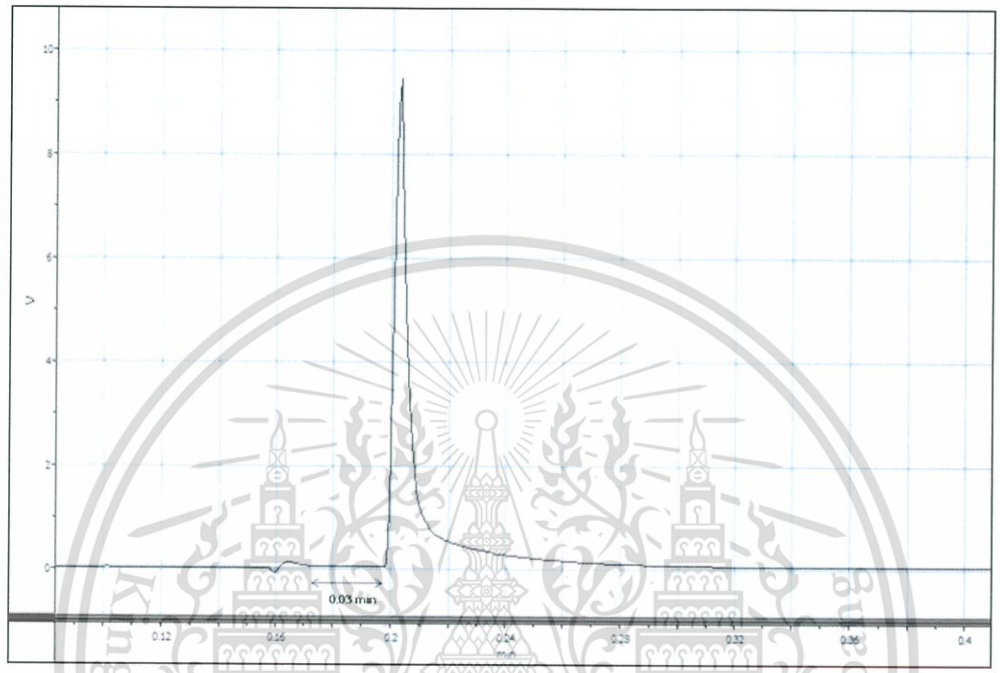

Figure D.1 TCD signal of standard ethylene

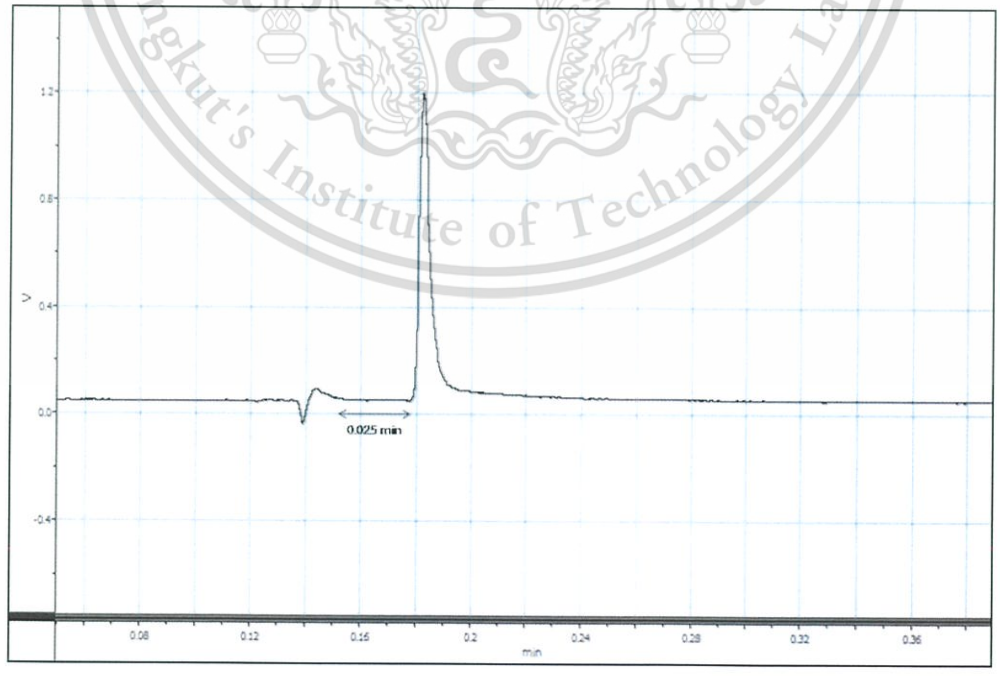

Figure D.2 TCD signal of ethylene in LL70S30 film

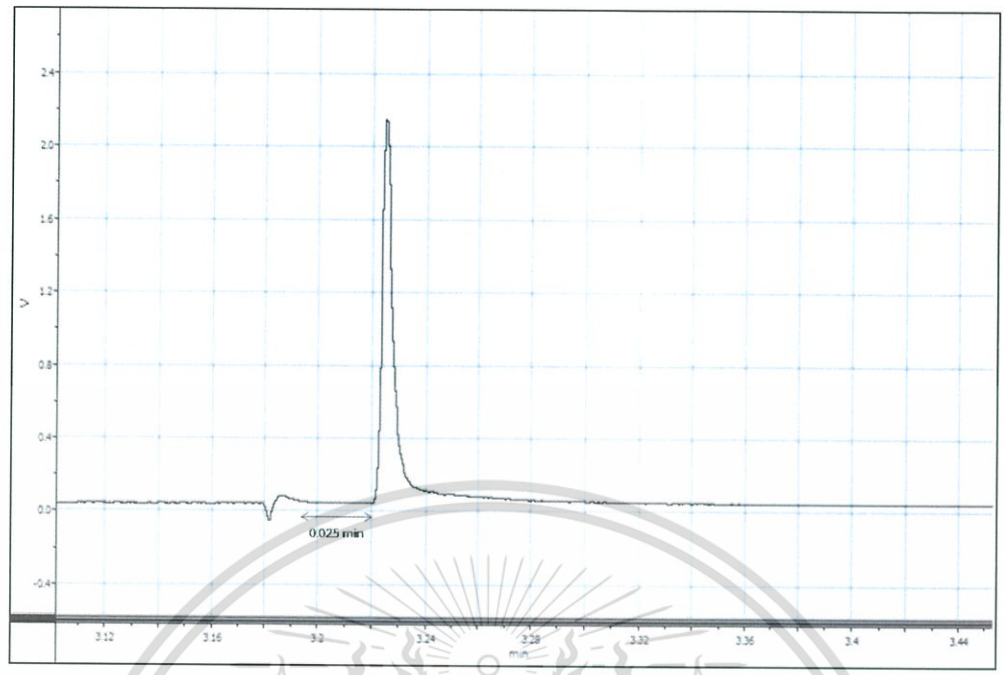

Figure D.3 TCD signal of ethylene in LL70S30Z5 film

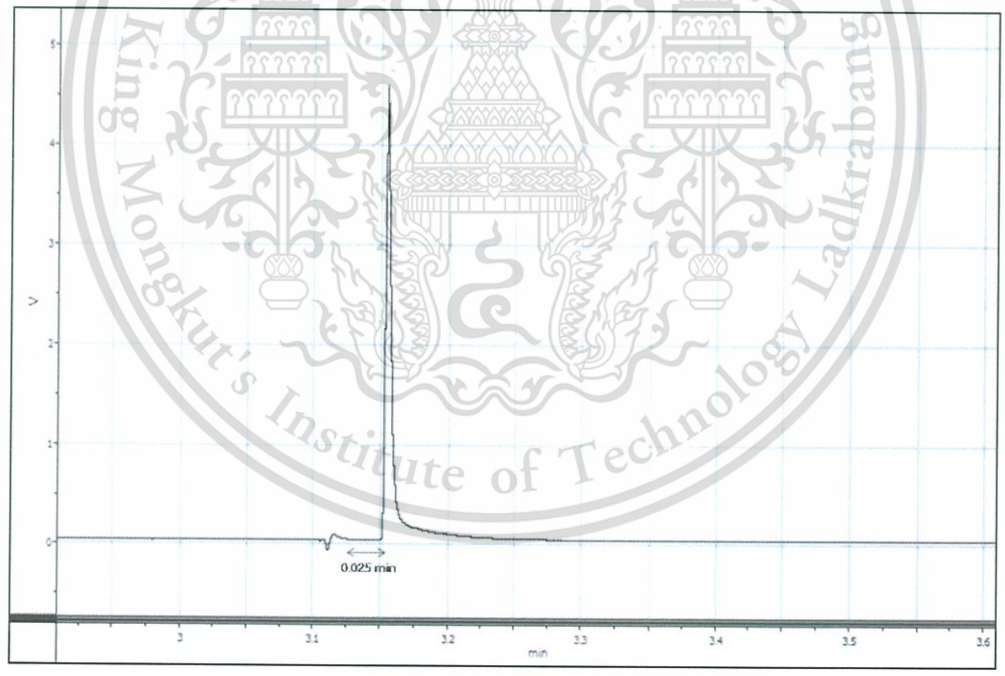

Figure D.4 TCD signal of ethylene in LL70S30Z10 film

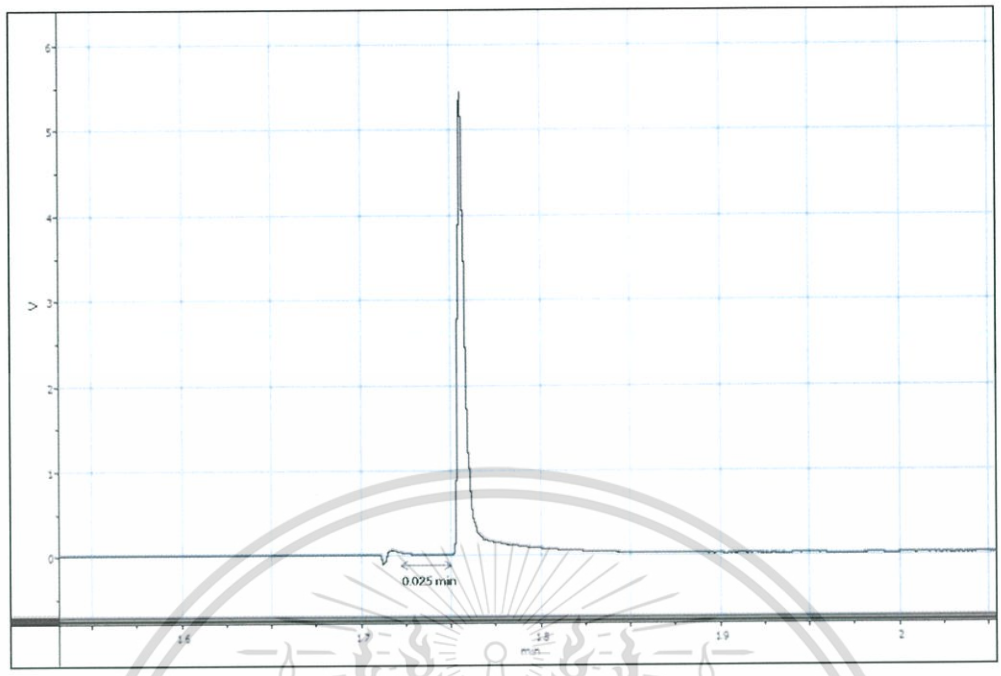

Figure D.5 TCD signal of ethylene in LL70S30Z15 film

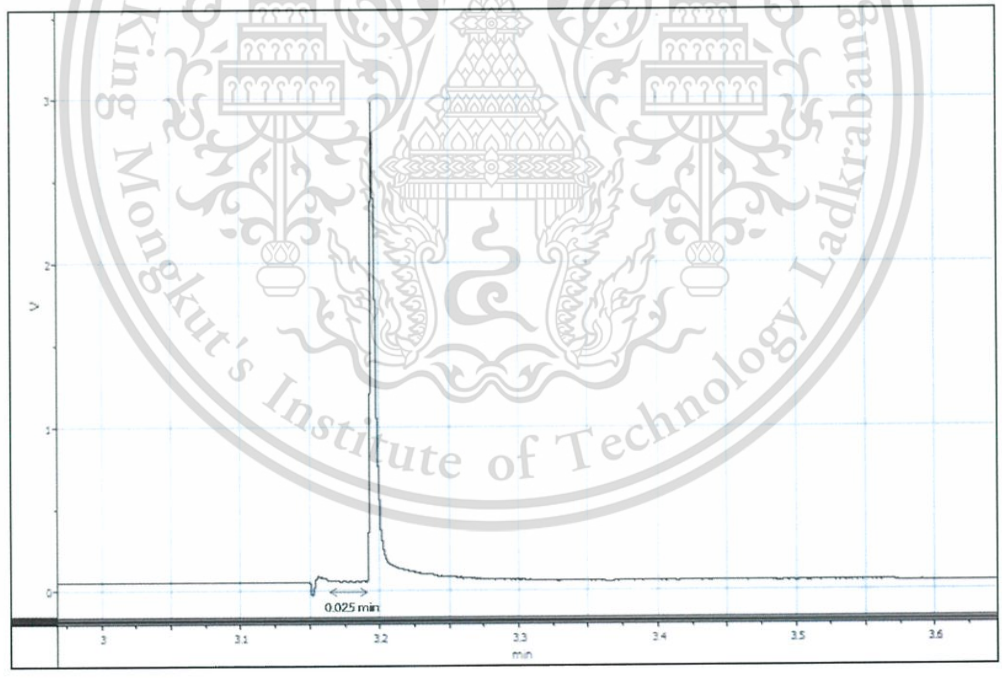

Figure D.6 TCD signal of ethylene in LL70S30ZO5 film

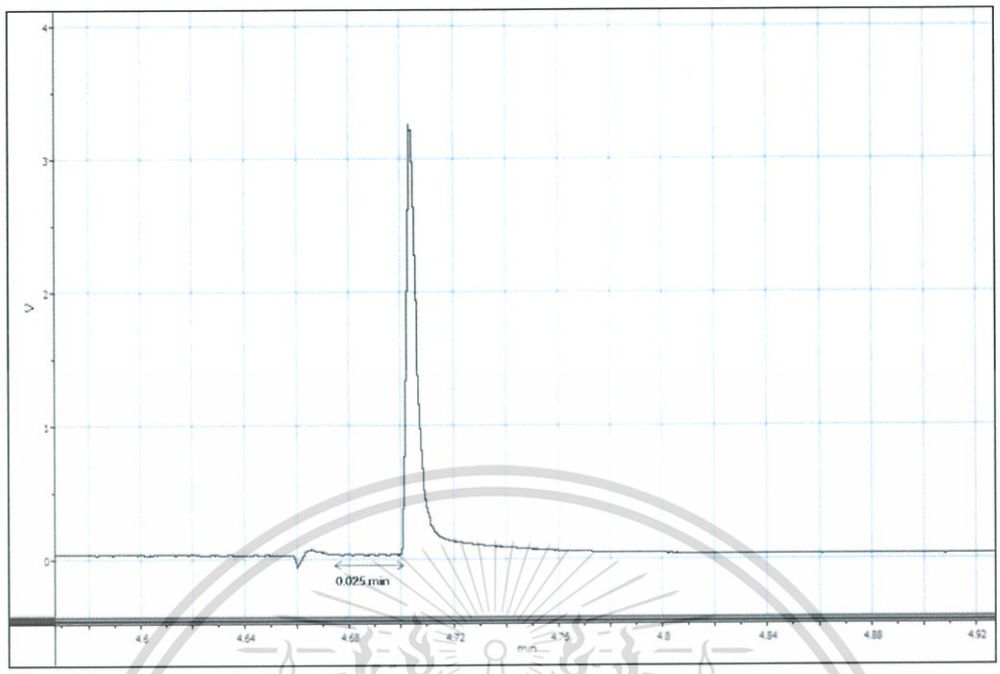

Figure D.7 TCD signal of ethylene in LL70S30ZO10 film

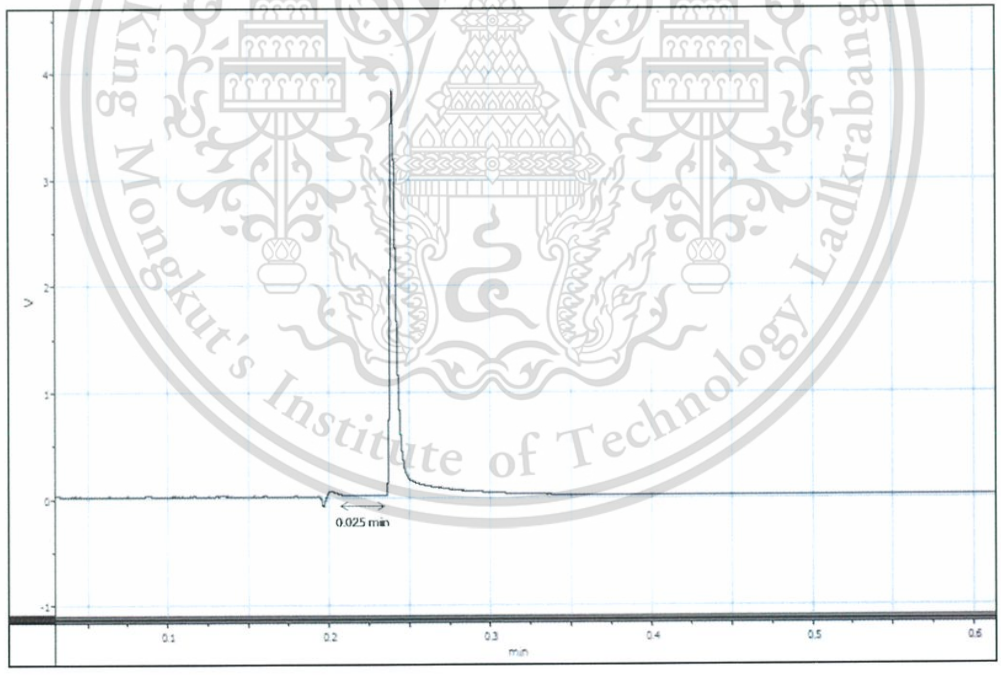

Figure D.8 TCD signal of ethylene in LL70S30ZO15 film

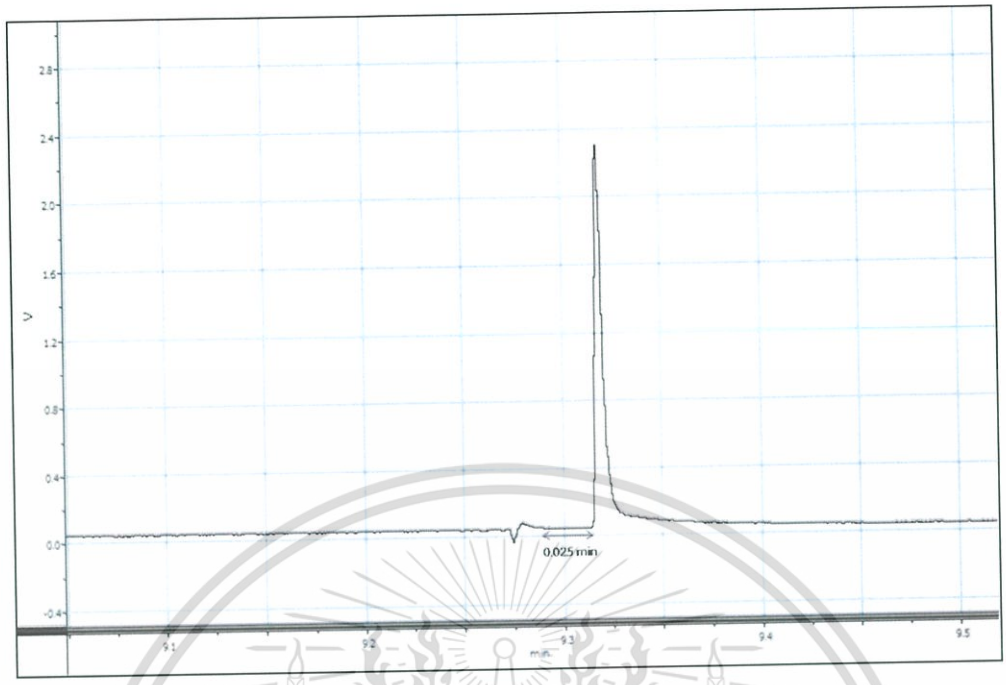

Figure D.9 TCD signal of ethylene in LL70S30ZA5P film (60 rpm)

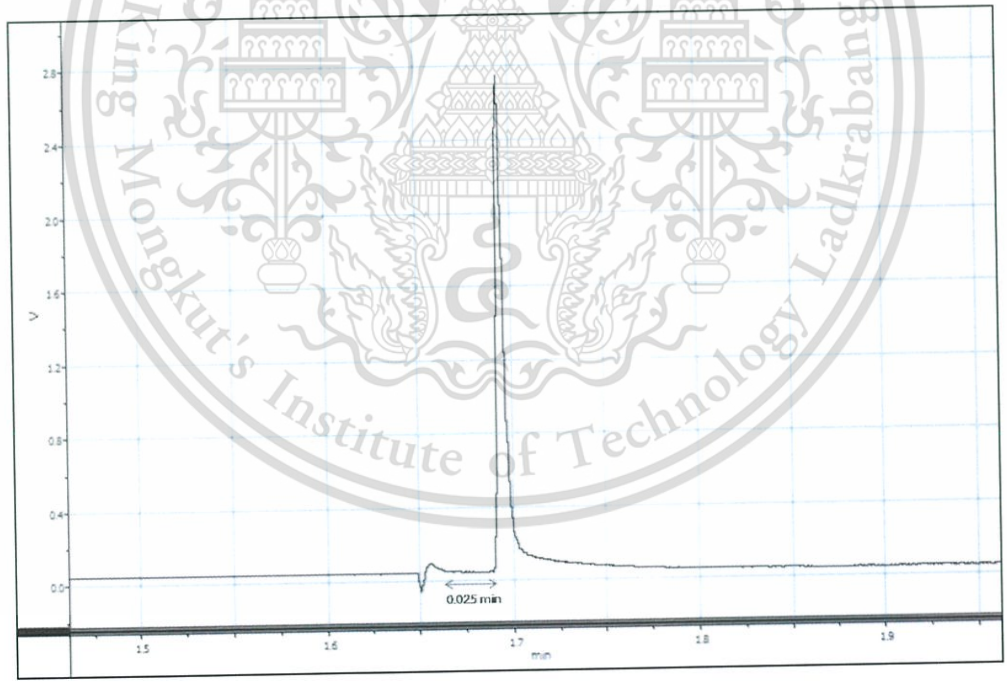

Figure D.10 TCD signal of ethylene in LL70S30ZA5P film (100 rpm)

Ethylene permeation calculation

Pressure drop (P_{drop})

$$P_{drop} = \frac{F}{A} = \frac{mg}{A}$$

When m = Mass of water in U-tube (kg)

g = Gravitational force (9.807 m/s^2)

A = Area of loop (m^2)

Mass of water in U-tube (m)

$$D = \frac{m}{V}$$

$$m = DV \; ; \; V = \pi r^2 h$$

$$= (1000 \text{ kg/m}^3)(\pi \times (3\times10^{-3})^2 \text{ m}^2 \times 7.1\times10^{-2} \text{ m})$$

$$= 2.0075\times10^{-3} \text{ kg}$$

$$\therefore \quad P_{drop} = \frac{F}{A} = \frac{mg}{A} = \frac{(2.0075\times10^{-3} \text{ kg})(9.807 \text{ m/s}^2)}{\pi (\frac{0.7875\times10^{-3}}{2})^2 \text{ m}^2}$$

$$P = 40{,}420.4108 \text{ kg/m.s}^2 \text{ or Pa}$$

$$= 0.40420 \text{ atm}$$

Concentration of the standard ethylene

$$PV = nRT \; ; \; n = \frac{PV}{RT}$$

When P = 1.4345 atm (Atmospheric pressure + Pressure drop)

V = 97.9404×10^{-6} L (Loop volume)

R = 0.0802 L.atm/mol.K

T = 300 K (Room temperature)

Mole of ethylene gas

$$n = \frac{PV}{RT} = \frac{(1.4345 \text{ atm})(97.9404\times10^{-6} \text{ L})}{(0.0802 \text{ L.atm/mol.K})(300 \text{ K})}$$

$$n = 5.8394\times10^{-6} \text{ mol}$$

Mole of ethylene gas (mol/L)

When loop volume 97.9404×10^{-6} L Ethylene gas = 5.8394×10^{-6} mol

Loop volume 1.0000 L Ethylene gas $= \frac{(1.0000\ L)\ (5.8394\times10^{-6}\ mol)}{(97.9404\times10^{-6}\ L)}$

$= 0.0596$ mol

Mole of ethylene gas (ppm or mg/L)

(0.0596 mol/L) (28.05 g/mol) $= 1.6718$ g/L

$= 1.6718\times10^{3}$ mg/L or ppm

$= 1,671.8$ ppm

Ethylene permeation of LL70S30

Peak area of the standard ethylene 1,671.8 ppm (A_s) = 3.99 V.s

Peak area of the permeated ethylene (A_E) = 0.35 V.s

Concentration of the ethylene in permeated gas (C_E) = $C_S \times (A_E / A_S)$

$C_E = 1,671.8\ ppm \times \frac{0.35\ V.s}{3.99\ V.s}$

$= 146.6491$ ppm or µl/L

$= 146.6491\times10^{-3}$ ml/L

$= 0.1467$ ml/L

Flow rate of the permeated gas (F_x) = 30.00 ml/min

Transmission rate of ethylene (J) $= C_E \times F_x$

$= 0.1467$ ml/L x 30.00 ml/min

$= 4.4010$ ml x ml/(L x min)

$= 4.4010\times10^{-3}$ ml/min

$= 0.0044$ ml/min

Surface area of the film (A_F) = 0.0025 m^2

Thickness of film (Δx) = 0.046 mm

Flux of ethylene gas (Flux) $= \frac{J}{A_F}$

$= \frac{0.0044\ ml/min}{0.0025\ m^2}$

$= 1.76$ ml/min.m^2

$= 2,534.4$ cm^3/m^2.day

Ethylene transmission rate (ETR) $= \frac{J}{A_F \times \Delta p_i}$

$= \frac{\text{Flux}}{\Delta p_i}$

$= \frac{(2{,}534.4\ cm^3/m^2.day)}{1.01\ atm}$

$= 2{,}509.3\ cm^3/m^2.day.atm$

Ethylene permeation (EP) $= \frac{J \times \Delta x}{A_F \times \Delta p_i}$

$= ETR \times \Delta x$

$= 2{,}509.3\ cm^3/m^2.day.atm \times 0.046\ mm$

$= 115.4\ cm^3.mm/m^2.day.atm$

Table D.1 Ethylene permeation of the films

Sample	Thickness (μm)	ETR ($cm^3/m^2.day.atm$)	EP ($cm^3.mm/m^2.day.atm$)
LL70S30	46±8	2,523±32	116±2
LL70S30Z5	50±9	4,674±106	234±5
LL70S30Z10	48±9	9,692±552	465±27
LL70S30Z15	54±10	11,312±293	611±16
LL70S30ZO5	54±7	5,878±134	317±7
LL70S30ZO10	50±0	6,380±355	319±18
LL70S30ZO15	50±8	7,656±171	383±9
LL70S30ZA5P (60 rpm)	50±9	4,789±128	239±6
LL70S30ZA5P (100 rpm)	50±8	5,635±64	282±3

Appendix E

Carbon dioxide permeation

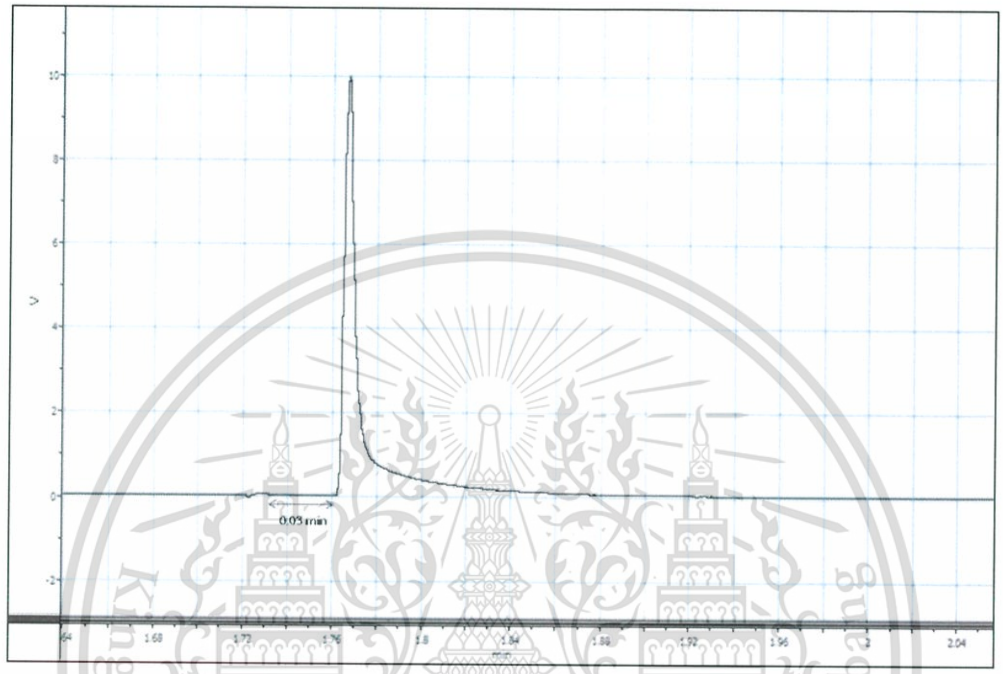

Figure E.1 TCD signal of standard CO_2

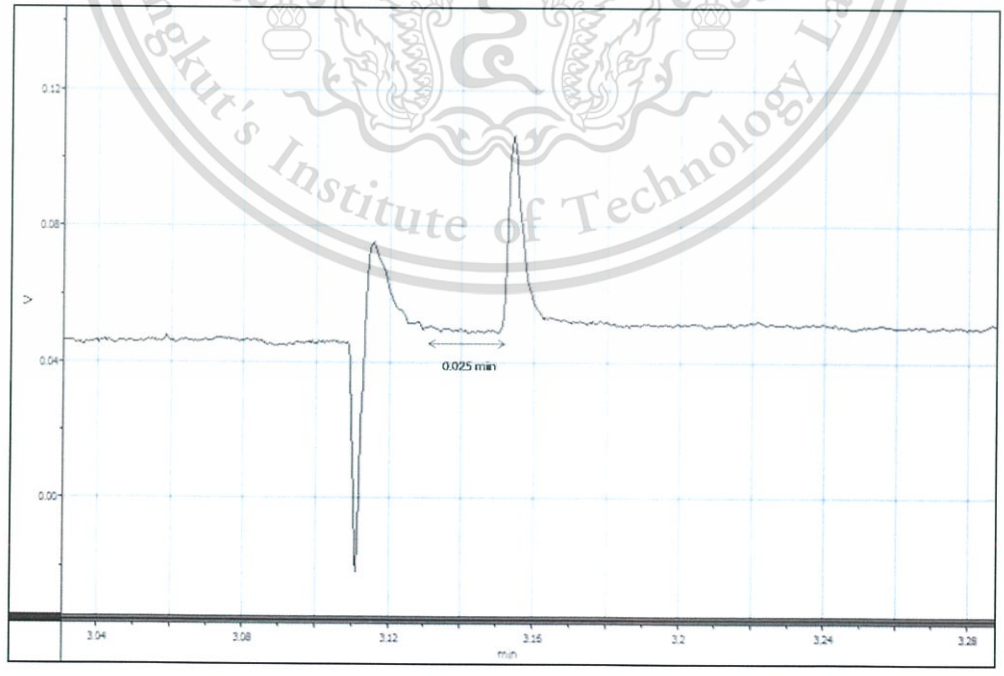

Figure E.2 TCD signal of CO_2 in LL70S30 film

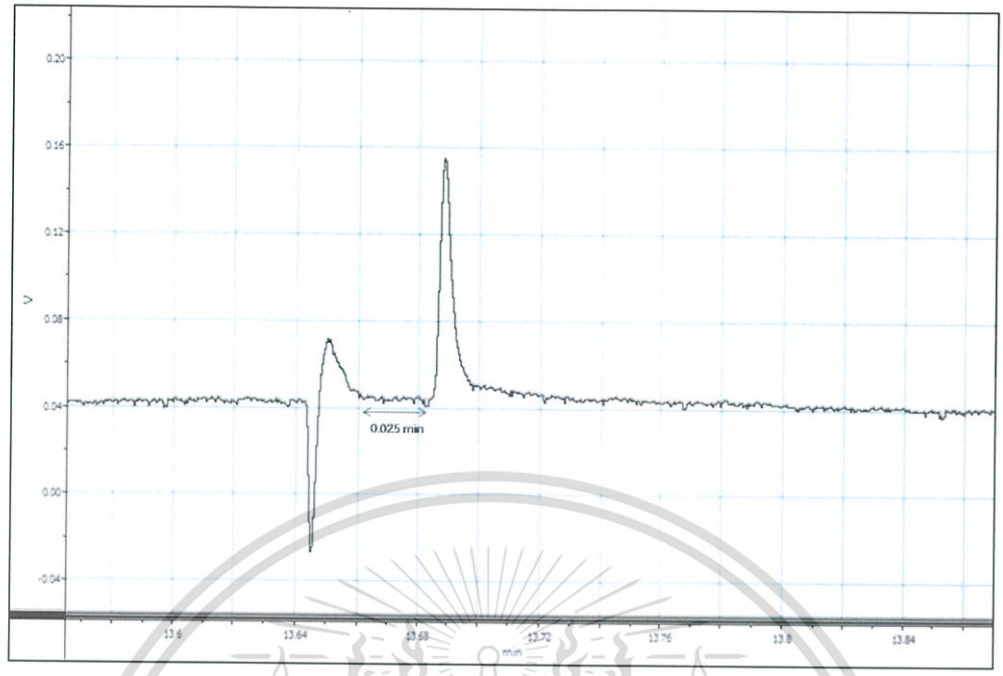

Figure E.3 TCD signal of CO_2 in LL70S30Z5 film

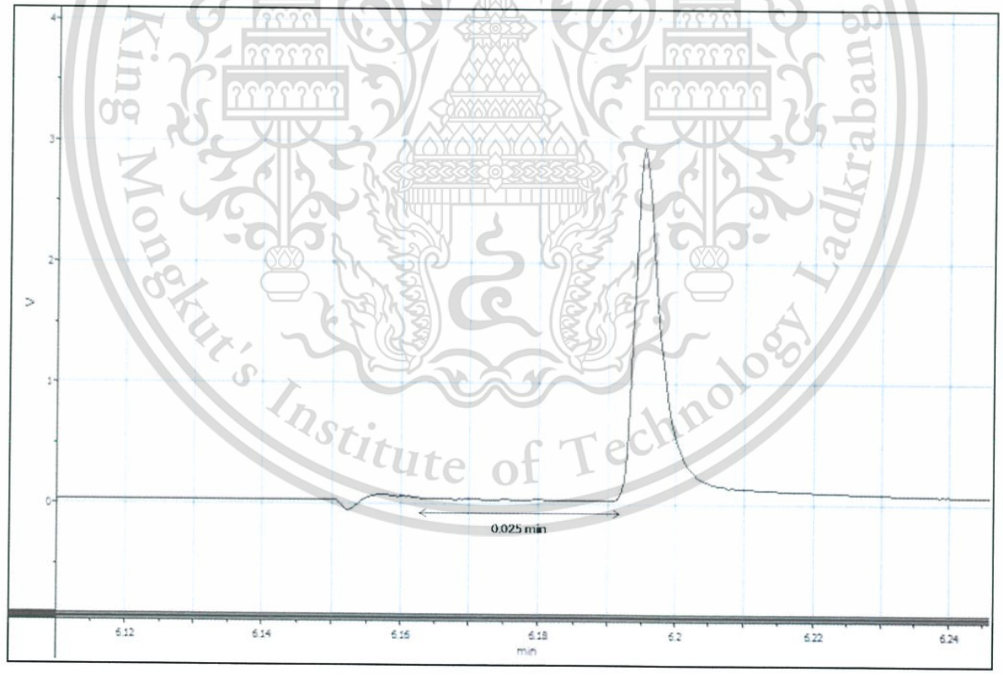

Figure E.4 TCD signal of CO_2 in LL70S30Z10 film

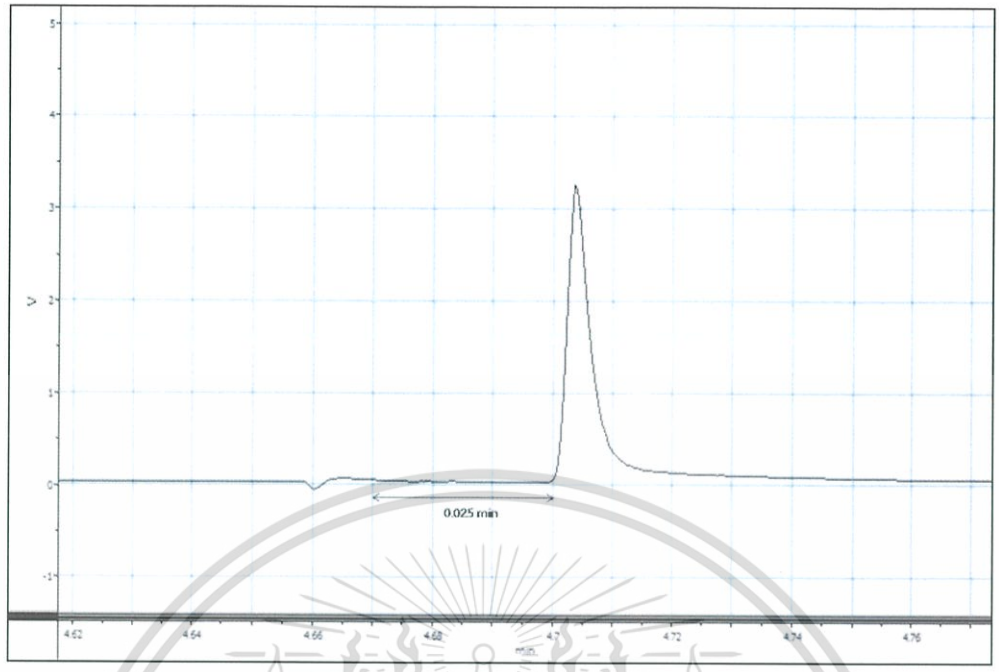

Figure E.5 TCD signal of CO_2 in LL70S30Z15 film

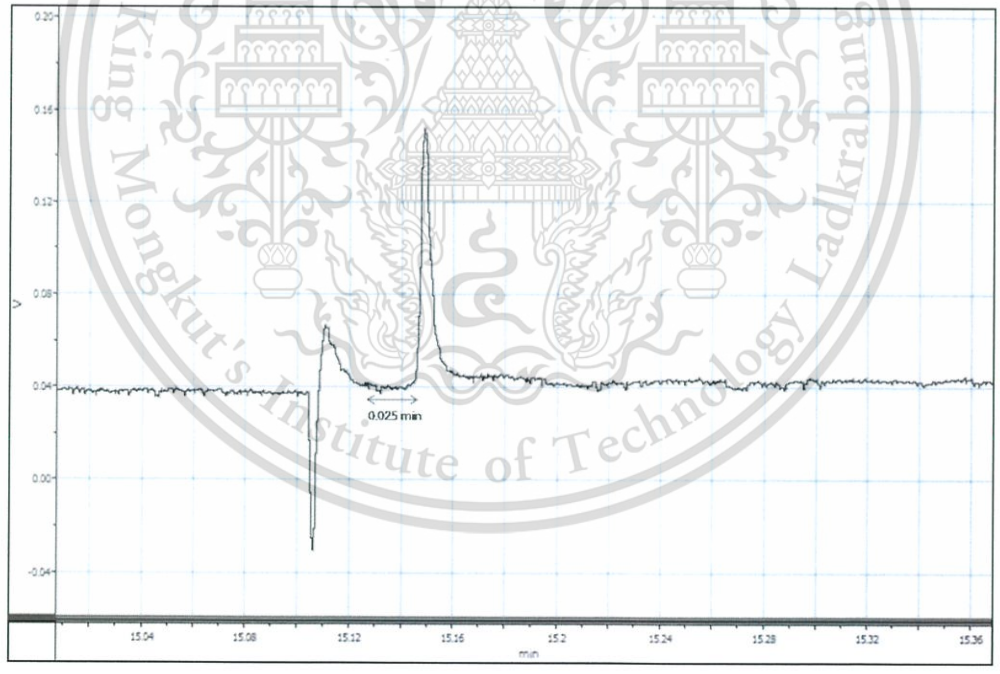

Figure E.6 TCD signal of CO_2 in LL70S30ZO5 film

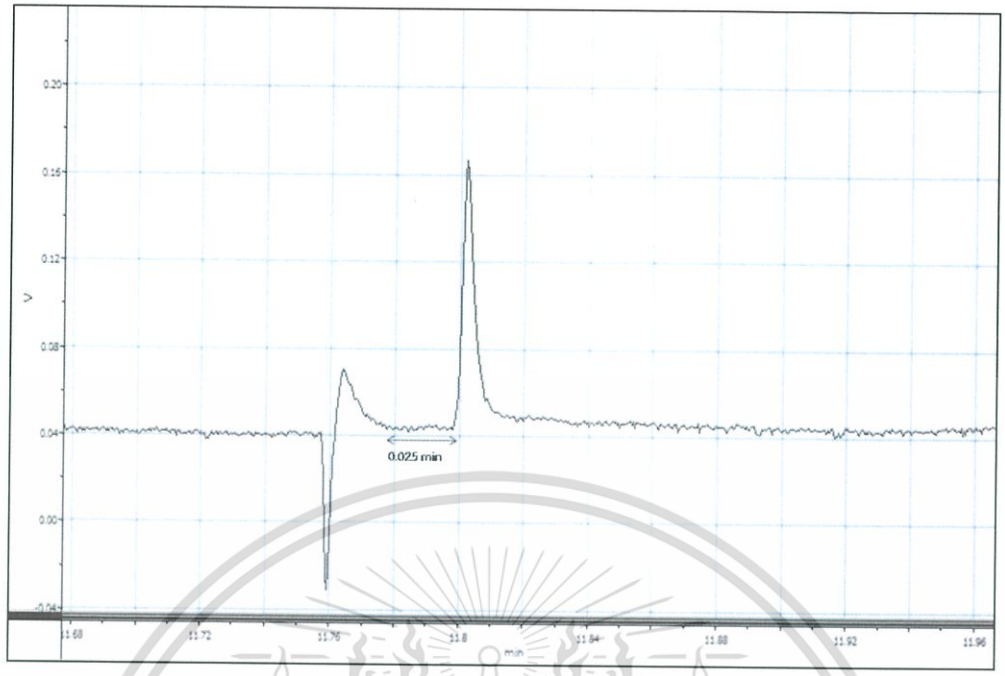

Figure E.7 TCD signal of CO_2 in LL70S30ZO10 film

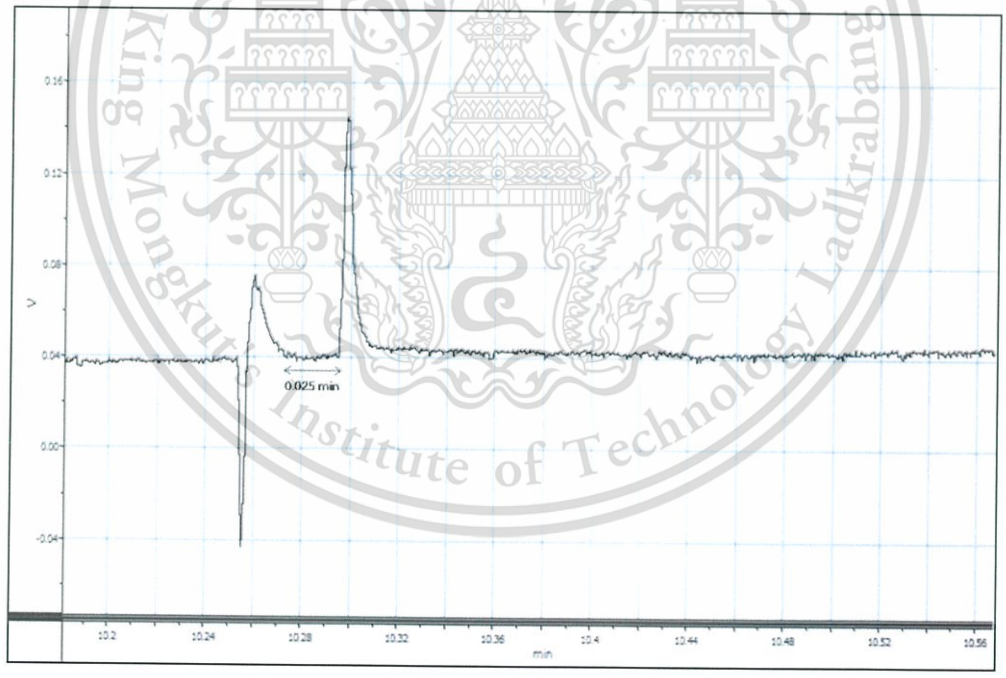

Figure E.8 TCD signal of CO_2 in LL70S30ZO15 film

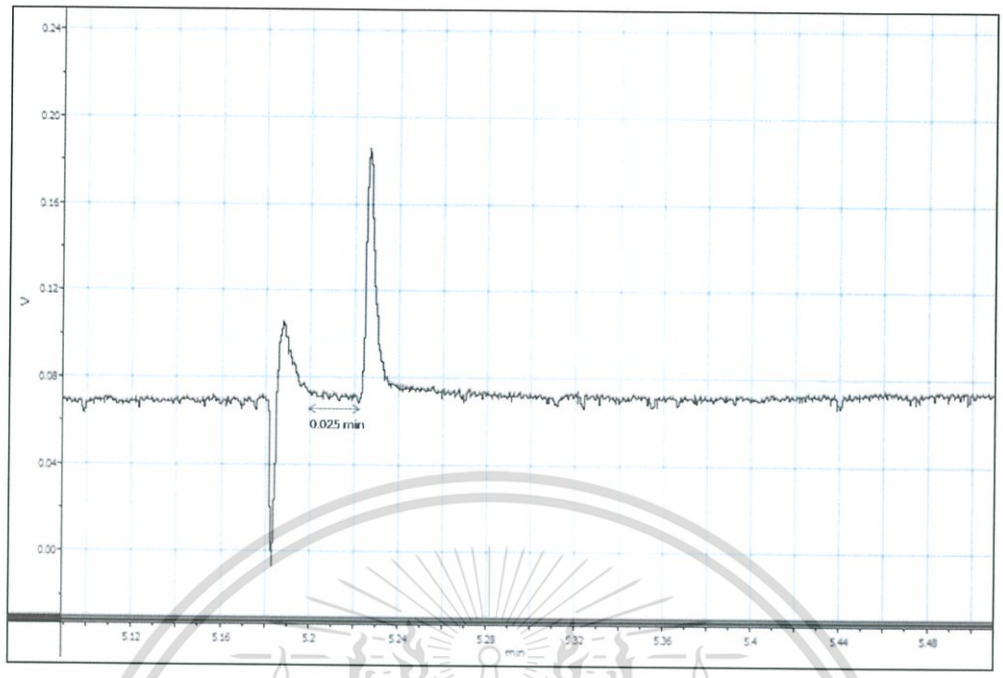

Figure E.9 TCD signal of CO_2 in LL70S30ZA5P film (60 rpm)

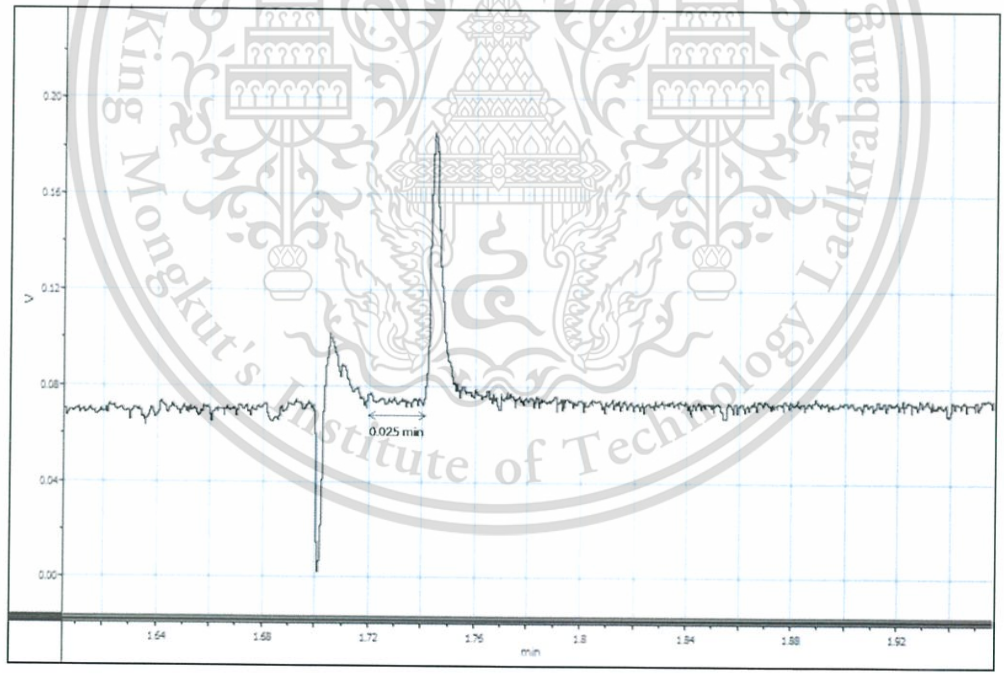

Figure E.10 TCD signal of CO_2 in LL70S30ZA5P film (100 rpm)

Carbon dioxide permeation was calculated as ethylene permeation.

Table E.1 Carbon dioxide permeation of the films

Sample	Thickness (μm)	CO_2TR ($cm^3/m^2.day.atm$)	CO_2P ($cm^3.mm/m^2.day.atm$)
LL70S30	46±8	215±44	10±2
LL70S30Z5	50±9	312±44	16±2
LL70S30Z10	48±9	8,122±44	390±2
LL70S30Z15	54±10	9,508±87	514±5
LL70S30ZO5	54±7	312±44	17±2
LL70S30ZO10	50±0	312±44	16±2
LL70S30ZO15	50±8	234±54	12±3
LL70S30ZA5P (60 rpm)	50±9	273±44	14±2
LL70S30ZA5P (100 rpm)	50±8	351±54	18±3

Author Biography

Name	Miss Kritsana Makphon
Date of Birth	2nd August 1992
Address	82/4 Moo.11 Nongbua Bankhai Rayong 21120
Education	(2014) Bachelor of Science in Industrial Chemistry GPA 3.16 King Mongkut's Institute of Technology Ladkrabang (2017) Master of Science in Polymer Technology GPA 3.50 King Mongkut's Institute of Technology Ladkrabang
Scholarship	1. Tuition fee from Faculty of Science, King Mongkut's Institute of Technology Ladkrabang 2. Financial support from Faculty of Science, King Mongkut's Institute of Technology Ladkrabang for visiting student at Japan Advanced Institute of Science and Technology (JAIST) 3. Scholarship from King Mongkut's Institute of Technology Ladkrabang for poster presentation of International Polymer Conference of Thailand 2016 (PCT-6)
Academic Publication	Makphon K., Rukchonlatee S., Sooknoi T., Yamaguchi M. and Ritvirulh C. 2016. "Mechanical and Rheological Properties of LLDPE/SEBS/Modified Zeolite ZSM-5 Blends." *The Proceedings of International Polymer Conference of Thailand 2016* (PCT-6), Pathumwan Princess Hotel, June 30-July 1, Bangkok, Thailand, pp. 355-360.